Luke Ian Richard

Delamination Arrest by Fasteners in Aircraft Structures Under Static and Fatigue Loading

Luke Richard

A dissertation

submitted in partial fulfillment of the

requirements for the degree of

Doctor of Philosophy

University of Washington
2017

Reading Committee:

Anthony Waas, Chair

Marco Salviato

Jeffrey Miller

Program Authorized to Offer Degree:
William E. Boeing Department of Aeronautics and Astronautics

University of Washington

Abstract

Delamination Arrest by Fasteners in Aircraft Structure Under Static and Fatigue Loading

Luke Richard

Chair of the Supervisory Committee:

Professor Anthony Waas

William E. Boeing Department of Aeronautics and Astronautics

Laminated composite structures convey tremendous benefits of specific strength and fatigue properties in plane, but are highly susceptible to interlaminar failures such as delaminations and disbonds. The initiation of this failure mode further complicates the design as delaminations initiate along termination points of bonded interfaces, such as a skin-stringer, or are often driven by discrete damage events. As a result, the service life cannot be predicted in the same manner as for metallic aircraft where fatigue analysis is used to substantiate the damage tolerance of the aircraft. In order to provide a substantiation for the FAA damage tolerance requirement of composite bonded structures (FAR23.573), fasteners are subsequently installed.

The delamination arrest by fasteners was studied in depth to create a detailed understanding of the process such that it could be accurately predicted under varying load conditions. The fastener itself provides crack arrest capability initially through mode I suppression, and subsequently through fastener joint shear stiffness and frictional load transfer. However, there is also

important interplay between these three fastener parameters, the laminate fracture toughness, fatigue properties and the expected loading conditions which ultimately determines the fastener's effectiveness in delamination arrestment.

Tests were conducted utilizing multiple fasteners to understand the capability of fasteners to arrest delaminations generated by in plane loading both under static and fatigue loading, i.e. mode II propagation. The test results show that the fastener is capable of crack arrest and retardation, but is highly sensitive to inclusion of clearance in the system. Testing, in conjunction with analysis, also demonstrated that the load transfer through friction, which is generated by fastener installation torque, is a critical parameter in the arrestment of fatigue delaminations and plays a dominant role under a number of fatigue loading conditions.

In conjunction with the testing and finite element analysis in Abaqus FEA, a high efficiency FEA based tool was developed in MATLAB which allowed for the more direct manipulation of the input parameters in order to best understand the influence of each. Comparisons between the predictive tool and experimental results showed agreement which indicated the ability of a highly simplified, one dimensional, model to capture the relatively complex fatigue delamination process, provided care was taken in establishing the input parameters.

LIST OF FIGURES

LIST OF TABLES

Acknowledgements

I would like to express my appreciation to my advisor Professor Kuen-Yuan Lin for advising this work, supporting and encouraging me, despite five challenging years of research. Without him, this would never have been possible. Special thanks to Wenjing Liu who helped teach me how to use Abaqus and Phillip Rodriguez who helped with many of the modeling challenges.

Additionally, I would like to thank Professor and Chair of the Department Anthony Waas for stepping in to chair the committee due to Professor Lin's passing.

For supporting the experimental manufacturing and testing, the expertise of Bill Kuykendall and Michelle Hickner of the Mechanical Engineering Department and Fiona Spencer and Dzung Tran of the Department of Aeronautics and Astronautics was invaluable. As well, the technical support and industry experience from Gerald Mabson, Matt Dilligan, Eric Cregger, Eric Saeger and Don Lee, is greatly valued and helped to guide this dissertation.

This research is jointly supported by the Boeing Company, Federal Aviation Administration and Toray Composites America

Chapter 1 Introduction

With the increasing use of composites in primary aircraft structures, delamination resistance has become a critical parameter. The increase in large, bonded structures has largely eliminated the need for fastened joints, but unlike in metals where the critical damage mechanism is fatigue cracking which tends to follow a predictable damage initiation and progression based on the load cycle count, delaminations are typically initiated at discontinuities where opening moments are high or by discrete damage events either within the manufacturing environment or during service. Coupled with the ability of a composite design to hide internal damage [1], delamination damage can go unnoticed and as a result unmanaged.

In order to address the safety of a structure under fatigue, the Damage Tolerant Design methodology was created. For metallic structures with fatigue cracking, a flaw is assumed to exist at the most critical location in the structure and the fatigue crack growth is calculated based on this initial damage. This leads to an inspection and repair protocol which will identify and repair this damage before it grows to the critical length, i.e. the size at which the residual strength of the structure drops below the regulatory load capability. However this approach requires extensive knowledge of the crack propagation for the designers to create an appropriate inspection and repair program to be carried out by the operators. Currently in service composite parts with delaminations are assumed to exist under a “no growth” condition, such that they are arrested statically and will not increase in length under fatigue loading.

Applying the same damage tolerant approach to composite primary structures, delaminations are the critical damage parameter instead of through-the-thickness fatigue cracks. Initial work [2]

focused on the quasi-static behavior of the delamination propagation and arrest through fasteners as it is critical to first understand the static propagation system.

Furthermore, for composite structures which consist of bonded joints, FAR Part 23.573 specifies requirements for the damage tolerant and fatigue evaluations, stating that:

> For any bonded joint, the failure of which would result in catastrophic loss of the airplane, the limit load capacity must be substantiated by one of the following methods:
>
> i. The maximum disbonds of each bonded joint consistent with the capability to withstand the critical limit flight loads (design limit load) must be determined by analysis, test or both. Disbonds of each bonded joint greater than this must be prevented by design features; or
> ii. Proof testing must be conducted on each production article that will apply the critical limit design load to each critical bonded joint; or
> iii. Repeatable and reliable non-destructive inspection techniques must be established to ensure the strength of each joint

For primary structures in a commercial jet aircraft, method (ii) can be understood to be impractical, it would be exceedingly difficult and expensive to proof test the joints in each aircraft. Meanwhile, current non-destructive inspection techniques such as C-scans can verify the integrity of the bond, but not the strength [3]. As a result, this leaves method (i) as the best solution to the damage tolerance requirements set forth by the FAA.

Delamination fasteners are one of many features used to improve the arrest of delaminations or disbonds, also called interlaminar cracks or simply cracks. For the purposes of the work presented here, the terms “crack,” “delamination” and “disbond” are used interchangeably. While through-the-thickness cracks can exist within a composite structure, they did not occur in the work presented here and thus the cracks referred to here are exclusively delamination or disbond type cracks. Various other reinforcement mechanisms including, but not limited to

fasteners, z-pins and stitches [4] all designed to provide a through-the-thickness reinforcement are in use currently and each have different pros and cons. Primary benefits of fasteners are that they are commonly "dual use." These fasteners already exist in the structural design serving to attach design details and they are installed post manufacturing and not limited in the maximum laminate thickness in which they can be installed. One example of a potential dual-use role is attaching shear ties; the fasteners run through the shear tie as well as the skin and stringer of the fuselage, positioning them to suppress skin-stringer delaminations.

The effective use of these fasteners, to prove compliance to regulations, requires a comprehensive understanding of their capability and limitations as implemented, as well as the primary drivers of the delamination arrest through the fastener system. There are three modes of delamination, modes I, II, and III. Mode I is well studied and tests supported by analysis have indicated that the very high axial stiffness of the fastener suppresses this mode extremely effectively [18]. Mode II delaminations however are less well resisted as the crack propagates through shear and previous research indicated the fasteners did not provide arrest in the same overwhelming manner as in mode I [18]. Mode III is least commonly encountered, and is not the topic of this work. This research focuses on the investigation of the effectiveness of multiple fasteners in suppressing delaminations under both static and fatigue loading in mode II, and the development of analysis tools which can predict the results.

A literature review of common delamination and fastener modeling techniques, as well as arrest techniques and previous work in this area is presented in Chapter 2. Motivations and background for this particular area of research is described in Chapter 3 and the description of the Abaqus based finite element modeling is contained in Chapter 4. The development of a MATLAB based FEA tool used for rapid prediction of the performance and various parametric studies is

discussed in Chapter 5. Testing is described in Chapter 6 for quasi static loading and in Chapter 7 for fatigue loading. Further tests and their methods, such as those to establish the material properties, are described in Chapter 8. A comparison of the experimental results and predictions, using the previously established material properties is presented in Chapter 9. Chapter 10 discusses various areas of the research conducted in the course of this research which was not pursued further and a brief explanation as to why each subtopic was not expanded upon. Parametric studies using the same tool are conducted and shown in Chapter 11 and finally a discussion on the applications of delamination arrest fasteners is presented in Chapter 12.

Chapter 2 Literature Review

Two keys to the accurate prediction of the delamination arrest performance of the fasteners using finite elements is to use the appropriate method to propagate the delamination and accurately model the fastener stiffness. The research here utilized the virtual crack closure technique (VCCT) to propagate the crack and Huth's fastener flexibility formula. However, various other methods are also presented here which offer superior performance in other applications.

Additionally, fasteners were chosen as the arrest mechanism. While other reinforcement mechanisms exist and are described in this chapter, fasteners were chosen for their flexibility in application and previously established knowledge on the topic for quasi static loading. The previous work on this topic which also utilized fasteners is discussed in this chapter as well as other work in similar areas.

2.1 Delamination Modeling

Four of the most common delamination modeling techniques are the Virtual Crack Closure Technique (VCCT), the extended finite element method (XFEM), Cohesive Zone Modeling (CZM), and Crack Tip Elements (CTE). The computational efficiency of VCCT was chosen for this research while the other three methods provide different abilities for modeling different delaminations. In particular, VCCT assumes an infinitesimal thickness of the "bondline" which for the co-cured specimens is a reasonable assumption but breaks down for thick bondlines.

Crack tip elements are one popular choice for capturing the effects of a crack in a structure, with formulations addressing different configurations [5] and elements derived from analytical fracture solutions. However, prior to Wang and Qiao's publication, shear deformation of the

orthotropic materials along the interface [6] were not incorporated. This limited the existing models to analysis where the shear effects could be safely neglected or required "tuning" of the element to match test results. Elements developed by using Wang and Qiao's solutions will subsequently have a more extensive scope.

The self-contained nature of the elements provides a benefit over other delamination modeling techniques. Developed from a closed form solution, these elements provide an accurate estimation of the stress intensity factor around the crack tip [7] with a single special element. Additionally, as only one element, the crack tip element, requires special treatment, the remaining entirety of the model can easily be meshed utilizing standard elements. As a result, crack tip elements have excellent computational efficiency for estimating the residual strength of cracked structures.

However, crack tip elements are not without their limitations, especially in areas where the propagation of a crack is desired. Typically, either element deletion and remeshing or cleaving is necessary to propagate a crack. Once the crack tip element has failed, the adherends separate and a new crack tip element is generated. This adds computational costs and complexity, increasing the probability of errors. Additionally, the crack tip element is placed along a prescribed crack path; the propagation is restricted to the element in question. This can be inaccurate in complex structures where ply jumping or crack branching is likely to occur as the crack follows the path of least resistance.

XFEM was developed to solve localized features, such as cracks, not effectively resolved through mesh refinement. Equations with discontinuous functions, known as enrichment functions, are incorporated for efficient analysis of cracking and fracture [8]. As well, crack tip

elements can be utilized with XFEM, for further improvements in the accuracy of the method [33].

This method eliminates the need for remeshing the discontinuity surface as the crack progresses. Nodes surrounding the crack tip are enriched with asymptotic functions and the crack interior is modeled by a discontinuous (Heaviside) function [9]. As well, only the subset of nodes which are close to the crack need to be enriched [9]. This relieves the need for the mesh to conform to the crack path; the crack is free to propagate between the enriched nodes. The decoupling of the mesh from the crack path also enhances the computational efficiency while allowing for reasonably arbitrary propagation, only constrained to the area or volume which is enriched.

Crack tip elements have also been incorporated into XFEM [33]. The principle enhancement is that the entire crack can be treated with only one type of enrichment function, including the elements containing the crack tip. As such, this formulation of XFEM for crack propagation offers another step in computational efficiency.

Not surprisingly, the enrichment functions and crack tip elements in XFEM require particular care. The "appropriate" function depends on the problem parameters, with a diverse set of choices. Also, for 3D solids XFEM, often requires extremely fine meshes [10], limiting its applicability to large structures. Finally, XFEM fatigue propagation results, a critical component of life cycle analysis, require intensive computational and human labor costs, with questionable results.

VCCT has received recent attention due to recent work by Boeing [11] which allowed for the efficient implementation into the ABAQUS FEA code. The technique assumes the force

required to propagate a crack is equal to the force required to close the same crack. This only requires the forces and displacements at the crack tip and the two nodes trailing the current crack tip, with formulae that calculate the appropriate strain energy release rates from these values.

The principle benefit of VCCT is that it does not require unique element formulations and works with common elements. Additionally, no remeshing is required, as the crack is propagated through the releasing of the tie constraint at the crack tip. Finally, this solution has been proven to be robust when other engineering features, such as fasteners [12], and provides reasonable agreement with fatigue experiments [13].

One principle drawback of VCCT is that the crack propagation is restricted to a single plane. This prevents analysis of crack paths which lead to ply jumps. However, current research has indicated a specific hierarchy of crack interfaces in carbon fiber composites, minimizing this limitation. Additionally, VCCT is mesh dependent and the standard VCCT formulation is less accurate when simulating ductile materials compared to brittle fracture, as plasticity around the crack is neglected.

A third method commonly utilized in fracture analysis is cohesive zone modeling. CZM can account for crack initiation, while the other methods cannot. This method assumes that the separation of the surfaces (fracture) takes place across a cohesive zone, instead of a sharp crack tip, and fracture is resisted by cohesive tractions along a finite size zone. This traction first increases to a maximum before relaxing to zero, indicating complete separation. This is then implemented in the finite element method through cohesive elements along the crack path [14].

As mentioned, CZM can predict the initiation of cracking in uncracked structures, including those with blunt notches [14]. This makes CZM uniquely suited for damage initiation.

Additionally, these cohesive elements which model the cohesive zone can be of finite or infinitesimal thickness, allowing for the simulation of structures with a finite bondline. Finally, these cohesive elements allow for further fine tuning of fracture behavior including incorporating the plasticity of the material, accounted for through the traction curve.

A primary disadvantage of CZM is complexity; cohesive elements are needed, decreasing computation efficiency [15]. This may introduce unnecessary complexity to analysis. As well, the result of introducing cohesive elements to simulate the crack also restricts the growth to the surface in which these elements are situated, similar to VCCT. Finally, the addition of these cohesive elements must be treated in such a way that they do not alter the elastic response of the structure both prior to and after separation.

Crack Tip Elements are one of the original methods of dealing with a crack tip in a finite element model and are still utilized in various applications. Standard finite element models cannot establish a stress concentration factor or energy release rate of a sharp crack tip, theoretically the stress at this point is infinite. A CTE solves this issue by implicitly modeling the crack with a closed form solution, with various solutions developed to deal with different material systems, including composites [6]. As a crack propagates through a material, the CTE is moved through the design in order to model the crack tip at the appropriate location. This leads to the first of two primary issues with utilizing a CTE, it requires meshing these elements along the crack path. Either elements must be placed at the appropriate crack locations or the model must be remeshed at each crack step, leading to additional computational complexity. Second, the element requires a closed form crack tip solution, which either must be derived or found from the literature again adding computation complexity, but typically not to a significant degree.

When comparing four commonly utilized fracture modeling methods, VCCT was chosen primarily because the additional capability conferred by the various other methods was not utilized in the modeling for this research. For the work here, the crack tip remained along a prescribed interface due to the design of the experimental specimen and the co-cured specimens conformed well to the assumption of an infinitely thin bondline. Secondly, VCCT was implemented in Abaqus FEA, allowing for rapid implementation of this solution technique.

2.2 Fastener Modeling

Various formulas have been developed for the shear flexibility of a fastener, which is necessary to determine the load sharing through a fastened joint. These various semi-empirical solutions all provide an estimate of the shear stiffness of the fastener, which is critical for the prediction of the mode II delamination arrest capability of the fastened joint. Two different methods are highlighted here, the Tate and Rosenfeld, and Huth solutions. Ultimately the Huth solution was chosen for use due to its use of carbon/epoxy beams during testing to generate the formula.

The Tate and Rosenfeld solution was one of the initial solutions derived to establish the load transfer through bolted joints. As shown below in Figure 1, the fasteners share the load depending on their relative stiffness, with the two bounding cases being infinite stiffness and zero stiffness in the fasteners. A simple spring model of the joint, utilizing the calculated stiffness values of the fasteners and stiffnesses of the fastened sections allows for the estimation of the load sharing between each fastener. Initial work in this area [16] did use the Tate and Rosenfeld solution [17], however the relative complexity of the solution resulted in work being shifted towards utilization of Huth's fastener flexibility formula [18].

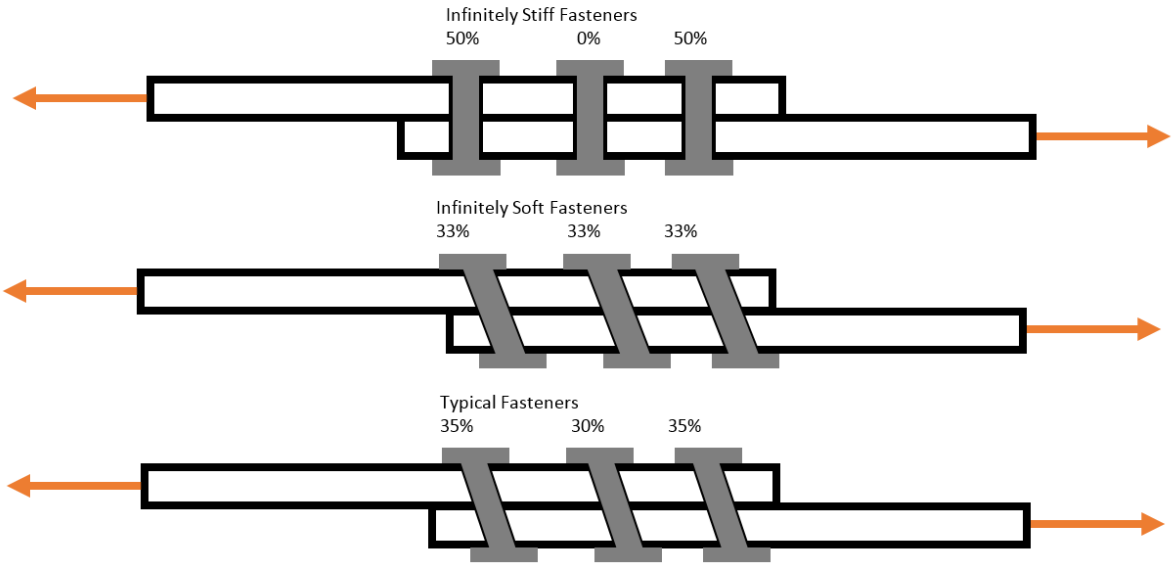

Figure 1: Joint Load Sharing

Huth's fastener flexibility formula was developed to predict the fatigue performance of jointed composites, and utilized graphite/epoxy joints in addition to the typical aluminum used with great frequency in aerospace composite structures [18]. Through experimental work, he arrived at the formula shown below in Eq 1.

$$C = \left(\frac{(t_1 + t_2)}{2d}\right)^a \frac{b}{n}\left(\frac{1}{t_1 E_1} + \frac{1}{n t_2 E_2} + \frac{1}{t_1 E_3} + \frac{1}{2n t_2 E_3}\right) \quad \text{Eq 1}$$

Where E_1, E_2, E_3 are the moduli of the first and second joint materials and fastener respectively, n=1 for single lap joints or n=2 for double lap joints, a, b are experimentally derived coefficients, which are provided as a=2/3, b=4.2 for a graphite epoxy joint. This formula can then be used in the spring-bar analysis which is commonly utilized to determine the fastener load sharing through a joint.

The spring-bar model utilized simplifies the fastener joint, such as shown in Figure 1 to a set of bars and springs which represent the stiffness of the bar segments and the shear stiffness of the fasteners. This solution also relies on the strip model assumption which is that for a repeating fastener pattern, a single strip with width equal to the fastener spacing will yield a result representative of the entire fastener pattern. This strip assumption greatly simplifies the problem in analyzing very wide repeating joints, such as those down the length of an aircraft fuselage.

For purely bolted joints these fastener flexibility formulas have provided proven results for aircraft in service, however another conclusion can be drawn from Figure 1; variations in fastener flexibility do not tend to change the load sharing dramatically. Variations in fastener flexibility from infinitely stiff to zero stiffness changes the load carried by the most stressed fastener only by 17%. Admittedly, more complex joints, such as those that are stepped down or with multiple fastener sizes in an effort to more evenly spread the loading, can see more variation. It should be noted that the predicted response tends to be relatively insensitive to fastener flexibility calculations, a statement which is not true for delamination arrest fasteners, as will be discussed in Chapter 6 and Chapter 7. Furthermore, provided a consistent fastener flexibility is utilized, it is the relative stiffness of each fastener which determines the load sharing, not the absolute value of each individual fastener stiffness.

Additionally, these fastener flexibility formulas, which are experimentally derived, tend to include the effects of all phenomena underneath a single equation for the shear stiffness of the fastener. One phenomena of particular interest in the current research, but not of particularly high importance in purely bolted joints is that of the interfacial friction. As tested by Schön [24], the coefficient of friction of carbon epoxy joints is on the order of 0.25 or greater, which generates non-negligible amounts of load transfer through friction such as in this research where ¼ inch

titanium fasteners can generate 1000 lbs. of preload of more. As a result, while traditional models do not decouple the shear flexibility of the fastener from the shear transfer of load through friction, this has shown to be of interest for delamination arrest features as discussed in Chapter 6 and Chapter 7.

2.3 Arrest Features

Arrest features for delaminations in composites all are designed to provide a through-the-thickness reinforcement which resists peeling stresses that cause mode I delaminations and provide shear load transfer to prevent mode II delamination growth. Many reinforcement types utilize thread of some variety to provide the out of plane reinforcement. Typically the thread for aerospace composites is either carbon fiber, to match the carbon/epoxy composites, or Kevlar (aramid) thread. While the carbon fibers have greater tensile strength, aramids are very tough, beneficial for damage resistance as well as being more forgiving than brittle carbon fibers during the stitching operation. Meanwhile, fastening utilizes a metallic fastener, typically titanium bolts in aerospace, to hold the laminate together in the presence of delaminations.

2.3.i Arrest Features

Stitching of laminates is highly similar to the operation utilized in cloth manufacturing, where various layers of material are joined together via thread inserted through the thickness. For composites, sufficient density of the stitching can suppress out of plane failure modes such as mode I delamination as well as improve damage tolerance, commonly measured by compression after impact (CAI) [4] simply by holding the layers together. Additionally, as the stiches are continuous thread and locked together, their effective pullout strength is greater compared to other reinforcement forms such as pins, which rely simply on the bond between matrix and

reinforcement. However, stitching of prepreg becomes more difficult as the laminate increases in thickness as the needles encounter significant drag from the tacky resin and eventually cannot penetrate the ply stack.

Tufting is similar to stitching but does not involve the locking stitch; instead a needle is inserted and returns along the same trajectory, leaving a loop of thread through the structure. This simplifies the process by eliminating the second, locking, operation [19], meaning the operation can be performed from a single side and with one needle. Additionally, with specific preparation, tufting operations may be employed on thicker pre-preg structures compared to stitching. However, the lack of the locking stitch means the tufts are more susceptible to being pulled out of the laminate in mode I type loading.

Z-pins are thin (about 0.25mm, 0.0098 in) fibrous or metallic rods that are driven through the thickness (z direction) of the laminate, often with an ultrasonic hammer. These pins work similarly to nails, holding the laminae together due to the friction between the pins and the laminae [20]. Additional pullout strength may be conferred by the bonding of the matrix to the pins during manufacturing, but the lack of a head on the pin limits their abilities. Pins have been found to improve the effective static and fatigue properties of laminates subjected to mode I and mode II delaminations, and can be more easily driven through thicker prepreg laminates compared to tufts or stitches. These are more typically used in prepreg materials as in dry fiber processes stitches or tufts provide greater benefit [21].

For thick structures, it becomes inefficient and/or impossible to drive z-pins in, nor stitch or tuft the material as all of these will fail to penetrate the laminate. In these cases, fasteners are employed to provide delamination suppression. Bolts, or derivatives thereof, are most commonly

employed and these serve to clamp together the laminate, preventing resistance to out of plane loading. As well, the fastener shank helps provide load alleviation at the crack tip, improving the mode II delamination resistance. However, because fastener installation requires drilling holes and installation of the fasteners after the part has cured, it has been of great interest to minimize the number of fasteners which are to be employed so these post-processing operations can similarly be minimized [22].

2.3.ii Reinforcement of Prepreg vs. Dry Fibers

The two primary methods for making aerospace structures currently involve either prepreg materials or dry fibers infused via some form of resin transfer molding (RTM, VARTM, CAPRI, SCRIMP, etc.). Each of these materials provides distinct challenges in materials processing, with pre-preg generally having higher part consistency, while dry fibers are significantly easier to reinforce in the z-direction. One general consideration for both of these material forms is to ensure that the third dimensional reinforcements do not experience significant buckling or damage during the ply consolidation process.

Three dimensional dry fiber reinforcement is very similar to the material processing in the textile industry; layers of fiber or woven cloth are stitched or knitted together to create a three dimensional structure. As the handling characteristics are much like other cloth types, the manufacturing of dry fibers utilizes much of the technology from the fabric making industry, leading to a higher prevalence of stitching and tufts as compared to pins and fasteners. Additionally, as the fibers are not held in place by a viscous resin, the needle can displace the fibers more easily compared to punching through a prepreg [4]. As a result, the maximum thickness which can be stitched together is primarily limited by the maximum needle length, not

the ability to penetrate the laminate as in prepreg structures, allowing thick laminates to be effectively reinforced in the out of plane direction [23].

Three dimensional reinforcement of a prepreg material is generally more difficult, but of interest because many aerospace structures are made of, and will continue to be made of, prepreg. The resin in the prepreg serves to maintain fiber alignment but also makes penetration of the laminate for the insertion of reinforcement much more difficult by preventing fiber displacement as well as creating drag [4]. Research has found that the tackiness of the resin tends to create flocking and "birdnesting" issues on the back side of the laminate as well as increasing the frequency of needle and fiber breakage dramatically. Tufting tended to cause less flocking problems compared to stitching thereby providing better results [4].

Fasteners can be considered to be the most practical of the reinforcement mechanisms as they are installed after the laminate has been consolidated. The primary tradeoff subsequently is that the installation of fasteners, which does not depend on the material starting form, requires post assembly manufacturing to drill and install.

2.4 Previous work in this area

Previous work in this area which formed the foundation for the topic of this dissertation has focused on the single fastener response to quasi-static loading. Additionally, work has been conducted using other reinforcement mechanisms which also show promising results [25][26]. The work on single fastener arrest features forms the initial basis for the research presented here.

The initial testing involved pure mode II specimens [16]. As it was already understood that the clamping of fasteners provided good mode I elimination, it was originally desired to investigate the arrest of delaminations independently of mode mixity. These mode II specimens however

presented problems as the twin cracks did not necessarily propagate symmetrically and certain configurations did not generate crack growth beyond the fastener. While this result is excellent for crack arrestment, it did not provide for studying the drivers behind propagation and arrest. Using the established filled hole failure strain of the sample, finite element models were utilized to investigate sample revisions, ultimately settling on a sample which provided an initially mixed mode crack front.

Subsequently, testing focused on a mixed mode delamination arrest specimen with a single crack front. Testing combined with analysis provided insights into the delamination arrest process using fasteners, with the key takeaway that the fastener provided mixed mode arrest through three mechanisms; mode I elimination, fastener shear engagement, and frictional load transfer [22]. Additionally, an analytical model along with finite element models were developed to provide predictive capability and showed good agreement with experimental results. However, it was shown that a single fastener, while slowing the crack growth significantly, did not immediately arrest the growth, as the crack extended significantly past the fastener. This shortcoming in the arrest capability lead directly to this research where additional fasteners are utilized to further reduce the crack growth.

Additional research focuses on arrest delaminations through different means, including, but not limited to z-pins and similar through-the-thickness reinforcements. Pins are generally restricted to thinner laminates compared to fasteners, and both act as complimentary arrest mechanisms; laminates too thin to be fastened can be pinned while thick laminates are bolted. Pins were also found to appreciably improve the arrest capability of the laminate. Their primary mechanism of action is providing load transfer through shear in resisting mode II delaminations and restraining the laminate in mode I [25].

The results of this work have shown the capability of a fastener to improve the delamination resistance of a composite, and identified the primary drivers behind delamination arrest to be mode I elimination, shear engagement of the fastener, and load transfer through friction. Limitations in the scope of the work also presented an area for future work, particularly in the areas of fatigue and the installation of multiple fasteners.

2.5 Fatigue in composites

While a common thought is that composites don't fatigue, this is particularly untrue with respect to fatigue delaminations. Through the thickness of the laminate the composites tend to be very resistant to fatiguing, but under mixed mode loading which tends to generate delaminations there is a distinct fatigue behavior which is similar to other homogenous materials [27]. As a result, effort has been put into predicting the fatigue delamination response of composites under various loading conditions. Much of the foundational work revealed that the matrix properties dominated the delamination fatigue response [28] while more recent work found that the introduction of fasteners to the system will alter the response [29] [30].

Work studying unidirectional composite laminates under fatigue loading found that the fatigue crack behavior of the laminates tested was largely controlled by the toughness of the matrix, with the fibers themselves playing a secondary role [28]. In relation to this research, the authors discovered that for a toughened matrix system, as is the standard T800/3900-2 material which was utilized for the specimens generated for testing here, the crack growth rate was mainly controlled by the stress range. Extending this into fatigue delaminations, the stress range can be related to ΔG, dependent on the geometry, which supports the idea that fatigue delaminations can

be treated similar to that of a homogenous material. In contrast, for brittle epoxies, the maximum stress tended to dominate the fatigue crack growth rate [28].

Further work specifically focused on mixed mode delaminations of composites [27] showed that this interlaminar fatigue behaved similarly to common homogenous material fatigue and thus could be analyzed using common fatigue life prediction techniques. Using a mixed-mode bending fixture, the same technique as used to determine the mode mixity parameters in quasi-static fatigue, samples were cycled in fatigue and the delaminations allowed to propagate in order to experimentally determine the fatigue growth rates. One important result of these experiments is that the authors subsequently observed a fatigue threshold which can be related to the ΔG that the specimen experiences. Later in the research presented here, it was found that the threshold value is important to the accurate prediction of the maximum crack length; neglecting to include this results in underprediction of the arrest performance.

Further work in the area investigated a composite double lap shear joint in fatigue using a single fastener. Esmaieli et. al performed fatigue tests as well as three dimensional finite element analysis to attempt to evaluate the behavior [30]. One of their primary conclusions was that hybrid joints have a higher fatigue life in comparison with simple bolted joints. They determined that the life was improved by increasing the clamping force which increased the compressive stresses created around the hole, and that increased clamping increases the fatigue life of both the simple and bolted/bonded joints.

In the above research they did not consider delaminations as a failure mode. However, their work instead serves to highlight the importance of clamping and maintaining bond integrity in order to

improve the performance of the component. Bolted/bonded joints are found to have an improved life, but it is essential to ensure that these bolted/bonded joints remain both bolted and bonded.

2.6 Fastener modeling and installation

2.6.i Cheung Correction Factor

Previous work by Chi Ho Cheung [2] theorized a correction factor of 0.4 for Huth's fastener flexibility when utilizing his formula applied to load transfer in the joint utilized in his research and the research presented here. This correction factor is applied such that $K_{spring} = K_{huth} * .04$ and arises due to differences in the test conditions and load parameters.

The equation as derived by H. Huth was created for the purpose of fatigue life prediction taking the joint and fastener to or near failure [2]. During the reduction and analysis, the joint flexibility value obtained in the linear part of the hysteresis loops was consistent for a given joint configuration (C_F in Figure 2). However, the flexibility value found this way is strongly influenced by the fatigue loading. In quasi –static tests, Huth found that the joint flexibility during the unload-reload curves remained nearly unchanged during stepwise increasing load until fracture. As the C_F values from fatigue tests and $C_{2/3}$ which is defined as the flexibility at 2/3 of the failure load were nearly identical, it was decided this was to be used to create the flexibility equation.

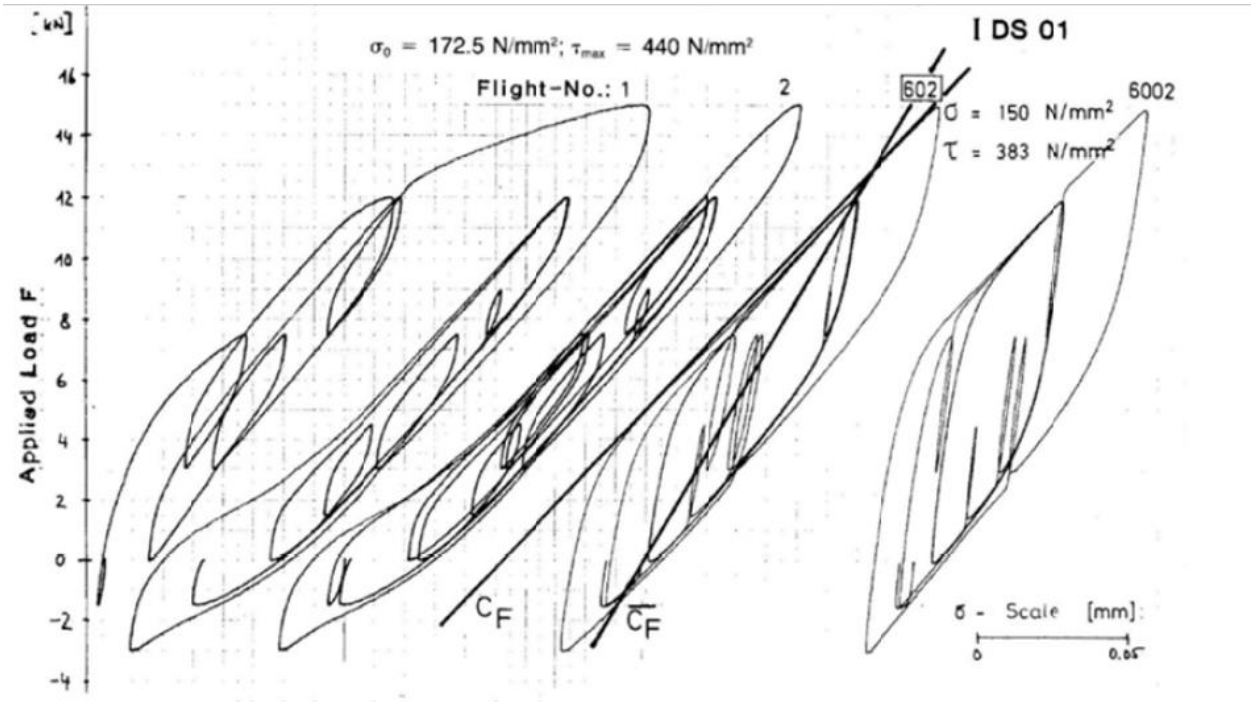

Figure 2: Fastener Joint Shear Flexiblity Under Cyclic Loading [18]

Cheung [2] reevaluated this application for static testing. Under the static loading cases, the sample test data shows that the joint load-displacement curve is almost completely nonlinear. As a result, considering a static test loaded to ultimate failure, the secant flexibility is found to be over 2.5 times that of $C_{2/3}$, translating to a static knockdown factor of 0.4 applied to the fastener joint shear stiffness.

2.6.ii Fastener Spacing [31]

Fastener spacing is primarily governed by the strength of the material and common failure modes of fasteners. The spacing is normalized to the fastener diameter, often abbreviated D, such as 5D means a spacing of 5 times the fastener diameter from center to center. Typical fastener spacing minimums are 4D from center to center in order to not too negatively affect the strength of the material due to the drilling of holes. A tighter fastener spacing than this will reduce the net

section strength of the part significantly enough without providing additional benefit. However, fastener spacing does not have a theoretical maximum amount, typical fastener spacing maximums are 6 to 8 fastener diameters, spacings greater than this tend to not produce adequate load transfer in a sufficiently short distance. Finally, fastener number is constrained by the loading and fastener sizing. The greater the number of fasteners, the lower the total load on any given fastener, as a result for heavily loaded joints, a greater number fasteners are included along the length of the joint in order to prevent static failure.

2.7 Paris Law and R Ratio Correction Factors [31]

The most common formulation for the Paris Law utilized in metals utilizes the Stress intensity factor K, as opposed to the more commonly utilized G for composite fracture. However, the value of K and G can be related as

$$\boldsymbol{G = \frac{K^2}{E}} \qquad 1$$

Where E is the Young's modulus of the material in question. Thus the Paris law is equally applicable for both ΔG as well as ΔK, with the important caveat that the exponent m and constant C will vary depending on whether the strain energy release rate G or stress intensity factor K is being utilized.

The Paris Law can then be utilized to calculate the crack growth for a give number of cycles, and is formulated for composite delamination growth, using ΔG as

$$\frac{da}{dN} = C\Delta G^m \quad (2)$$

Where da/dN is the infinitesimal crack growth for the infinitesimal number of cycles, C and m are experimentally derived parameters and ΔG is the value of $G_{max} - G_{min}$, where G_{min} and G_{max} are the values of G calculated at the maximum and minimum loads.

In order to find the given number of cycles for a known crack extension, equation **2** can be rearranged as

$$\frac{da}{C\Delta G^m} = dN \quad (3)$$

And integrated as

$$\int \frac{da}{C\Delta G^m} = N \quad (4)$$

If one then assumes that the crack growth is small, and thus the value of ΔG is constant for a given crack growth, this allows the above integral to be readily solved as

$$\frac{\Delta a}{C\Delta G^m} = N \quad (5)$$

And thus, for a known crack growth of Δa, the number of cycles can be calculated.

In order to account for the R ratio effects of fatigue, a correction factor is utilized to the original equation such that

$$\frac{da}{dN} = \frac{C\Delta G^m}{1 - R} \quad (6)$$

Which, following the same integration procedure, can be solved for N as

$$\boldsymbol{N = \frac{\Delta a}{C \Delta G^{m}} (1 - R)} \qquad 7$$

Chapter 3 Motivation and Background

3.1 Motivation for multiple fasteners

The primary motivation for initially extending the work into multiple fasteners was to understand the benefit of these additional arrest features in providing delamination resistance. A single fastener, as shown below in Figure 3, slows the crack growth significantly compared to a lack of a fastener with a load increase of up to 100% when comparing the initial load and the load just prior to failure. However, there is still non-negligible crack growth, even with transition fit fasteners.

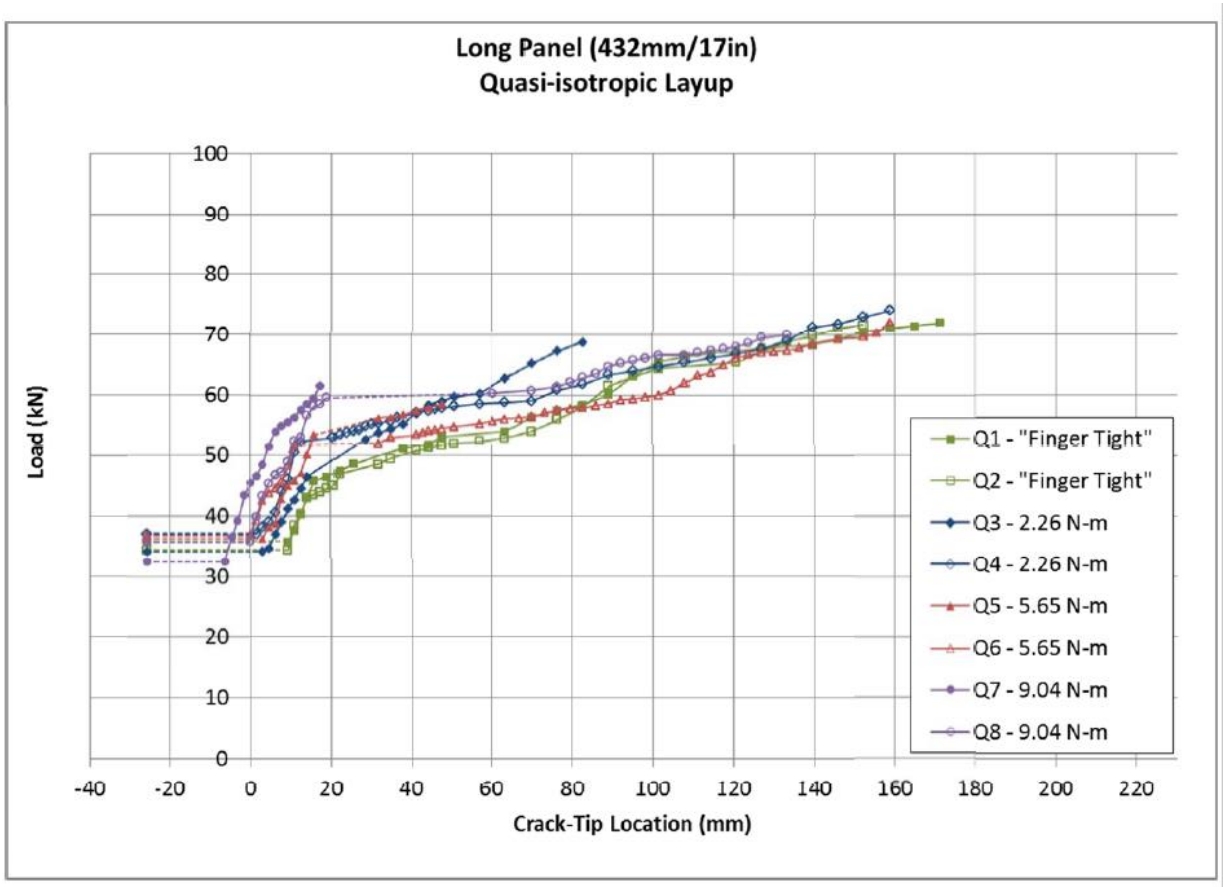

Figure 3: Single fastener results [2]

As a result, there was an interest in investigating the improvement provided by including a second fastener. In particular, mode I propagation had already been eliminated, and during single fastener testing had not reappeared. Thus the arrest mechanism of the second fastener would be limited to load transfer through friction and shear engagement of the fastener shank. Additionally, as shown in Figure 4, large parts will tend to utilize multiple fasteners working in concert as opposed to isolated single fasteners, increasing the interest in understanding how sets of fasteners will contribute to arrest.

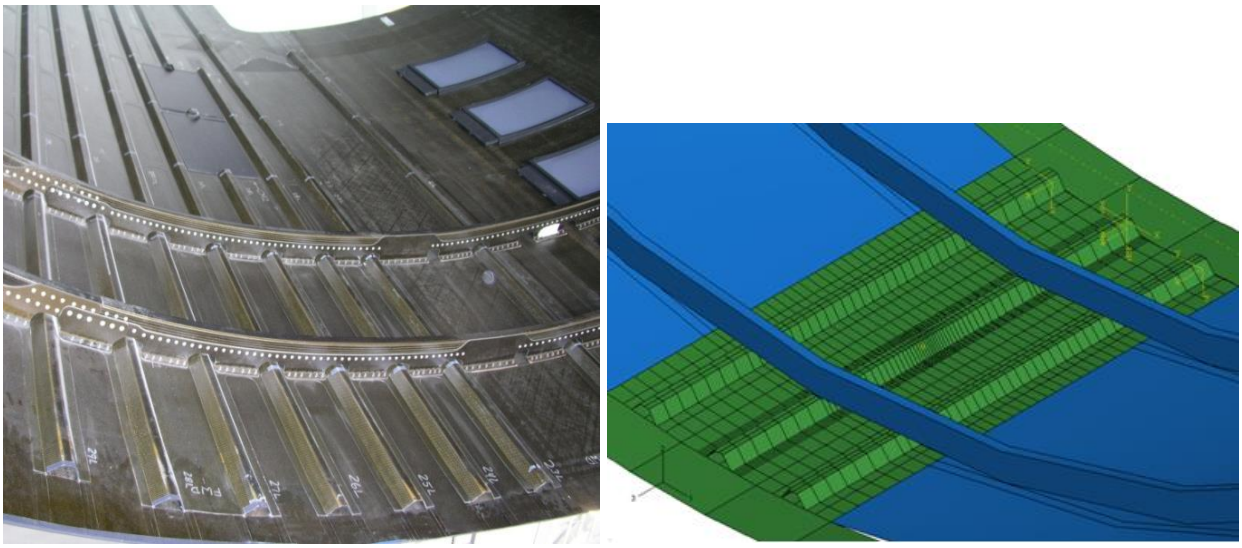

Figure 4: Skin-Stringer of a fuselage barrel section, fasteners visible on frames (left) and FEA (fasteners not modeled)

Initial finite element modeling, as discussed in Chapter 4 showed a non-negligible increase in arrest effectiveness when a second fastener is installed, possibly arresting the crack growth at the location of the second fastener under ideal conditions. Additionally, previous single fastener testing had been limited to these ideal conditions, in particular, zero clearance between the fastener and its associated hole and as a result, testing was to be conducted to verify the theorized loss in arrest effectiveness which would arise due to clearance within the fastener hole. In the

case of this, and preceding work, zero clearance, also known as a transition fit fastener, is defined as a fastener installed in a tightly fitting hole such that there is zero gap between the fastener shank and hole walls.

3.2 Defining "arrested" and "arrest effectiveness" in context of delaminations

One of the key points of discussion is what defines "arrested" and when delamination features are considered sufficient. Generally speaking, once the failure mode has been shifted to a mode that is not delamination, the crack can be considered to be arrested at that load. Eventually a load will be reached such that there is net section failure of the sample prior to additional crack growth. At this point, the crack can be considered "arrested" at that length, as the load which causes net section failure cannot be exceeded.

Additionally, "arrest effectiveness" can be quantified one of many ways, although the simplest is to consider the increase in load, or increase in the number of cycles that an arrest feature will provide for an equivalent crack growth. For the purposes of this research, crack lengths are measured with respect to the first fastener location as the arrest fasteners only become effective once the crack has reached their location. As done in this research, the arrest effectiveness is measured as the relative increase in load between the initial growth away from the starter crack and a given crack length. Typically, this specified crack length is either the length at failure, or location of a fastener.

While quantifiable, the arrest effectiveness of a given fastener and laminate cannot be generalized to all load conditions. For example a 0.25 inch titanium fastener, depending on the application, could vary from infinitely effective in arresting a mode I crack to minimally

effective in arresting a pure mode II fatigue crack when the fastener is installed with clearance. Thus the arrest effectiveness must be evaluated for the application at hand. The research presented here gives guidelines on important parameters to consider, such as hole clearance, fastener installation torque, fastener size and fastener pitch, but each application will have a different ideal answer.

This, among other conditions, also determines what arrest features are sufficient. If the maximum crack growth of a system with a single fastener is less than the critical crack length, then it is possible that the single fastener is sufficient, and additional fasteners will add weight without adding needed capability. Meanwhile, the additional weight of multiple fasteners which limit the maximum crack length may instead confer a benefit. This becomes a design choice, with no specific guidelines possible beyond the statement that additional fasteners at a tighter pitch will tend to arrest a crack by shifting the failure mode away from delamination at a shorter crack length.

3.3 Fatigue Delaminations

Through-the-thickness, composites are often said to not fatigue. While this is arguably not true, depending on various factors including the loading parameters and material system, it is generally true that the millions of fibers serve to naturally arrest cracks. Additionally, work has been shown [34] that for a composite there exists a damage zone surrounding a crack as opposed to a sharp geometric discontinuity as in homogenous materials. However, there is no natural through-the-thickness reinforcement of typical laminates, which rely simply on the matrix material in the interlaminar region to maintain laminate integrity.

As a result, delaminations are a significant danger, and delamination arrest features have been introduced and tested successfully under static loading. However, the fatigue response of these designs with arrest features installed is largely untested. With no natural through-the-thickness reinforcement, the interlaminar matrix region can be treated as a homogenous material and as a result is expected to fatigue in a similar manner. The research presented here subsequently tackles this issue through experimental work and analysis in order to predict the behavior of the arrest features under this fatigue loading.

Chapter 4 Finite Element Modeling

Finite element modeling was conducted in Abaqus FEA in order to develop predictive tools which would accurately capture the delamination response of the system. One of the primary decisions for choosing Abaqus FEA over other comparable finite element packages was due to the implementation of VCCT within the software package. Previous work by Cheung et. al [3][12][16] showed experimentally that the crack propagated along a well-defined interface that could be consistently predicted, allowing the use of VCCT and its reduced computational cost compared to other prediction techniques.

Three different levels of models were detailed that could be classified as 1, 2 and 3 dimensional. The 1D and 2D models both assumed a flat crack front while the 3D model allowed for crack front curvature within the model. The tradeoff was accuracy of the crack shape near the fastener compared to computational cost. The 1D and 2D models, which both modeled a side view of the crack propagation were differentiated by the element utilized, 1D models used bars/beams and smeared laminate properties while the 2D model used plate elements and allowed for lamina level material property modeling.

As shown in Figure 5, all the different models conformed to the same basic dimensions. As the grips were not modeled, the length was reduced to 10 inches, while the width was nominally 1.25 inches and thickness of 0.36, matching the nominal material thickness. The total length of the experimental sample, as discussed in Chapter 6 is nominally 17 inches, with 4 inches lost to the grips, and the final 3 inches typically not utilized during testing to avoid boundary effects, resulting in a net test length of approximately 10 inches.

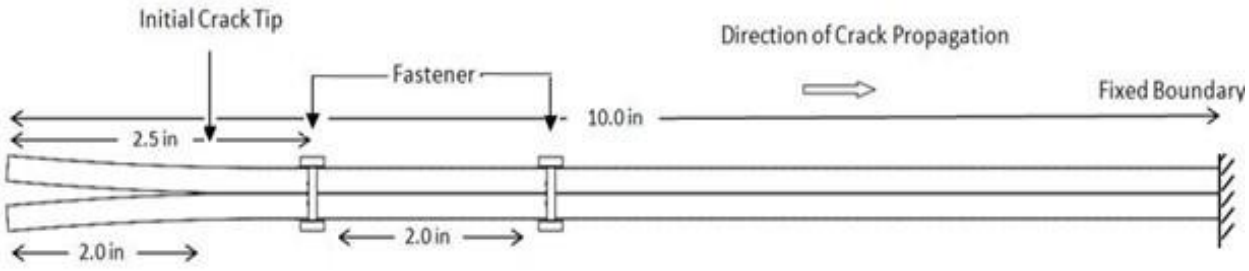

Figure 5: Model Dimensions

4.1 Material Properties

The same material properties were used consistently across each of the finite element models. Lamina level material stiffness properties were sourced from literature, initially utilizing AS4 properties, to verify the solution in comparison with previous models and subsequently T800/3900-2 material properties summarized in Table 1 to match the experimental material. During testing, laminates were strain gaged and the resultant stiffness was compared to the predicted value from the simulations. Due to good agreement between the results shown in Chapter 9, it was determined that lamina level material property testing was not required.

	English Units	SI Units
Ply thickness	0.0075 in	0.1905 mm
E_1	20.6×10^6 psi	142.0 GPa
$E_2 = E_3$	1.13×10^6 psi	7.79 GPa
$G12 = G13$	0.58×10^6 psi	3.99 GPa
G_{23}	0.52×10^6 psi	3.6 GPa
$v12 = v13$		0.34
$v23$		0.40
G_{IC}	1.6 in-lb./in^2	280.2 J/m^2
$GIIC$	14.0 in-lb./in^2	2452 J/m^2
η	1.75	

Table 1. Composite laminar material properties (T800/3900-2) [2]

Two additional materials were utilized due to availability in order to provide a brief investigation of the response in other carbon/epoxies. One material was labeled M46J and a second BMS 9-17, however material properties for these were not readily available. During testing, it was found that the laminate moduli were comparable to that of the T800/3900-2, although the G_{IIC} of the M46J labeled material was noticeably less, resulting in poorer arrest performance as shown in Figure 11. Due to the limited nature of the material, additional tests of the material properties were not conducted for this research to quantify the differences.

Initial model predictions using the primary T800/3900-2 material properties resulted in overprediction of the delamination arrest capability of the system, finite element modeling showed that changing the value of G_{IIC} results in a shifting of the crack length-load curve along the vertical axis, allowing for a post facto fitting of the results. In order to then resolve the discrepancy in a more thorough manner, three point bend testing of the material was conducted using ASTM D7905 [38]. The resultant value of G_{IIC} was found to be 12 in-lb/in^2 (2101 J/m^2), a difference of almost 15%. As shown in Figure 11, altering this value of G_{IIC} allows for the improvement in agreement between the experimental and finite element based results.

The fastener modulus was not directly tested; instead this was taken to be the typical value of titanium, $E = 16.5\,Msi$. Similarly, when clearance was introduced to the system, the values were derived from published drill sizes, which dictated the available values of clearance which could be tested experimentally without undue effort in custom fabricating drill bits. Listed in Table 2 are the nominal and measured values of the properties necessary to model the clearance, which is defined as the difference between the fastener shank diameter and the hole diameter. The fastener shanks were measured using a vernier micrometer with a scale accurate to 0.0001 inches while the hole diameters were measured utilizing an inside micrometer accurate to 0.001

inches. Due to the relative accuracy of the nominal material properties compared to those of the measured values, it is assumed that if proper machining practices are followed, accurate predictions can be made from utilizing the nominal values.

	Nominal in.	Measured (average) in.
0.25 Inch Fastener	0.25	0.2495 $\pm$0.0005
0.25 Inch E Drill	0.25	0.2495 $\pm$ 0.0005
F Drill	0.2570	0.257 $\pm$0.0005
6.5 mm Drill	0.2559	0.2555 $\pm$0.0005

Table 2. Measured vs. nominal fastener properties

The fastener flexibility and friction were experimentally verified using previously delaminated samples. The fastener installation torque vs. preload curve for the fasteners utilized is shown below in Figure 6, an assumed installation torque of 40 in-lbs. was then taken to equal a preload of 1000 lbs. Interfacial friction was subsequently tested using a static frame and the results agreed well with those published by Schön [24].

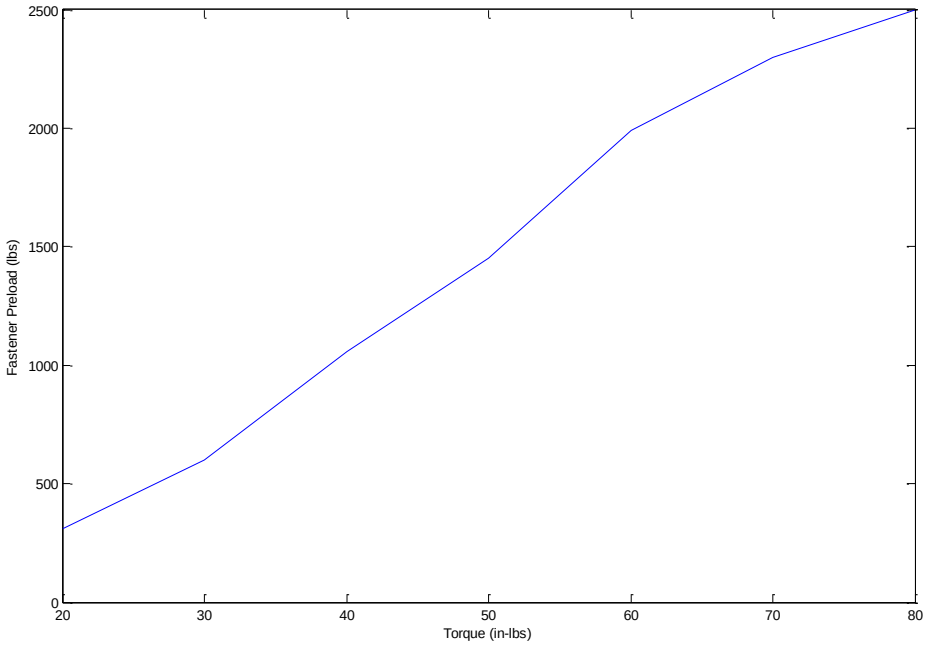

Figure 6: Fastener torque vs. average preload

4.2 Model Descriptions

4.2.i One Dimensional Model

The one dimensional model consisted of beam/bars, element B21 which represented the axial and bending stiffness of the laminate. In order to determine these values, Classical Lamination Theory (CLT) was utilized. Abaqus also has built in laminate property calculation tools, however these were not employed. As a minor goal was to evaluate the ability of CLT to calculate the laminate properties for this configuration in order to ensure its applicability for future modeling endeavors. As such, the laminate level properties were input to Abaqus with initially a modified bending stiffness to capture the composite response. For the model in question, it was determined through sensitivity studies that the bending stiffness did not influence the solution, however for a more generalized application, it is necessary to account for the bending stiffness of the layup which can differ significantly from the calculated isotropic bending stiffness.

Huth's fastener flexibility was utilized to estimate the fastener flexibility in shear while the fastener was assumed to act as a constant diameter bar in tension. The element spring2, a nonlinear spring which allowed for preloading in tension and the inclusion of clearance, was used to model the fasteners. Two springs were utilized for each fastener, one for shear, one for tension; each spring only acted in its assigned degrees of freedom.

The boundary conditions consisted of one end fixed (encastre) and a monotonically increasing load applied to the opposite end, simulating the test conditions. However, the grips were not modeled in order to reduce the computational cost, instead the point load was distributed across the face of the model in two and three dimensions by an infinitely stiff element. The Virtual Crack Closure Technique was then utilized to propagate the crack, with the load and crack tip

location saved to the output file as the simulation progressed. The simulation was terminated once the crack reached the end of the specimen; typically results well beyond the experimentally determined load capability of the sample were neglected.

4.2.ii Two Dimensional Model

The two dimensional model, in contrast with the one dimensional model, allowed for lamina level modeling, potentially improving the accuracy of the solution. Delaminations have been found to be sensitive to the interface along which they propagate [16]. As a result, modeling the interfacial plies had the potential to provide a better solution compared to a one dimensional model, which utilizes the smeared material properties generated through CLT and thus does not capture the stress variation through the thickness inherent in an anisotropic structure.

As before, the fasteners were modeled using the spring2 element, while the laminate was meshed using CPE4R and CPS4R elements, which represented plane strain and plane stress conditions respectively. Initially, it was assumed that the plane strain solution would represent the crack front at the center of the laminate while the plane stress solution would represent the solution along the edge of the laminate. Shown in Figure 7 both elements tend to provide a near identical solution shape but different load levels. As pictured in Figure 10, these predictions are misleading, the different load levels suggest a continuously curved crack front, where at a given load, the crack length along the edges of the sample is greater than that in the center. The C-Scans only show a significantly curved crack front when the crack is nearby the fastener. In general, the predictions using a plane strain element provided better agreement with the experimental results, with some disagreement in locations near the fasteners.

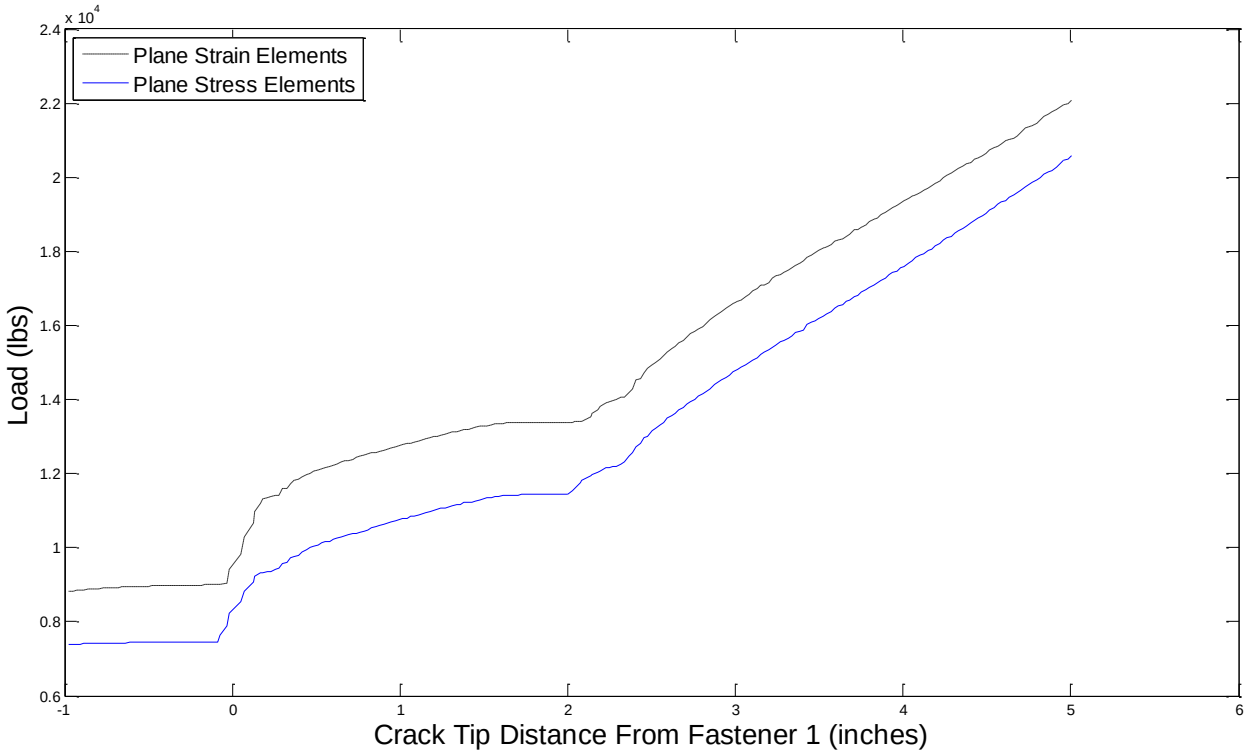

Figure 7: Comparison between plane stress and plane strain elements

As the aspect ratio of the elements is limited, the small elements required to model individual plies lead to a computationally complex model, with a 48 ply model this leads to over 7,500 four noded elements with an aspect ratio of 10. Although this is a relatively small model, the delamination propagation requires hundreds to thousands of individual static runs in order to advance the crack node by node along the defined bondline, with small increases in computational complexity leading to large increases in run time. In order to reduce the computational cost of the two dimensional model, as it was determined that the solution was largely independent of the bending stiffness, the ply count was reduced to the minimum number possible to still model the symmetric, quasi isotropic model with individual ply properties. The layup was changed from $((0/45/90/-45)_{3S}/Crack)_S$ to $((0/45/90/-45)_S/Crack)_S$ where each ply was three times the thickness. Comparing the results of these solutions in Figure 8 suggests that this

solution method provides equally accurate results and thus was used due to the order of magnitude reduction in model complexity.

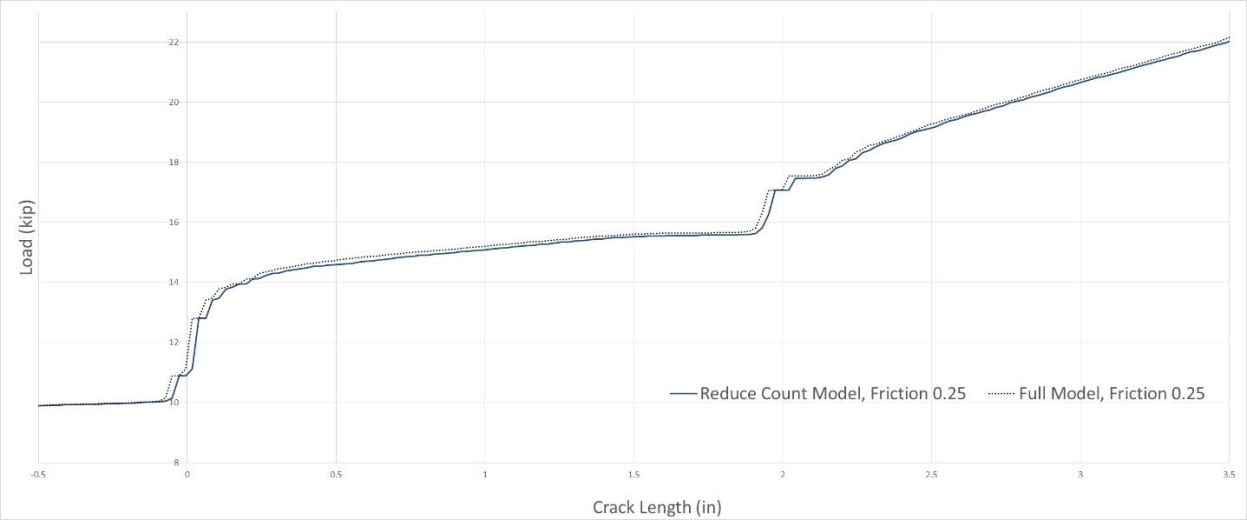

Figure 8: Comparison of 48 (full) and 16 (reduced count) ply models

The fasteners in shear were attached to specific nodes in the model located at the appropriate length along the sample. Previous work [35] showed issues with attempts to create a distributed load via "fastener walls," where the performance was greatly overpredicted. Meanwhile, "fastener heads," which consisted of rigid bodies, were utilized to spread the preload generated by the tensile springs in an attempt to more accurately capture the physics of the actual experiment.

A result of this method is issues with the attachment of the fastener in shear. When the spring was attached to a node along the bondline, the load necessary to overcome the initial resistance of the fastener deformation in shear at this element lead to an artificial spike in the load. By placing the fastener one element above and below the bondline, or including a nominal value of

clearance such as 0.001 inches, the problem was rectified as the interaction between the VCCT calculation and fastener was prevented.

A coincidence of this attachment to a single node was that it artificially softened the fastener as the stress was concentrated on the corner of four elements. Ignoring the excessive deformation of that element compared to those surrounding it allowed for a reasonable solution but the fastener stiffness reduction factor as found by Cheung provided too soft of a fastener in shear. Instead, the combination of the stiff fastener deforming a single element allowed for the serendipitous arrival at an accurate prediction. A better solution would be to distribute the spring through the laminate thickness to provide a more accurate distribution of the fastener engagement in shear. As work transitioned to the MATLAB based FEA, this avenue was not pursued in depth.

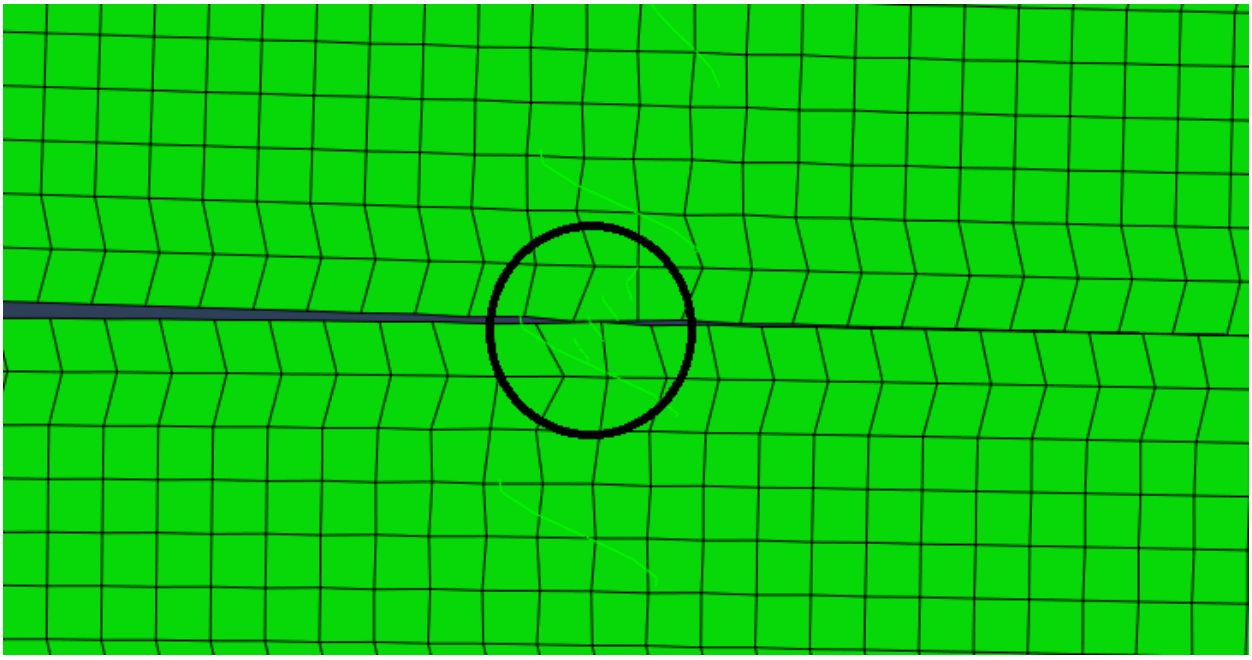

Figure 9: View of fastener attachment point (shear attachment point circled)

4.2.iii Three Dimensional Model

The three dimensional model was generated in order to attempt to capture the crack curvature around the fastener and better understand this process. C-Scans of the sample, as shown in Figure 31 indicate that the crack tip is curved around the fasteners. Being able to capture this effect was then found to be of interest.

The first attempts were made modeling the system entirely using brick elements C3D8R and the reduced ply count, in order to attempt to minimize the computational complexity. Further modeling was performed using quasi-isotropic material properties as this allowed for a further increase in element size in the regions not of interest but lost the unique distribution of the preloading which resulted from the anisotropic material properties through the thickness. The decision was made that model run time was to be prioritized over preload distribution.

The second attempts were made by Phillip Rodriguez which utilized continuum shells, SC8R. As described in greater detail in [36], the solutions presented resulted in good prediction of the crack front curvature around the fastener, and agreement with the experimental work.

In both cases, the fastener was modeled as a solid, with the preload applied utilizing the "preload" feature in Abaqus which deforms the defined plane of the model until the desired force across that plane has been achieved. Additionally, by using the three dimensional model, the interaction of the shank along the fastener hole would be most accurately captured.

The primary benefit of this model was the ability to estimate the fastener flexibility through analysis as opposed to test. Running a static test with the two halves fully delaminated and correlating the displacements with a one dimensional result then allowed for the computational estimation of the fastener flexibility.

4.3 Model Changes for Fatigue Modeling

In order to capture the fatigue delamination response in contrast to the static delamination response, the fatigue properties were utilized using VCCT. For each delamination growth, two runs are performed, one at the minimum load, one at the maximum load, in order to determine G_{Min} and G_{Max}, allowing for the extraction of ΔG. Using material properties $\frac{da}{dN} vs. \Delta G$, where $\frac{da}{dN} = C\Delta G^m$ and the crack growth da can be solved for. This formulation, which is the Paris Law, is identical to that used in metallic fatigue, with the caveat that ΔG is utilized instead of ΔK in the course of this research [31]. Because the matrix is a homogenous material, this solution is applicable to interlaminar fatigue but is not applicable to through-thickness fatigue cracks in composites.

4.4 Results and Discussion

4.4.i Primary arrest mechanisms

The three primary drivers of fastener arrest under quasi-static loading are the elimination of mode I, fastener engagement in shear, followed by load transfer through friction. Meanwhile, for fatigue, the load transfer through friction plays a much greater role, as will be discussed in greater detail in Chapter 5 and Chapter 7.

As seen in Figure 10, the first fastener, located at 0 inches, effectively shuts down mode I as soon as the crack reaches it. However, it can be noted that mode I reappears as the crack travels down the sample, with the second fastener, located at 2 inches in this model, again reducing the value. The reasons for this are due to the modeling approach. The first reason is that the tensile stiffness is modeled as a spring that typically has both tensile stiffness as well as compressive

stiffness. The second reason is that the fastener head is attached to the laminate in the model, resulting in a minor change in bending stiffness at the tip of the fastener head and opening rotation at the crack tip. By eliminating the compressive stiffness, most of this reoccurrence of mode I is removed. If the fastener is modeled purely as a spring, and the model is reduced in thickness due to Poisson ratio effects, the fastener spring will cause the two model adherends to separate. However physically this will not happen, as the fastener is not attached to the laminates in any matter and will only compress the laminates together. Removing the fastener head further reduces this phenomena but the decision was to sacrifice the small artificial spike in mode I for improved preload distribution via the fastener head modeling.

Visible in Figure 10, with the modified fastener, there is still a resurgence in mode I however as the crack progresses further down the model, and this too can be attributed to the Poisson's ratio effects of the laminate, since when it is sufficiently strained in tension, it becomes thinner than the clamped fastener and as a result, the laminate is able to separate, resulting in mode I delamination growth. As the crack reaches the second fastener, this is again removed, and then reoccurs further down the laminate as the crack grows. When visually comparing the two different modeling techniques, for most cases it is suspected that the small difference in response does not justify the additional modeling complexity of removing compressive stiffnesses and modifying the method of fastener head modeling required.

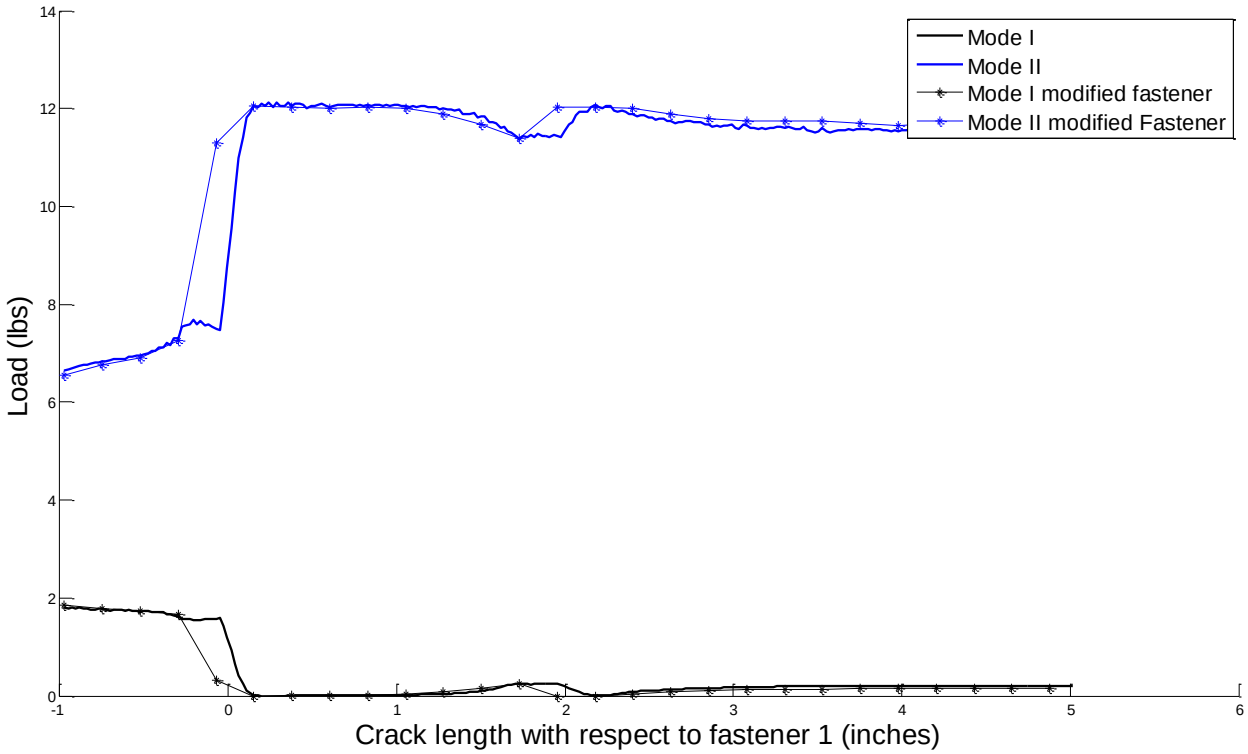

Figure 10: Mode Decomposition of Finite element Model

4.4.ii Fastener Spacing

One of the desired effects when performing experimental work was to be able to decompose the response of the first and second fasteners by adequately spacing the fasteners such that they did not influence one another. Using ¼ inch fasteners, the standard fastening spacing is approximately 4-6D or 1-1.5 inches. Finite element testing however showed that increasing the spacing to 2 inches would ensure there was no interaction between the fasteners. One area in which this can be seen is in the mode decomposition in Figure 10, where the fasteners are sufficiently far apart that mode I can reappear to a minor degree.

Fastener pitch can also become a design parameter, as seen in Figure 12, changing the fastener distance in the direction of the crack will change the crack length for a given load. However,

within the confines of this research, there has not been significant work dedicated towards evaluating the response of changing the fastener pitch in the perpendicular direction. Although the fastener spacing in the direction of the crack has been altered, the width of the specimen has remained largely the same due to constraints in the scope of the work and machine resources.

4.4.iii The Effect of G_{IIC}

Two of the most immediately apparent and expected results are that changing the value of clearance and G_{IIC} alter the arrest capability of the fastener significantly. As shown in Figure 11, reducing the value of G_{IIC}, in this case from 12 to 8 lb/in results in an over 20% drop in load carrying capability for the same crack length, or conversely, greater crack growth at the same load. Additionally, but not as readily apparent, is that the inclusion of friction does play a beneficial role in the crack arrest capability. The lines in Figure 11 with the inclusion of clearance, consistently sit above those which do not include clearance, but only by 1-2%.

Modeling was conducted at 0.007 and 0 inches of clearance as these were two commonly available drill sizes. There was no readily apparent "critical" value of clearance found through the modeling, increasing the clearance increased the decrement in performance.

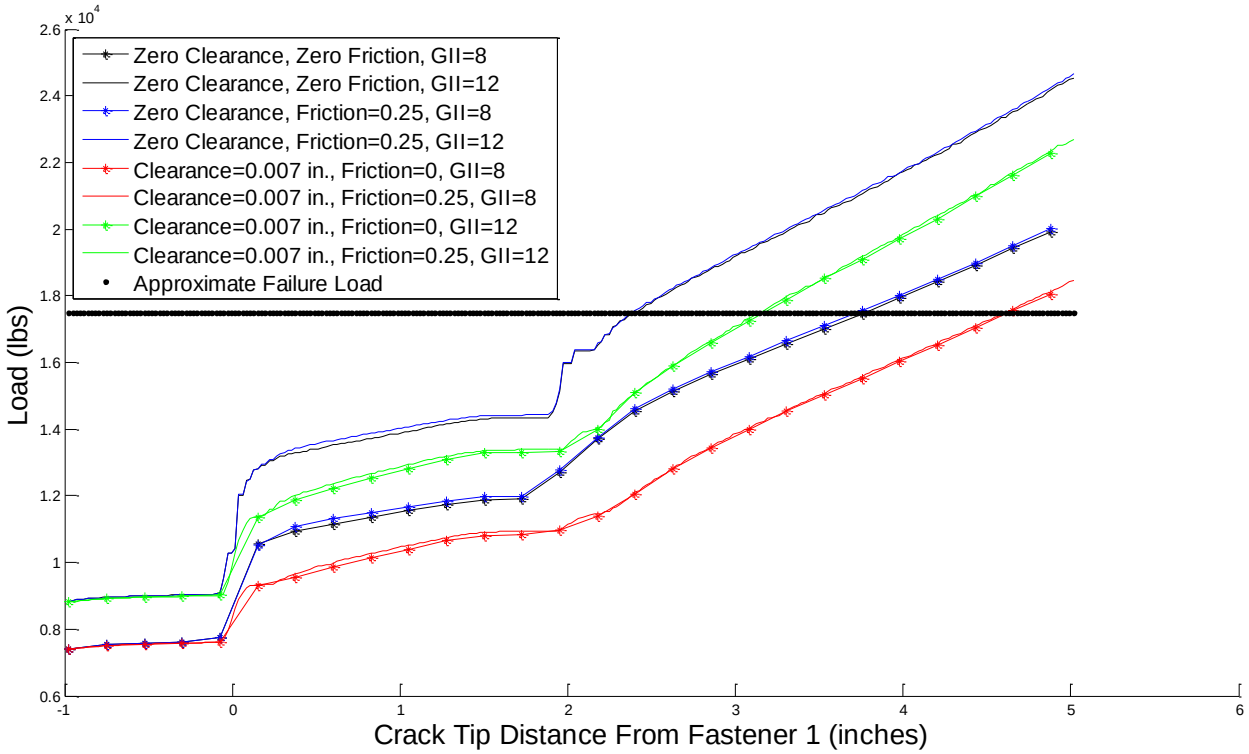

Figure 11: Load vs. Crack Tip Location for Various Simulations

4.4.iv Effects of Fastener flexibility

Additionally, changing the fastener flexibility as well as the fastener spacing affects the delamination arrest capability. As the fasteners do not provide arrest benefit until the crack has reached said fastener, increasing the fastener pitch, as shown in Figure 12 results in greater crack growth for a given load, as the crack must grow further before the second fastener can provide arrest benefit. Meanwhile, changing the fastener flexibility, either by using a stiffer material such as stainless steel or using a larger diameter fastener alters the slope of the line. A less flexible fastener will result in a steeper slope of the crack tip location vs. load curve. Note however that the curves remain the same prior to engagement of the first fastener, and the curves of different fastener pitch only diverge after the engagement of the second fastener occurs for the sample with a shorter fastener spacing.

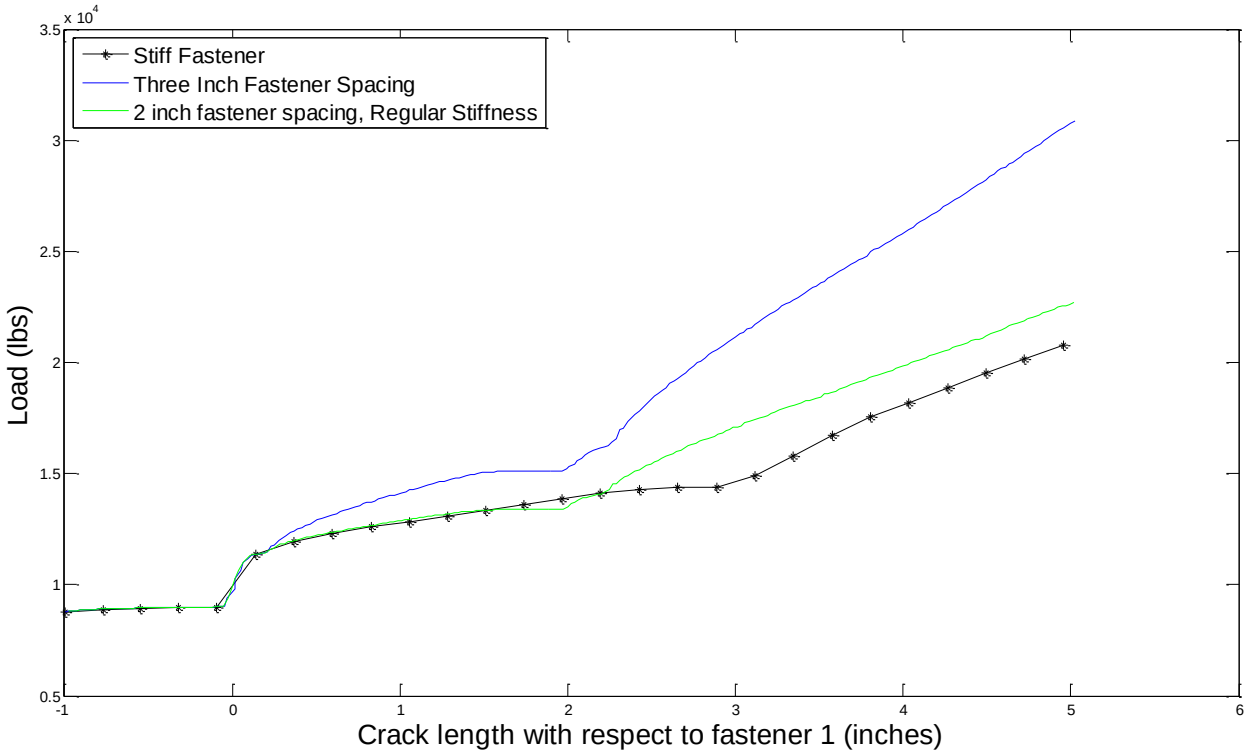

Figure 12: Comparison of varying fastener stiffness and spacing T800/3900-2

These results subsequently guided the delamination arrest experimental design. Under static loading, some of the key design parameters were the fastener spacing, fastener size, and fastener preloading, which correlates to the load transferred through friction. Fatigue delamination simulations were primarily conducted using the custom developed MATLAB based FEA discussed in Chapter 5 as it provided greater flexibility for simulating the conditions and allowed for more direct evaluation of the effect of various input parameters on the fatigue response. One of the primary drawbacks of utilizing an established finite element code is that the solving software is closed source, preventing detailed investigation into how each parameter is treated.

4.4.v Three Dimensional Results

Both Rodriguez's model as well as the model developed in this research provided a reasonable approximation of the crack curvature. As shown below in Figure 13, the three dimensional brick model reasonably approximated the shape of the crack front around the fastener if the average shape is taken, however the various "peninsulas" of bonding, particularly on the far right image, indicate issues with the simulation, as these have not been found to occur in actual testing.

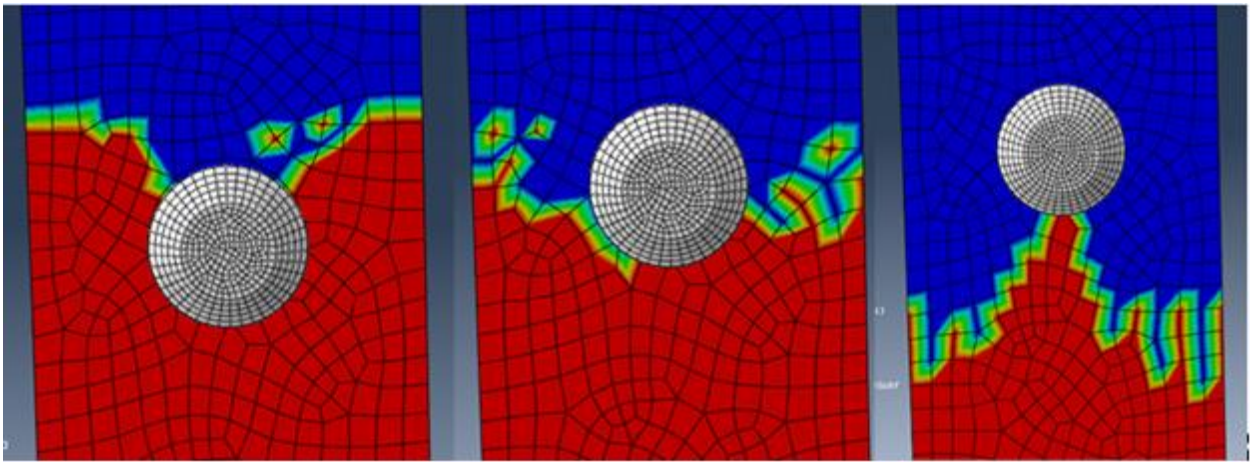

Figure 13: Crack shape during propagation (red is still bonded)

Further development of the three dimensional model by Rodriguez provided better results, as shown below in Figure 14 [36]. One of the notable reasons for this is that better partitioning of the model provided a more uniform mesh, compared to that of the original brick model. Further pursuit of these techniques can yield valuable insights into the crack shape, particularly for cases of more varied geometry compared to the straight samples simulated here, however this is outside the scope of the research presented.

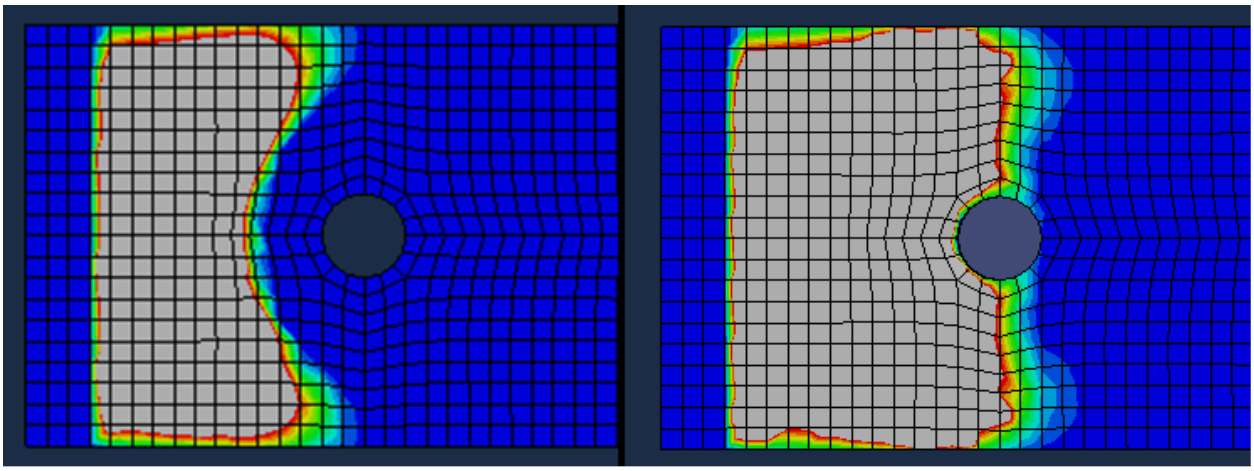

Figure 14: Crack shape during propagation of revised model (blue is still bonded)

An additional use of the three dimensional finite element models is to simulate the fastener flexibility in order to obtain an accurate estimate of the fastener flexibility for various configurations, as well as verify the fastener flexibility formulas. Simulations of the current configurations gave good agreement with the corrected fastener flexibility as proposed by Cheung [35].

Chapter 5 Development of MATLAB Based FEA Tool

In order to run various parametric studies as well as investigate the ability to predict the delamination response in the most efficient manner possible under fatigue loading, a MATLAB based one dimensional FEA tool was developed. MATLAB was chosen due to its relative ease of code implementation and robustness as a programming tool. The simulation was written with relatively easy translation into additional programing languages as well, although that has not occurred at this time.

This decision to make this tool finite element based was due to the high level of complexity required to generate an analytical tool which relied on energy methods. One of the primary benefits of creating an energy methods based tool is such that it provides a "closed form" solution through which understanding can be derived about the system. Previous work [2] successfully implemented a Principle of Minimum Potential Energy (PMPE) based simulation, however, the sheer number of shape functions required to describe a single fastener version of this solution did not allow for any significant insights into to the solution. In contrast, a FEA based solution was expected to provide more ability for customization, particularly changing the fastener pitch without needing to recalculate the functions.

Additionally, the departure from established finite element codes allowed for greater flexibility in how the fastener and delamination were modeled. Various frictional modeling techniques and fatigue delamination propagation solutions were attempted in order to thoroughly examine the design space.

Finally, the tool was written such that it is rapidly translatable into other programming languages and provides a standalone program that does not require design and development of a finite element model.

5.1 Method of Model Development

In order to develop a model which could be utilized for the prediction of static and fatigue delaminations using the finite element method, it was determined to program the system in Matlab. A 1D beam/bar/spring model was chosen based on the rapidity of results and success in Abaqus FEA using a model of this type. Additionally, the choice to employ Matlab allowed for greater control over the entire solution, the solver for Abaqus is not open source and as a result, the influence of individual input parameters is much more difficult to determine. The process of developing the model followed four main steps: static development and validation, implementation of VCCT, implementation of the Paris Law and implementation of the effect of R ratio and compressive loading.

The process for the static implementation of this code is shown in Figure 15 while the fatigue implementation is shown in Figure 16.

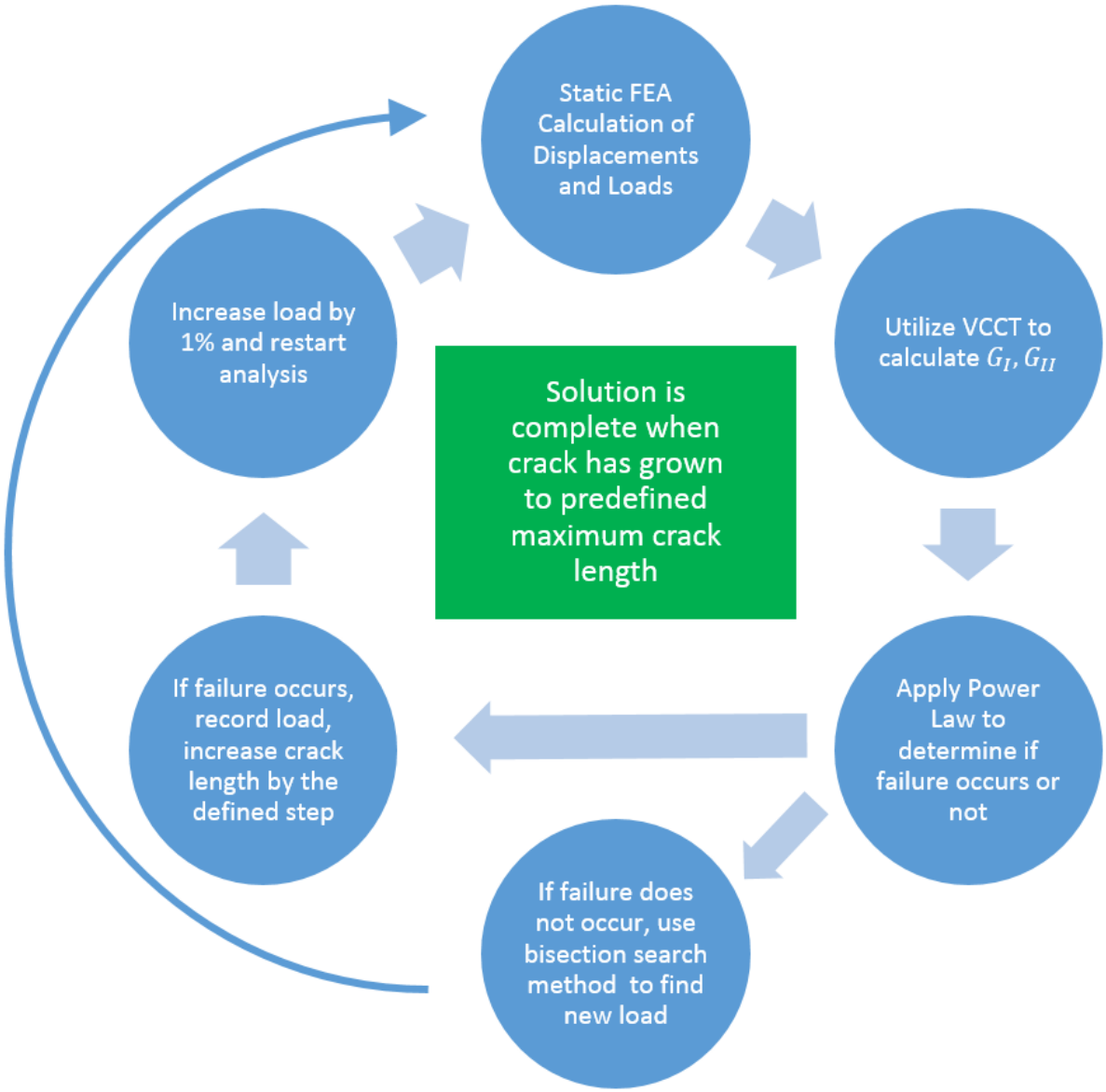

Figure 15: Static Implementation Flow Chart

5.1.i Static development and validation

The first step in creating the Matlab FEA tool was the creation of the static beam/bar/spring model solution. Each plate was discretized into up to four main pieces depending on crack length, the end piece which consisted of the distance between the grips and delamination or first fastener, the between fasteners piece which was of a length equal to the distance between the fasteners, the post fasteners piece which was of length equal to the distance between the crack front and final fastener and the bonded portion, which was the length from the disbond to the end of the model. When the delamination had not reached one or both of the fasteners, all parts past the disbond were merged together, resulting in a simplified model.

Second, the fastener spring stiffnesses were implemented into the model, with if statements checking if the load was sufficient to cause the fastener to engage, should it be a clearance drilled fastener. This "takeup load" was back calculated by scaling the initial loading to the point where the displacement at the hole edge equaled the clearance in the system. If the load was not greater than the takeup load, the fastener was assumed to have not engaged in shear, if the load was greater than the takeup load, the solution was found based on the sum of the displacements from 0 lbs to the takeup load and from the takeup load to the applied load.

In order to verify the implementation of this model, a load was then applied to this and the solution was then compared against Abaqus FEA as well as hand calculations. The displacements and internal forces at varying crack length were matched at different clearance values and loads under static loading.

5.1.ii Implementation of VCCT

After verification of the static implementation of the solution accurately calculated the resultant forces and displacements, the virtual crack closure technique was implemented in the model. In Abaqus FEA, additional "crack tip elements" are applied which calculate the forces and displacements needed for VCCT more readily. However, in the interest of efficiency, additional elements were not applied in this implementation.

Instead, it is possible to calculate the displacements and forces at the crack tip using the existing elements. The displacements in each beam/bar element can be calculated utilizing the known displacement along the length, rotations of the ends and thickness of the beams. The total relative displacement of the upper and lower sections were then calculated a small but finite distance away from the crack tip node. Similarly, the crack tip forces were recovered based on the forces within the beams prior to the crack tip location.

In order to then determine whether or not the crack tip was to propagate, and at what load, the power law was utilized. If the value was equal to $1 \pm tol$ then the crack was allowed to propagate one crack length step and the load was recorded. The tolerance was taken as 1% or 0.01. If the value was less than $1 - tol$ then the crack would not propagate, if the value was greater than $1 + tol$ then the load was too great for the load to be considered the "failure load." In order to find the appropriate value, a bisection method was employed.

These solutions were again compared against the Abaqus FEA solutions of an identical model, providing good agreement, suggesting the modeling methodology was valid.

5.1.iii Implementation of the Paris Law

Shown below in Figure 16, the initial steps of the fatigue implementation follow a similar procedure to the static case, with the caveat that two static calculates are run, at the minimum and maximum loads in order to calculate the value of ΔG

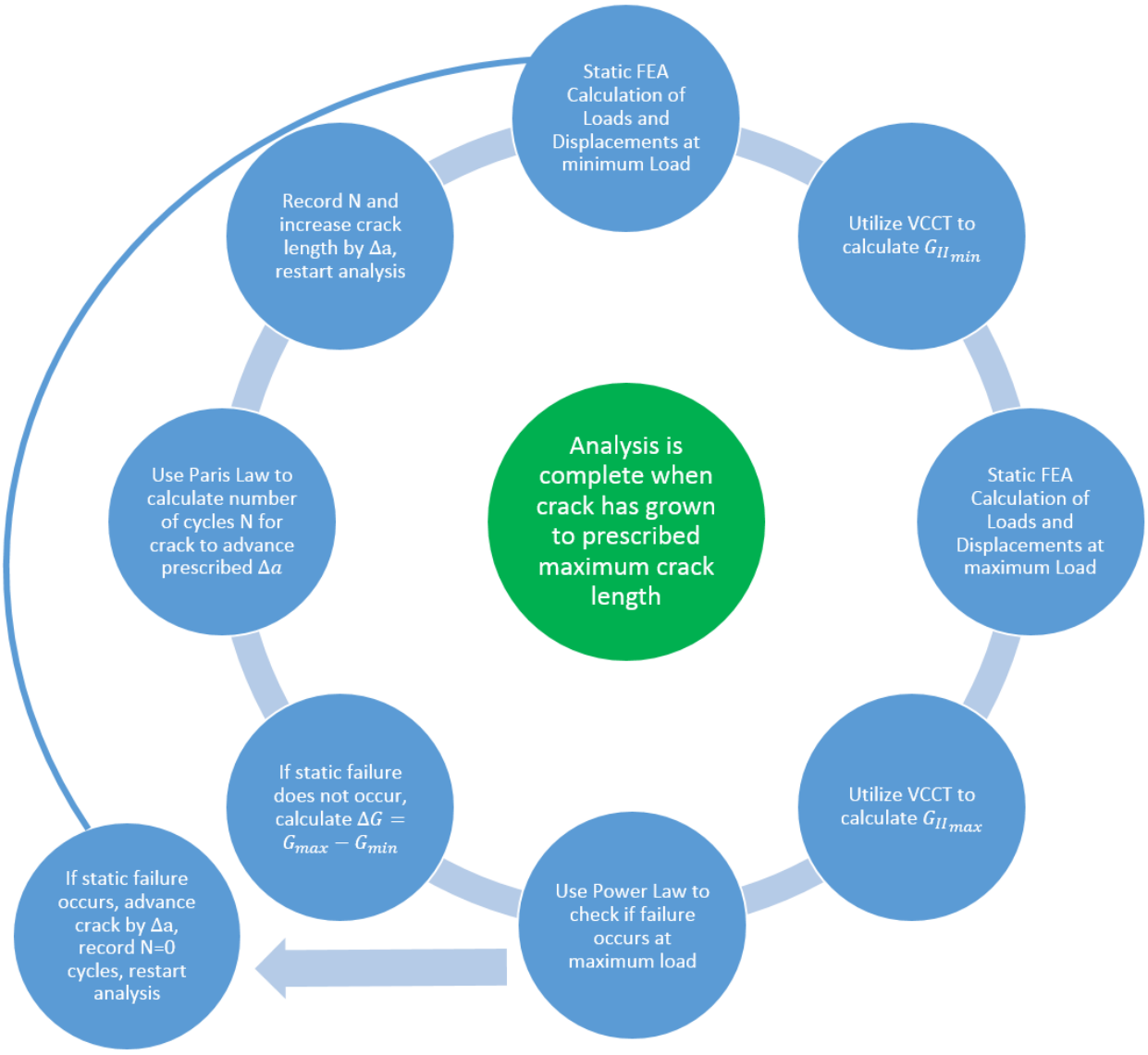

Figure 16: Fatigue Implementation Flow Chart

Once the static finite element model had been validated both through comparison of tests and Abaqus FEA, the fatigue solution was implemented. For each fatigue step, two static load cases were run with VCCT. The first at the maximum load, and the second at the minimum load. This would then provide a value of $G_{max}$and G_{min} which was utilized to calculate $\Delta G = G_{max} - G_{min}$. Using ΔG and the material properties derived through testing of unfastened samples, the value of N for a given crack extension Δa could be calculated as described in Section 2.7

One modification of the static VCCT however was the assumption of crack propagation if the load resulted in a value greater than $1 + tol$. In this case, the crack was assumed to grow one value of Δa (typically taken as 1/100-1/1000th the total length) and the simulation re run. Until the value was less than $1 - tol$, the crack was assumed to have continued growing at 1 cycle. After this, the solution reverted to the above described method for calculating N for the prescribed increase in crack length.

5.1.iv Implementation of the effect of R ratio and compressive loading

The initial implementation of the Paris law did not include the effects of R ratio, which can be accounted for as discussed in Section 2.7 Initial testing was at an R ratio of 0, which from examination can also be seen to have no effect on the solution. For additional testing which included an R ratio that was non-zero, it was necessary to utilize this modified Paris law, and good agreement was found to occur.

However, during testing of an R ratio of less than one, the solution was found to be less accurate. At R=-1, the compressive and tensile maximum loads are equal and opposite. For metallic structures and mode I loading, the crack growth will only occur with tensile loads, compressive

loads serve to close the crack tip. However for mode II loading, the shear growth is independent of direction. As a result, the solution required modification. First, the ΔG was separated into ΔG_{tens} and ΔG_{comp} in order to represent the independence with respect to loading direction, and second R was set to zero.

Calculating ΔG the standard method where R=-1 and $\Delta G = G_{max} - G_{min}$ will give a resultant $\Delta G = 2\Delta G_{comp} = 2\Delta G_{tens}$ with subsequently a much higher crack growth compared to separating each cycle into a compressive and tensile section, where $N_{Total} = N_{tens}(\Delta G_{tens}) + N_{comp}(\Delta G_{comp})$. Using this methodology works well, however for R ratios other than -1, the solution presented here must also account for variable amplitude loading.

5.2 Model Description

The model is based on a one dimensional beam/bar finite element formulation. This solution provides the most rapid results without sacrificing significant accuracy compared to a two dimensional model and avoids the issues of the stress concentration due to the attachment of the fastener spring in shear to a single node.

Subroutines were written to calculate the laminate properties based on CLT as well as the fastener spring parameters based on the fastener and calculated laminate properties. As before, each of the fastener springs is calculated as a constant diameter bar for tension and a using Huth's fastener flexibility for the shear stiffness. Different methods of calculating the laminate stiffness and fastener flexibility formulae can be substituted in via the calculation subroutines, as well as implementation of the fastener flexibility correction factor proposed by Cheung.

The total clearance input into the simulation is the difference between the diameter of the shank of the fastener and the hole. When the fasteners become non-linear springs in order to model this clearance, the problem inherently becomes non-linear, and typical finite element solutions require iteration in order to find the intersection point. However, as the fastener engagement is binary and otherwise linear, it is possible to develop a semi-closed form solution which allows for a more rapid response. An initial run is performed with the fastener assumed to not be engaged in shear, and the displacements calculated. The relative displacement of the upper and lower panels is then compared with the input value of clearance in the system. If the relative displacement is less than the value of clearance, the fastener is assumed to not have been engaged in shear.

Once the relative displacement is greater than the value of clearance, the fastener has become engaged and the load is decomposed into the load prior to engagement and the load after engagement of the fastener. As the simulation is a linear finite element analysis, this can easily be done by using a scale factor to find the load at which the clearance will be exactly taken up. The load can then be separated into the load prior to engagement and after engagement and respective displacements calculated. The final displacement is then the sum of these two displacements.

Another primary driver of arrest is the load transfer through friction. In order to simplify the model, the load transfer through friction is assumed to occur entirely at the point of the fastener location. In reality, the load transfer through friction occurs in a zone underneath the fastener head, with the exact size of said zone dependent on a myriad number of design details including the layup and thickness of the part in question which influences how widely the preload is spread at the bondline. Testing, as described in Chapter 8, indicated that the “effective” coefficient of

friction when using a bolt was approximately 0.35, greater than the value of 0.25 published previously and found during standard testing. This higher value of friction was utilized in the simulations and provided good correlation with experimental work.

In order to minimize the complexity of the simulation, the number of elements was limited to those minimally necessary. In order to avoid generating contact conditions and the associated spring elements to join the members, elements were merged together prior to crack propagation. The model was subdivided into a region in front of the first fastener, between the fasteners, from the second fastener to the crack tip, and from the crack tip to the fixed boundary conditions. This resulted in a maximum of 7 elements for the two fastener system. As the computational cost of the finite element solution is directly related to the number elements, this minimized the cost and thus maximized the speed of the solution.

5.2.i Necessary Inputs

A number of inputs are required for the calculation of the solution are these are detailed below, these values do not require any particular order:

- Lamina properties: each material must have the in plane ($E_1, E_2, G_{12}, \nu_{12}$) properties defined
- Laminate Layups and width
- Fastener Young's Modulus and diameter
- Fastener Pitch
- Fastener Preload
- G_{IIC} and G_{IC}: the critical fracture parameters
- Total length of the beam system
- Initial and maximum crack lengths
- Crack extension length Δa
- Power law exponents
- Tolerance for evaluation of the fracture criterion
- Number of fasteners
- Fastener hole clearance
- C and m for fatigue analysis

- Fatigue threshold

Multiple different cases can be input for each of the above, with the crack length vs load or number of cycles recorded in an indexed array corresponding the various load cases being evaluated

5.2.ii Calculations Performed

Various calculations are performed in the model, briefly detailed below in the order of operations. The calculations must be performed in order as the initial calculations provide the inputs for the subsequent analysis.

- Classical Lamination Theory is used to calculate the beam/bar stiffness values of the laminate
- Huth's Fastener flexibility formula calculation with knockdown factor calculates the spring stiffness values of the fasteners in shear.
- Static FEA analysis using beams and bars
    - Local stiffness matrices are created
    - Merged to create global stiffness matrix
    - Fastener springs inserted at the appropriate nodes
- Virtual Crack Closure Technique is utilized to calculate G_I, G_{II} at the crack tip for the applied loading
- Power law fracture criterion
    - Check to see if $\left(\frac{G_I}{G_{IC}}\right)^{\alpha} + \left(\frac{G_{II}}{G_{IIC}}\right)^{\beta} = 1 \pm tol$ is satisfied
- Bisection search method
    - If the failure criterion was not satisfied, a bisection search method was utilized to either increase or decrease the load, repeating the analysis until the fracture criterion was satisfied
- Calculation of number of cycles from Paris Law
    - As described in 2.7 , the value of N is calculated based on ΔG

5.2.iii Calculating the takeup load with the inclusion of clearance

One of the primary speed benefits of the solution developed here beyond typical finite element models is that the design of the model and order of fastener engagement is known a priori. As a result, it is possible to calculate the load at which the fasteners become engaged in shear when clearance is introduced into the system without being forced to iterate through the solution.

As the finite element model is linear elastic, scaling the loading by a prescribed value will scale the displacements by the same factor. First the displacements are calculated assuming that the fastener has not engaged in shear, and the relative displacement of the fastener holes in the two plates is calculated. If this value is less than the prescribed value of clearance, then the fasteners are assumed to have not engaged in shear. If this value is greater than the value of clearance, then the fasteners are engaged in shear and the load is decomposed into that required to close the clearance and that after which the fasteners have engaged in shear.

5.2.iv Static Delamination Response

In order to then extract the delamination response, it is necessary to determine the strain energy release rates of the system. The virtual crack closure technique was implemented in this solution as it provided a simple implementation and had already been found to yield accurate results from finite element simulations. However, VCCT is mesh sensitive, which does not work well with the extremely large elements generated in the solution as described above. This can be rectified by discretizing the solution in the region of interest to create smaller elements in order to calculate the forces and displacements at a location close to the crack tip.

The finite element model is comprised entirely of beam-bar elements, which assume a constant tensile stress, linear axial displacement, cubic vertical displacement and linear change in rotation

along the length. As a result, knowing the values at both ends of the beam allows for the calculation of the solution at any point within the beam. Consequently, the displacements are calculated a short distance away from the crack tip, taken as $1/1000^{th}$ of the length of the cracked segment as this provided good convergence, and the strain energy release rates are calculated.

Using either the power law or BK law, depending on personal choice, the model is checked to see if the applied load causes delamination. If it is within the tolerance the user selects, the crack is advanced by a user defined amount and the simulation re-run. If the solution is outside the tolerance, the load is either increased or decreased, whether G_{Total} is less or greater than one respectively.

5.2.v Fatigue Response

In order to then propagate cracks in fatigue, the modified Paris law is implemented. VCCT is still utilized to extract the values of G, however, based on the assumptions of mode I elimination, only G_{II} is utilized. There is no existing accepted prediction method of fatigue growth in mixed mode, so the crack is assumed to propagate under purely mode II fatigue. Previous research supports this assumption as simulations and tests have shown that a fastener effectively forces propagation into near pure mode II. The original attempts were made to utilize a modified Paris law, which accounts for a critical value, G_C and a threshold value G_{th}, which represent where the fatigue data departs from the Paris region as well as the R ratio.

For highly loaded fatigue, if the value of G_{IIMax} is greater than the value of G_{IIC}, the crack is assumed to propagate, accomplished by releasing one node and re-running the analysis. This process is repeated until the value of G_{IIMax} is less than the value of G_{IIC}. Additionally, a G_{IICrit} and a ΔG_{th} can be programmed into the model. These allow for the capturing of the low

cycle fatigue and fatigue limits. During testing, it was found that for values of G_{IIC} of 10 lb/in or greater for T800/3900-2 material, the crack propagation occurred at a much greater rate than predicted from the Paris Region. Similarly, for values of ΔG_{II} less than 5 lb/in, the fatigue cracks did not propagate after 1 million cycles; thus for the purposes of this research, this threshold was programmed into the model.

Note that the critical and threshold values are absolutes, not values of ΔG. This was determined experimentally, when G_{IIMax} was less than 5 lb/in, fatigue crack propagation was found to cease up to the number of cycles tested in this research however there was no readily observable threshold of ΔG. Similarly, for high values of G_{IIMax}, taken to be above 10 lb/in for this material system, there was a significant departure from the Paris law and the simulation was modified to account for this. These material properties must be determined experimentally for each specific model, there is no expectation that the relative ratios between the critical and threshold values and G_{IIC} will remain the same.

5.2.vi R Ratio

The R Ratio in this case is calculated as F_{Min}/F_{Max} as this is the R ratio experienced at the crack tip. This value can be a significant departure from the R-Ratio of the load, depending on the conditions. For example, a loading of 12,000:4000 lbs. has a load R ratio of 0.33, however the ratio of loading at the crack tip varies from 0.33 (prior to fastener engagement) to 0.0619 at the minimum. In this example, as well as others, the R ratio of the loading is significantly different from the R ratio of the crack tip loads, largely due to the introduction of the fasteners, and thus careful attention must be paid towards which R ratio is utilized in the calculations. The suggestion is that the R-ratio of the crack tip loads is utilized as it remains independent of

configuration and loading. In addition, if it is desired to utilize the R-Ratio of $\frac{G_{Min}}{G_{Max}}$, this is another viable approach, but will require a different correction factor compared to the solution commonly utilized in homogenous fatigue. The R-ratio relationship during testing, assuming a pure mode decomposition, can be derived from VCCT, among other solutions, with relative ease. The expression for the mode II strain energy release rate is [32]

$$G_{II} = -\frac{1}{2}\,(F_i) * \frac{(u_1 - u_6)}{\Delta \mathrm{a}} \qquad \text{Eq. 2}$$

Where F_i is the force at the crack tip, u_1 and u_6 are the displacements of the nodes ahead of the crack tip and Δa is the distance between the nodes in front and the crack tip. For a pure mode II extension, the displacements and forces are easily related via uniaxial tension, thus for a specimen as described in the unfastened fatigue testing in Chapter 8 as well as previous work by Gray [16], the value of G_{II} is proportional to the square of the crack tip loads as is the relationship between the R ratios.

5.2.vii Compressive vs. Tensile Loading

Under mode II loading, compressive and tensile loading can be treated the same, assuming that buckling does not occur. From the formulation of VCCT, Eq. 2, the result of the multiplication makes the value of G_{II} direction agnostic. This can then be taken advantage of in the programming of the simulation, as compressive loading can be treated identically in all manners except for the direction of deformation. Shown below in Figure 17, if the tension and compressive response of a sample in Mode II were not identical, this would entail an orienting of the lamina such that a 0° and 180° prepreg would need to be analyzed in a different manner.

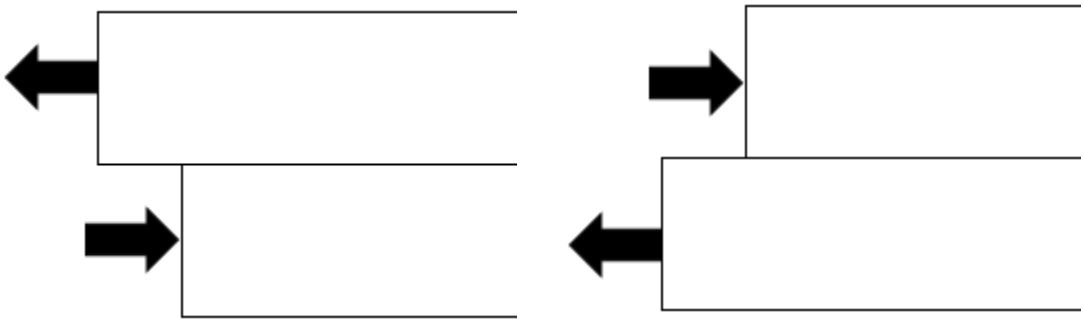

Figure 17: Comparison of stress state in mode II tension vs. compression

For fatigue loading, this remains true as well, however the value of ΔG is not the difference of G_{Max} and G_{Min} when the values have different signs. Instead, research into this situation during the course of this dissertation has indicated that the loading should be separated into two different sub-cycles, the above zero and below zero values. Each cycle which crosses zero can then be treated as two cycles, one $\Delta G = G_{Max}$ and one $\Delta G = |G_{Min}|$. Experimentally, this approach has been validated, with the caveat that it was for cycles such that $|G_{Min}| = G_{Max}$. If these values differ, the analysis becomes a variable amplitude loading analysis, which is beyond the scope of the work here. Furthermore, before using this methodology in certification, further work is required to verify its general applicability in estimating cyclic life.

5.3 Key Results

When comparing the two dimensional finite element model to the one dimensional model, it is found that the one dimensional model tends to be more conservative in the crack growth vs. load curves and tends to show a dramatically more linear trend comparatively. However, the runtimes are incomparable. For a single simulation, the clocktime for the MATLAB model averages 0.4

seconds on a single core while a two dimensional finite element model tends to require 30 minutes of wall time using the same computer operating with 8 cores enabled.

When comparing the one and two dimensional finite element models in Figure 18, the one dimensional model can be seen to be much more linear; considering it is made of bars, beams and springs, this is to be expected. All of these models are linear elastic formulations, while the elements through the thickness of the two dimensional model provide for more flexibility. However, as discussed further in Chapter 6 and Chapter 7, the loss in non-linearity does not negatively affect the simulation's predictions and the experimental work shows good agreement with the simulations.

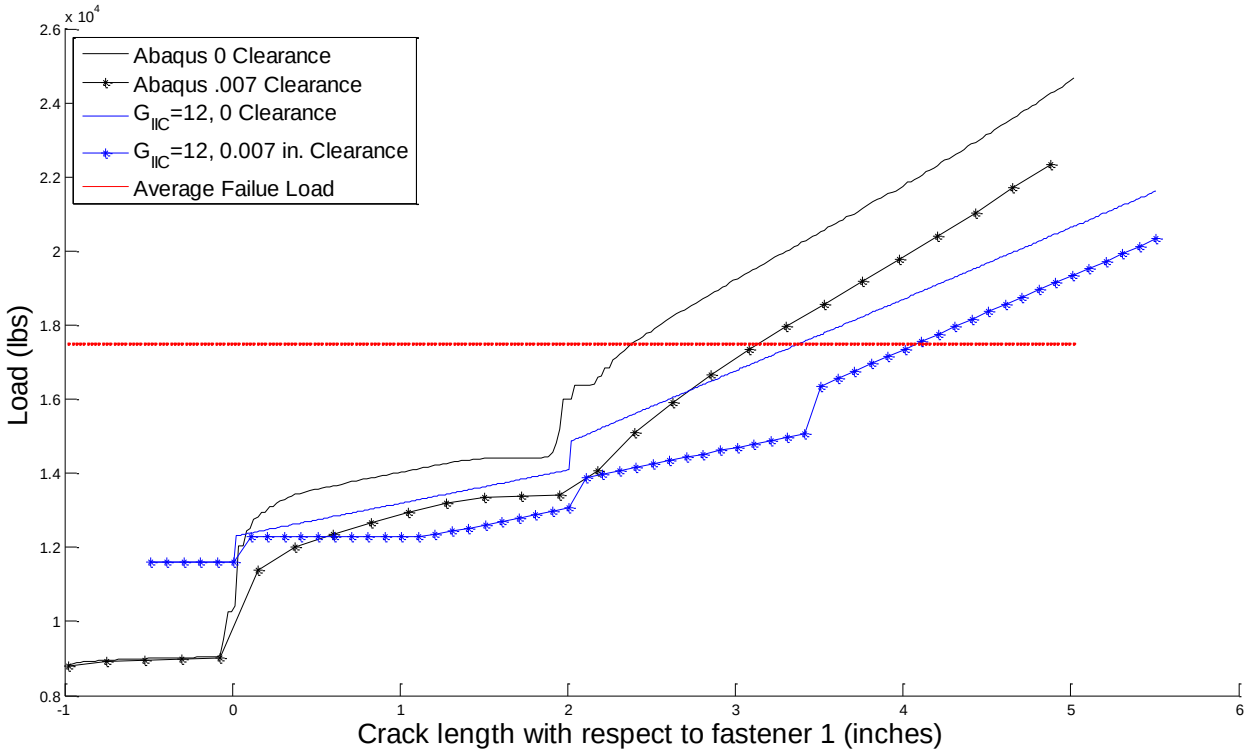

Figure 18: Comparison of one and two dimensional models

An additional item of note is the assumption that the frictional load transfer happens at the moment the crack passes underneath the fastener and the fastener instantaneously becomes 100% effective as soon as it contacts the fastener hole in the one dimensional model. This results in the load spikes, most visible in the clearance simulation. The initial spike in load at 0 inches is the load transfer through friction providing load alleviation at the crack tip. Once this resistance is overcome, the solution is flat as the crack propagates unstably until the fastener shank becomes engaged in shear and resists further propagation. A second spike due to load transfer through friction is visible at the second fastener and a very distinct spike in load is visible as the crack propagates further and the second fastener becomes engaged in shear. Because the fasteners with zero clearance are instantly engaged in shear, these load spikes are subsumed within the increase in load due to frictional load transfer as the crack passes underneath the fastener head.

Various modeling techniques could be employed to reduce this dramatic jump in load at these locations, such as distributing the load transfer through friction across a region equal to the fastener head diameter, and similarly having a non-linear fastener spring which represents a slower engagement of the fastener shank within the hole. However the additional modeling complexity adds computational cost, which is antithetic to the goal of this development.

Further studies using this analytical tool conform to the behaviors found through FEA, one of the most obvious being the change in fastener stiffness, which alters the slope of the curve as shown in Figure 19. Stiffer fasteners offer greater load alleviation at the crack tip and thus permit a higher load without an increase in crack length. Additionally, it can be noted that the second fastener engages later when clearance is included because the stiffer first fastener is providing greater load transfer; taken to the extreme, a single infinitely stiff fastener results in no additional fasteners.

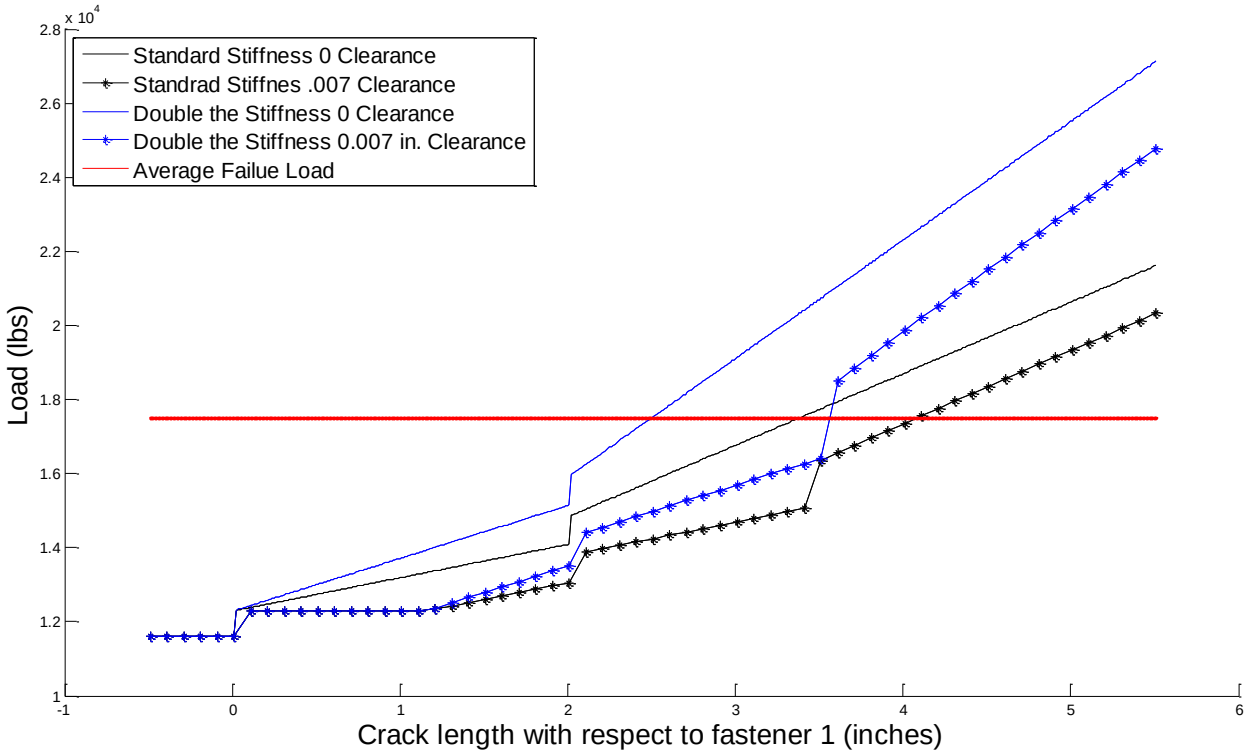

Figure 19: Comparison of varying fastener stiffnesses

Meanwhile, when simulating fatigue, the arrest tool shows the expected responses, zero clearance fasteners provide better delamination arrest, as pictured below in Figure 20. Significantly greater crack growth is experienced for samples where clearance is introduced, and this is exacerbated for cases, such as those shown below, where the minimum load is zero or negative because this means the fastener is disengaged for a portion of the loading spectrum, providing zero load alleviation. Reducing the clearance by one half reduces the maximum crack growth significantly, providing better arrest capability for the same fastener. While using zero clearance fasteners tends to become economically unfeasible due to the difficulty in installing these transition fit features, controlling the clearance as tightly as possible provides the next best arrest capability.

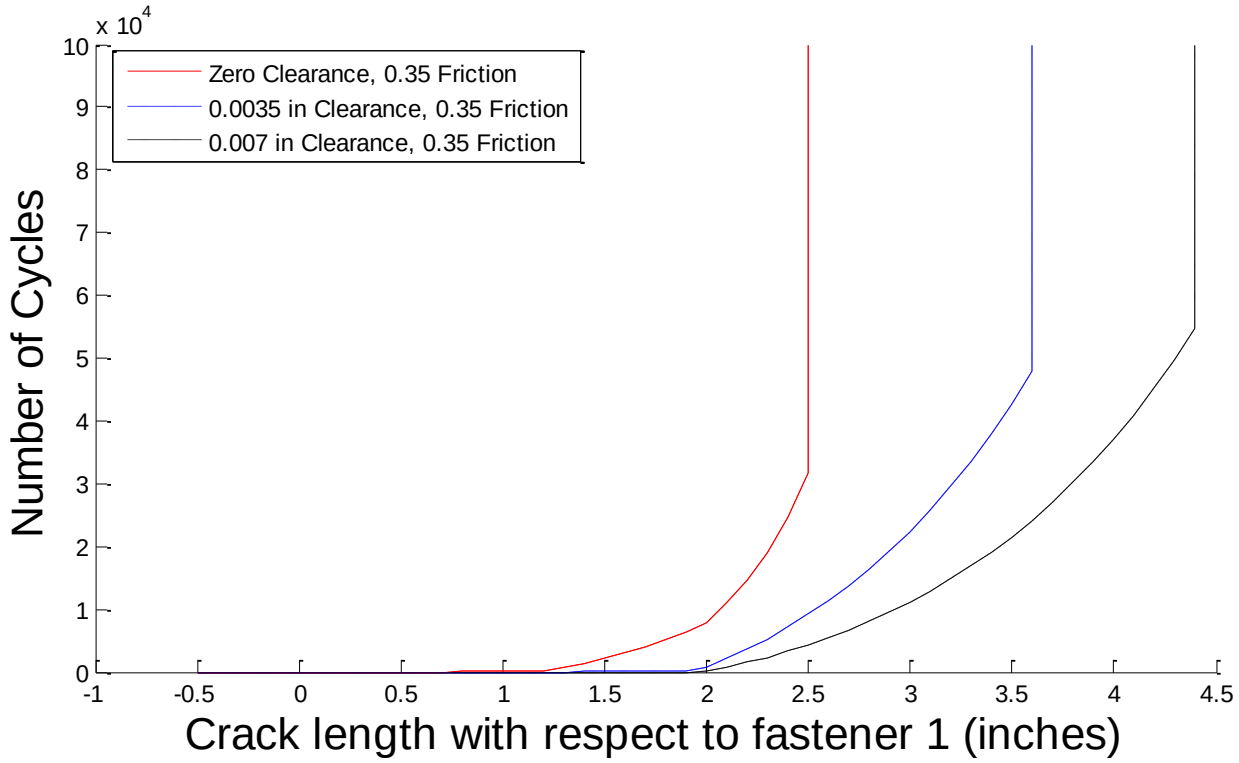

Figure 20: Comparison of Clearance in Fatigue, Cyclic Load 0:12,000 lbs.

While under static loading the load transfer through friction provides a non-negligible benefit in arrest capability, as visible in Figure 19, the benefit is more distinct in fatigue testing, particularly when the loading is relatively low and nearly all of the load transfer can occur through friction. Comparing Figure 21 with Figure 22, the difference between the assumption of zero friction and a coefficient of friction of 0.35, which was the measured value in testing, is much more dramatic. While the second fastener arrests the crack growth rather effectively when there is load transfer through friction, with friction not accounted for, the crack growth extends well past the fastener and continues to grow for a significantly larger number of cycles.

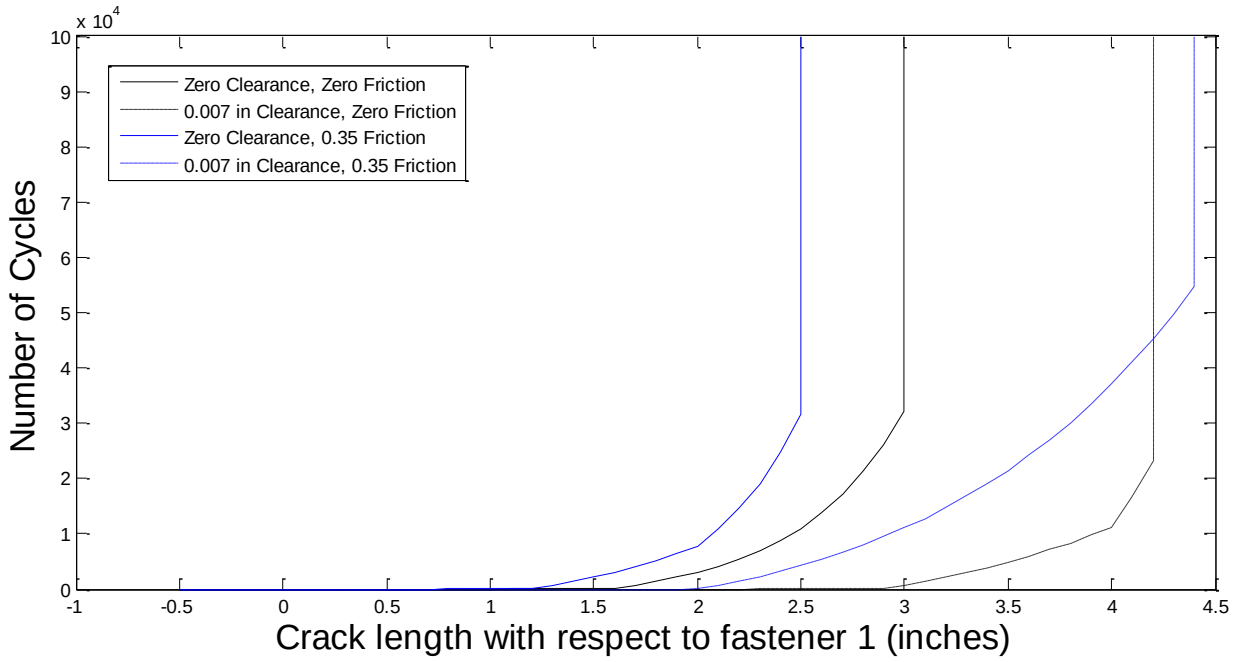

Figure 21: Comparison of zero and realistic coefficient of friction, cyclic loading 0:12, 000 lbs.

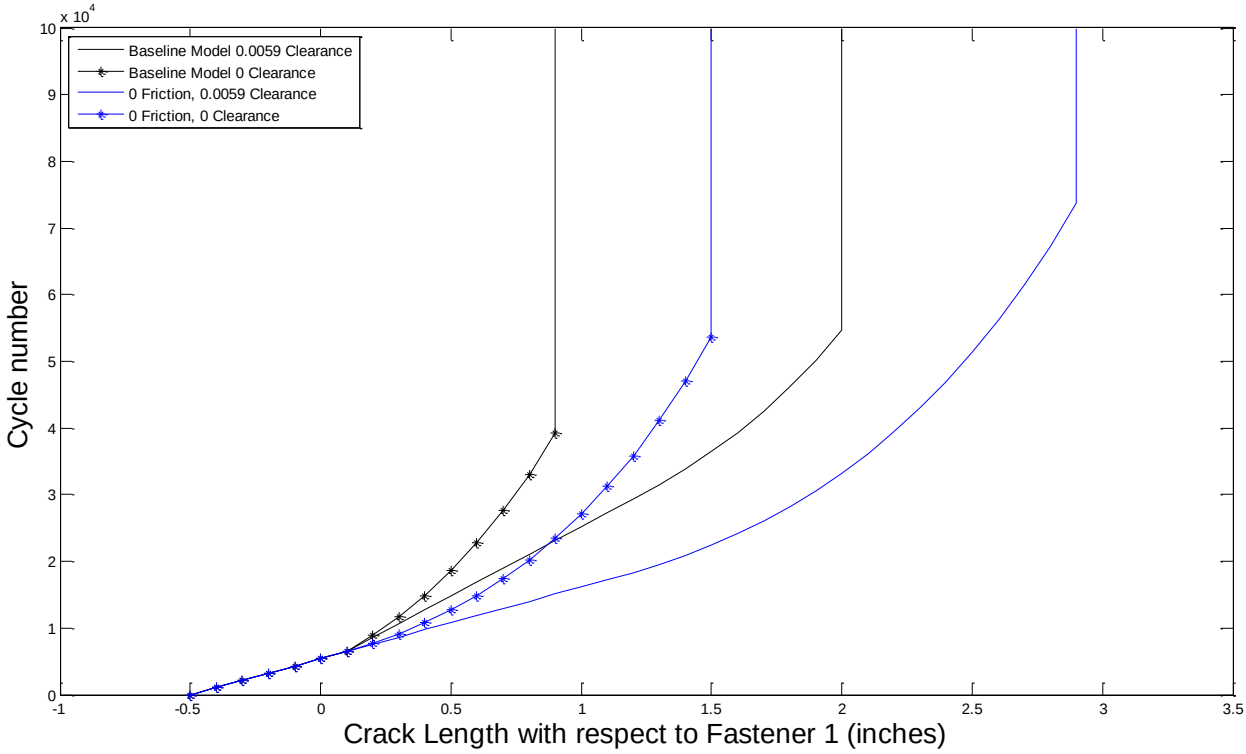

Figure 22: Comparison of zero and realistic coefficient of friction, cyclic loading 0:8,000 lbs.

The results of this analysis, in conjunction with the FEA analysis described in Chapter 3, subsequently guided the testing in static and fatigue testing. Previous work by Cheung et. al [2][16][12] had established that fastener preload played a role in propagation and speculated that clearance would reduce the capability. In the analytical studies presented in this research, fastener spacing, fastener preload/load transfer through friction, and clearance control were assumed to be the primary drivers of arrest capability, while understanding the fatigue threshold and critical values would aid in accurately gauging the fatigue delamination arrest capability of the system.

5.3.i Sensitivity of Varying Parameters

As will be discussed further in Chapter 11, the sensitivity of the model varies with respect to different input parameters, of particular note are C and m, the fatigue threshold, the fastener load transfer through friction, and the fastener stiffness. The values of C and m can be utilized to control the shape of the curve, the greater the value of C or m or a combination of both, the more horizontal the curve will be, leading to a greater crack growth for an equivalent number of cycles. Meanwhile the fatigue threshold, defined as a set ΔG will determine the length at arrest. With no fatigue threshold, the crack will continue to grow as the value of ΔG approaches zero, however this is not what we found in the experimental testing. As a result, a fatigue threshold, found experimentally, was implemented. The greater the value of ΔG_{thresh}, the shorter the crack length at arrest. Finally, the load transfer through friction and fastener flexibility both influence the total length of the crack at arrest as well as the growth vs cycle number. Greater load transfer through either method provides improved crack tip stress alleviation and thus a lower ΔG and slower crack tip growth rate.

Chapter 6 Quasi Static Delamination Arrest Testing

In order to validate the current modeling and understand the delamination arrest process for multiple fasteners, tests were conducted using quasi-static load conditions. Based on the modeling discussed in previous chapters, as well as a key assumption that strip modeling is applicable, it was decided to perform experimental work to test two fastener specimens with a two inch and three inch spacing as well as specimens which were double the width and contained a 2x2 fastener array.

6.1 Test Description

Testing was performed using Instron machines, both an 8801 servo-hydraulic machine as well as a 5585H screw driven machine. Mechanical grips were utilized in the 5585H machine while hydraulic grips were utilized for the 8801 machine which allowed for compression loading. Testing consisted of displacement as well as load controlled methods.

Initial testing was displacement controlled, with a displacement rate of 0.004 inches per minute. This slow displacement rate was utilized so that the crack growth could be recorded, higher displacement rates led to rapid crack growth which could not be captured quickly enough. Tests were typically conducted until sample failure, either through net section failure, typically at the first fastener hole, or if the delamination propagated the entire length of the sample.

The second method of quasi-static testing was load controlled. The loading was stepped by 500lbs. until the crack began to propagate and then stepped by 250 lbs. Each load step was held for 5 seconds to allow the crack growth to occur and/or stabilize, and the crack length at the applicable load was recorded. Using both methods subsequently allowed for comparisons to be

drawn to evaluate if the testing method played a role in the measured arrest effectiveness. When examining the data, no detectable difference was found in the propagation behavior, and thus in the work presented here, the testing method is not delineated in the results.

Crack tip tracking was done visually as this was the most robust method. The sides of the sample were painted white in order to provide contrast for the crack tip. Low cost, high gloss paint tended to provide the best results as it provided a relatively thin coat which did not obscure the crack tip and higher gloss provided more contrast compared to matte paint. Side lighting was also employed to highlight the crack tip. Comparing experimental results with predictions and C-Scans indicated that this method was highly reliable as good result to prediction agreement was observed.

For quasi-static testing, a scale was marked on the side of the sample with a mark spacing of 0.1 inches, with 0 inches at the first fastener location. The markings allowed crack length measurements to an accuracy of approximately 0.05 inches, with estimation of the crack length to be between marks. Unstable crack growth frequently occurred during testing frequently. The load at which the crack stopped growing was the load which was recorded along with the final length of the crack. When plotting the experimental data, this leads to near flat portions of the load displacement curve where the crack growth was too rapid to accurately record data as it extended.

Attempts were made to calculate the crack length using a potential drop or through changes in conductivity of metallic paint applied to the edge of the sample. However, these did not provide results consistently in agreement with the visual tracking and thus were not pursued further.

In order to test samples in compression, an anti-buckling fixture was utilized consisting of rollers which supported the sample and constrained it's out of plane displacement. Rollers were chosen as this minimized the influence of friction between the fixture and the sample. Should simpler supports be utilized, it was suspected that there would be undue influence on the results. A total of 5 rollers were utilized with a semi uneven spacing in order to accommodate the installation of the fasteners. A schematic with the spacing is shown below in Figure 23.

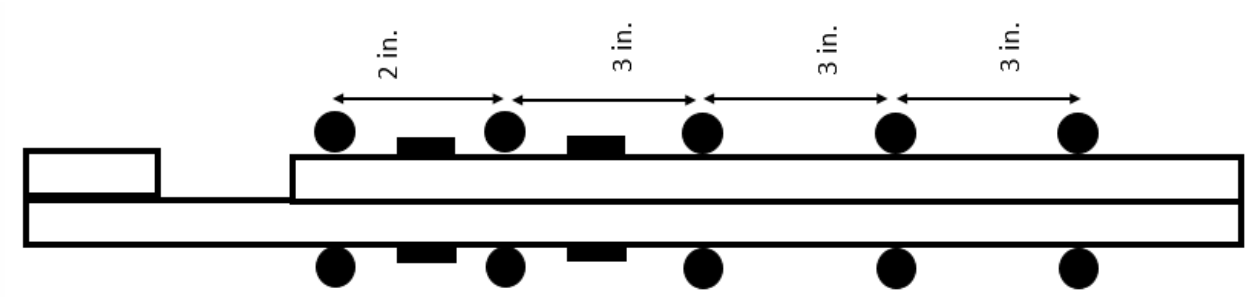

Figure 23: Anti buckling fixture schematic

6.2 Sample Description

Shown in Figure 25 are the sample dimensions. The sample length of 17 inches was chosen both for ease of manufacture as well as sufficient sample length so that crack propagation could occur; a 17 inch sample also allows for 100% utilization of a 12 inch prepreg roll in the assembly of samples. Donated T800/3900-2 Toray prepreg was utilized for the primary samples, as well as various other materials which were available and discussed previously. The standard width of 1.25 inches was chosen to be 5 fastener diameters while the nominal thickness of 0.36 was calculated from the nominal ply thickness. The average manufactured laminate thickness was thinner at 0.31 ± 0.02 inches.

Initial test sample lamina were entirely manually cut, which led to issues with alignment of the 45 degree plies. However, any relative inaccuracy did not appear to dramatically affect the response of the laminate. Subsequent samples were cut using an Autometrix Advantage fabric cutter, which, in particular improved the accuracy of the angle on the $\pm$45 degree plies. These laminates were still manually laid up for curing.

In order to generate the pre-cracked samples, two plates were laid up together, with a length of 17 inches, one plate was subsequently cut into two pieces of 2 and 15 inches in length respectively in order to insert the crack tip and also co-cure a tab so that bending was not applied to the sample as it was gripped in the test machine. A Teflon film was inserted in order to provide an initial crack length of approximately 0.25 inches. The two plates were subsequently combined and cured in a hot press. Initial samples were manufactured without a pre-cured insert at the crack tip which resulted in a significant bow in the plies at the junction between the termination of the plate and the portion which was to be gripped. The curved plies, combined with the eccentric loading, served to create additional delaminations which propagated to the first fastener prior to their arrestment. Subsequent samples had a pre-cured insert placed within the laminate in order to better control this and a comparison of this is shown in Figure 24. Those with the precured insert and less ply curvature around the initial crack tip tended to have fewer additional delaminations.

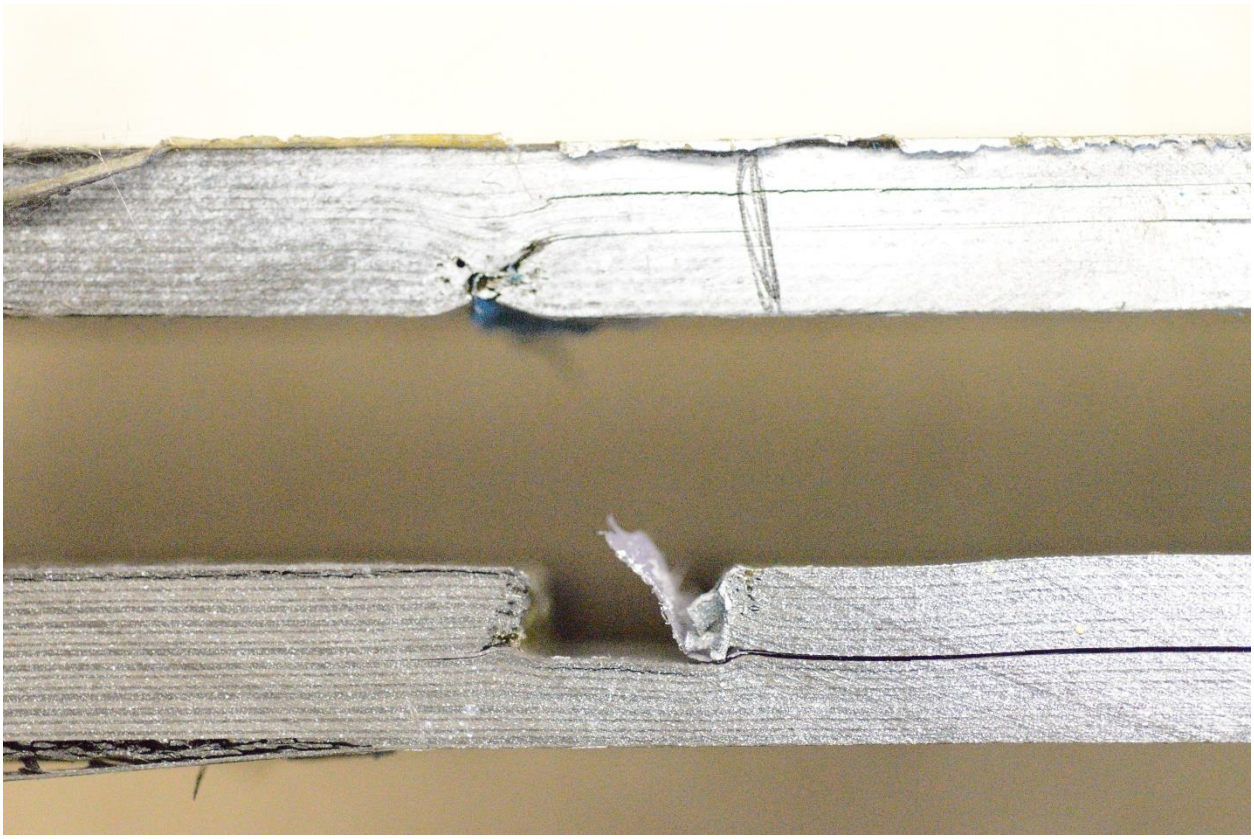

Figure 24: Comparison of samples with (below, insert removed) and without insert (above) to control initial crack tip shape.

The cure cycle consisted of a single stage cure, ramping at a rate of approximately 5°F/minute, a soak time of 2 hours and a cool down rate of approximately 15°F/minute. Programming of the machine does not specify the ramping rate directly, instead the final temperature and time to reach this temperature are specified. The linear ramp rate is then calculated by the machine based on the initial platen temperature. Due to the limitations of the machine, it was also not possible to reduce the cool down rate, the Wabash 50 Ton platen press controller simply pumps cooling water through the platens at a fixed rate, leading to the very fast cool down rate. This rapid cooling did not appear to negatively affect the final laminate based on visual inspections. Each sample was cut using a continuous rim diamond wet saw, allowing for cutting of the samples

with minimal heating. A wet saw was chosen over a waterjet both due to ease of access, as well as improved consistency in the alignment of the cuts with respect to the 0 degree fiber direction. With 0 plies consistently being the exterior ply, it is possible to align the direction of cut very accurately. However, this is only applicable for straight cuts, a waterjet would offer greater flexibility for cutting irregularly shaped designs. Samples were lightly sanded by hand to remove potential splinters along the edge in order to improve their handling characteristics and then painted white along the edges to improve crack visibility.

In addition to the T800/3900-2 material, other materials, specifically M46J and BMS 9-17 as noted in 4.1 which were graciously donated by various groups were utilized to provide a survey of results from additional material systems. These unfortunately did not necessarily have published material data, and no testing was done in the scope of this research beyond measuring the laminate stiffness. Additionally, due to the inability to find published cure cycles, the same T800/3900-2 cycle was utilized, which may have been a cause of the lowered fracture toughness of the M46J material as noted at the end of this chapter.

The primary layup utilized for testing was a quasi-isotropic, symmetric laminate, $((0/45/90/-45)_{3S}/Crack)_S$. This layup was chosen as each sublaminate was balanced and symmetric so that residual thermal stresses would not alter the delamination response. After testing, each sublaminate was found to have remained flat, supporting this assumption. The second laminate tested was a 50% zero $((0/45/0/-45/90/0)_{2S}/Crack)_S$ which represented a significantly harder laminate which could also reasonably be assumed to have fasteners installed within it. Stiffer laminates were not tested as highly directional laminates cannot be expected to support fasteners without splitting failures.

The crack interface plies were consistently chosen as 0 degree plies because they provided the lowest and most consistent delamination resistance by avoiding ply bridging as the laminate was tested. The delamination was found to preferentially jump to a 0 degree interface within the laminate during the delamination so by having the crack interface plies by 0 degrees, the crack was effectively constrained to the midplane. Initially, laminates utilized a small offset angle between the two interface plies. However testing using more precisely aligned 0 degree plies did not change the delamination response or result in fiber bridging.

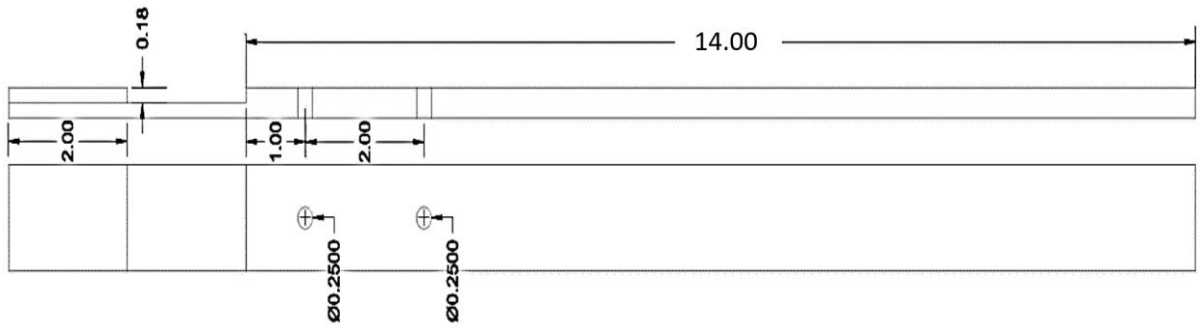

Figure 25: Experimental Sample schematic

Holes were drilled in the samples using carbide tipped drills of varying diameter. Zero clearance drilled holes were made using a ¼ inch E drill which was ground down 0.0005 inches less than the average diameter of the fastener using a lathe and sharpening stone in order to provide the most accurate transition fit fasteners. Other samples were drilled using F (0.257" diameter) and 6.5 mm carbide drills which were purchased and not modified. Samples were clamped with an aluminum backing plate into a milling machine and the drill centered over the sample. Holes were drilled utilizing a pecking motion and vacuum removal of the dust in order to help minimize the heating. Coolant was not utilized as the relatively low number of samples fabricated at any one time prevented overheating of the drill bits. Drills were resharpened using a

commercial “Drill Doctor” machine whenever the drilling resistance increased noticeably or punchout was observed, on average every 10 samples or 20 holes. Holes were measured after drilling and any aberrant samples were either reworked to a larger diameter hole or removed from testing.

Strain gages were installed on certain samples to measure the stiffness and response of the sample. Not all experiments were strain gaged; identical samples were assumed to have a similar strain response as their macroscopic delamination propagation and load/displacement response was similar. The strain gages utilized were MicroMeasurements EA-06-125AC-350 strain gages, both fully encapsulated as well as exposed. Each gage was wired individually in a quarter bridge and the strain response was captured using a Vishay System 5000 system or a MicroMeasurements Model D4 data acquisition system, depending on the application and test frame utilized. A representative sample is shown in Figure 26

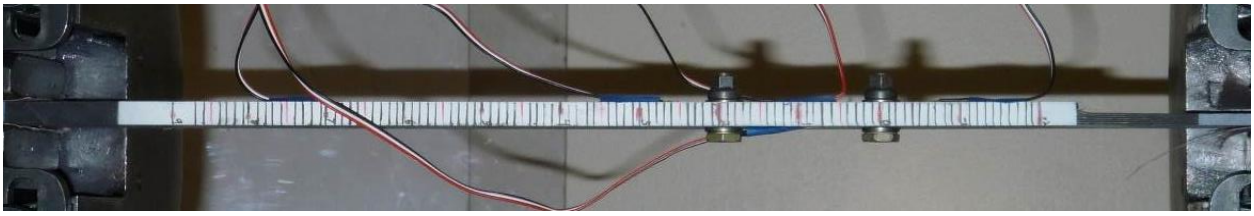

Figure 26: Sample in tensile test machine

During testing, the fasteners were installed to a specified torque of 40-in lbs. using a click type torque wrench. This was approximately ½ of the typical installation torque of the ¼ inch titanium fasteners when new in order to account for the viscoelastic stress relaxation which occurs for a laminate in service over an extended period of time. Previous work tested other fastener installation torques [2] and found a correlation between torque and arrest capability, which can be attributed to higher torques contributing more load transfer through friction. After testing, the

fastener installation torque was again checked in order to verify that the fasteners had not loosened for any reason and the values were found to have remained consistent for each test.

6.3 Quasi Static Testing Results

One of the immediately obvious results is that mode I remains eliminated during testing, identical to the one fastener model results. Additional tests using much smaller fasteners, such as 6-32 fasteners which are approximately ½ the diameter of the standard 0.25 inch fastener, also showed mode I elimination. This can be checked visually in images such as shown in Figure 27 where the crack has propagated entirely through the frame yet no visible separation is observed. This held true in compression as well, provided that the specimen did not buckle.

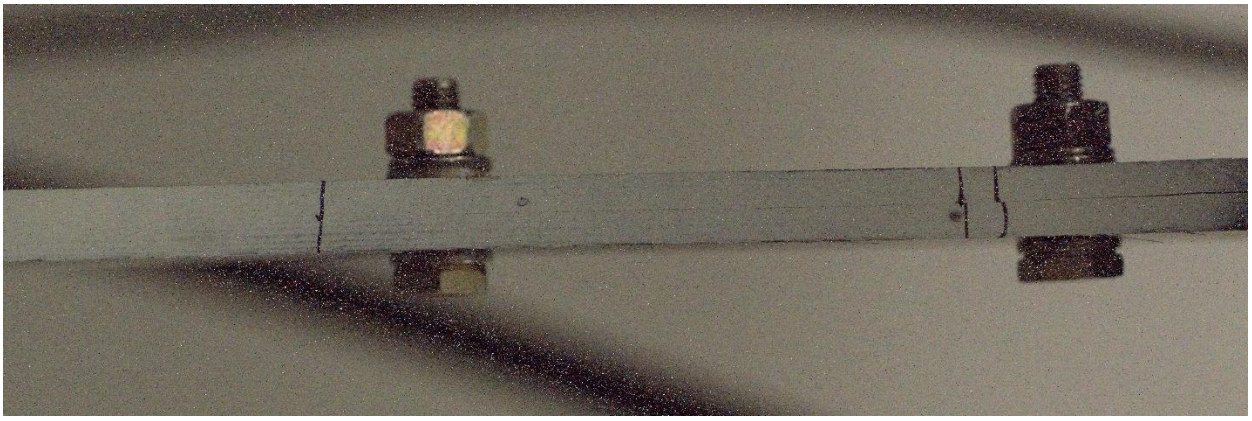

Figure 27: Image of crack during growth from right to left

Secondly, shear engagement of the fastener was visible after testing by examining the fasteners after removal. Prior to installation, the fastener shanks were clean, which allowed for examination after installation that showed black markings on the shank indicating it had come into strong contact with the carbon fiber hole walls. A comparison of a clean and a marked fastener are shown in Figure 28.

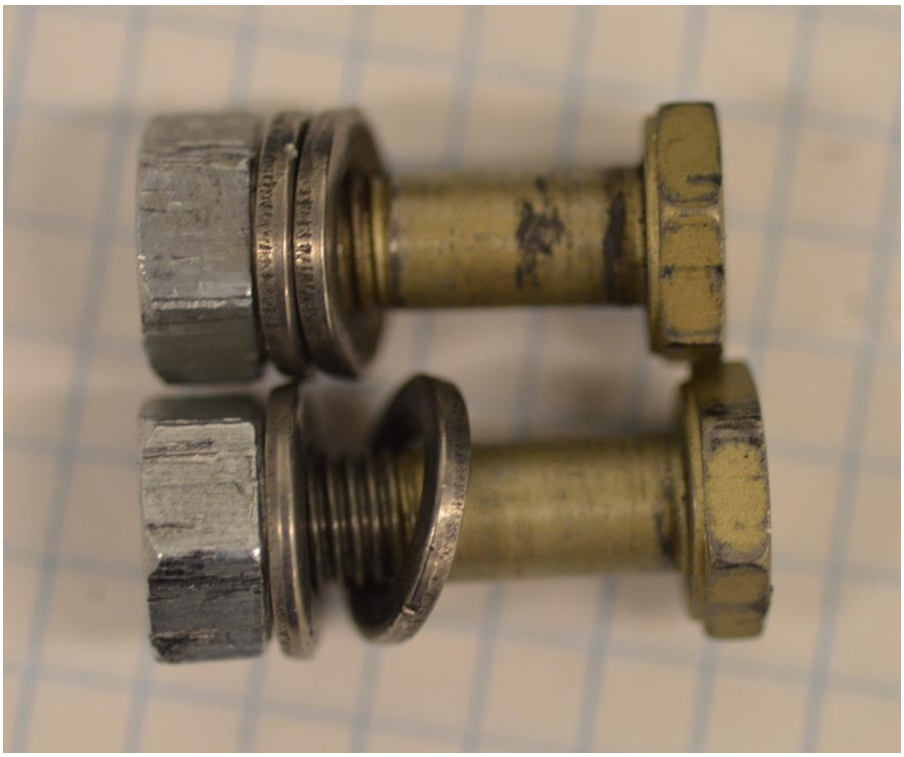

Figure 28: Comparison of fastener shank before (below) and after (above) testing.

Meanwhile, for clearance drilled holes, if the test was stopped partway through the loading cycle, or should the hole have sufficient clearance, the fasteners would remain unmarked when removed from the sample. This supports the assumption that the fastener does not engage in shear immediately when clearance is introduced to the system, and only once the crack has propagated a sufficient distance past the fastener will it engage in shear.

However, as seen in Figure 29, the fastener still provides some arrest as the crack has passed the fastener, but prior to the theorized fastener engagement point in shear. This is due to load transfer through friction, which is controlled by the installation torque of the fastener.

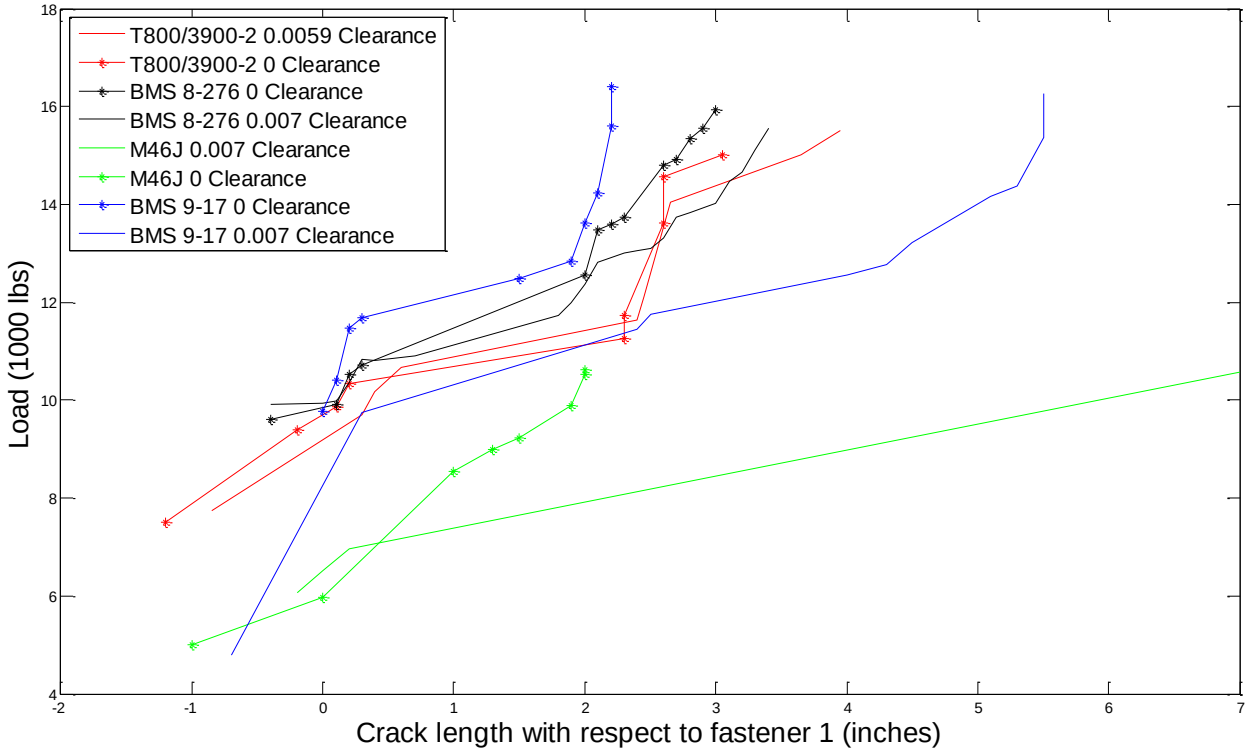

Figure 29: Test results Quasi-Isotropic Laminates

Additionally, visible in Figure 29 is that the arrest capability of the two fastener system is greater than that of the single fastener system, however the curves only diverge to a significant degree once the crack has reached the second fastener. For loading that does not cause propagation to the second fastener, the behavior is identical, as the second fastener does not provide any arrest benefit prior to the crack reaching it.

6.3.i Effects of Clearance

Clearance in the fastener hole has been found to be one of the primary drivers of arrest effectiveness in quasi-static testing. When comparing the test results, shown in Figure 30 of otherwise identical arrest specimens with and without clearance in the fastener hole, it becomes clear that a loss in delamination resistance occurs. Greater values of clearance will reduce the

capability further, and lesser values of clearance, which provide a tighter fastener to hole fit will reduce the loss due to more rapid engagement of the fastener shank in shear.

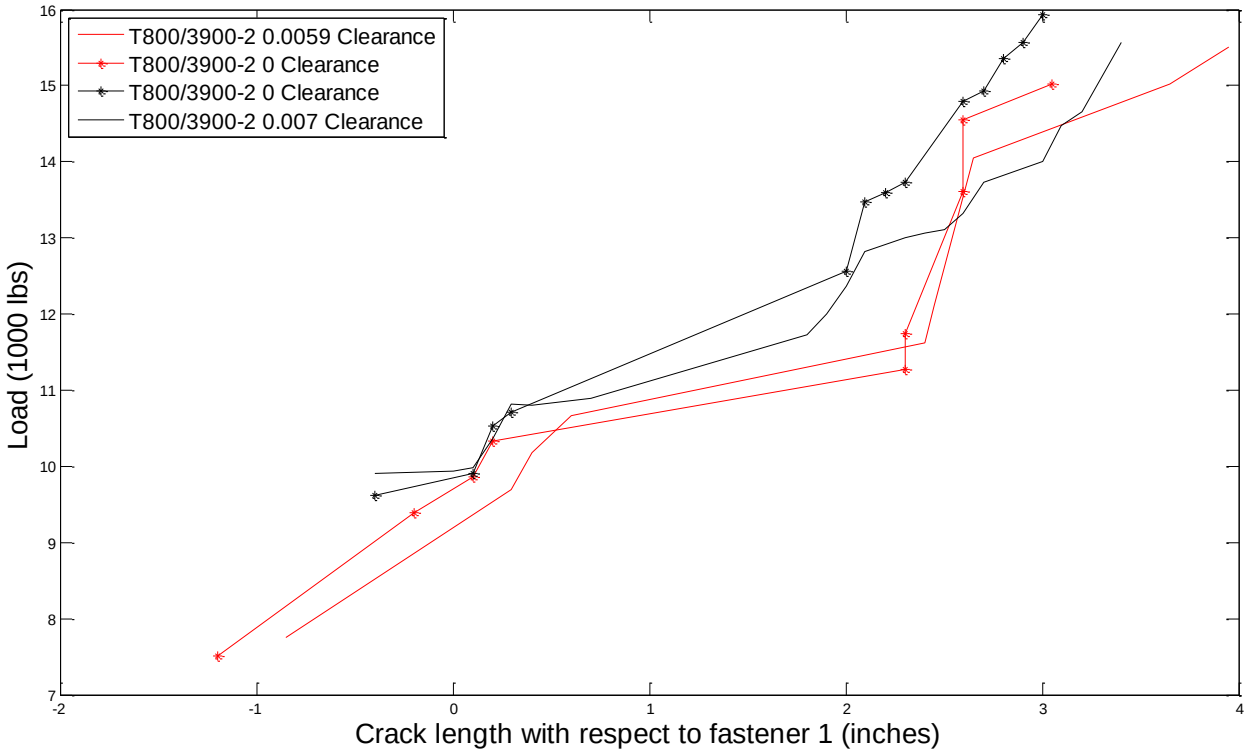

Figure 30: Test results Quasi-Isotropic Laminates

6.3.ii Crack Curvature

As visible in Figure 31, scans of the sample show a curved crack front near the fastener and a relatively flat crack front outside the area directly adjacent to the fastener. This indicates that the fastener is providing load alleviation at the crack tip as the crack propagates past the fastener, with the V shaped crack front focused with the point touching the fastener. However, once the load is increased sufficiently, the crack departs from the fastener zone and flattens out again, as the load distribution across the crack front becomes more even.

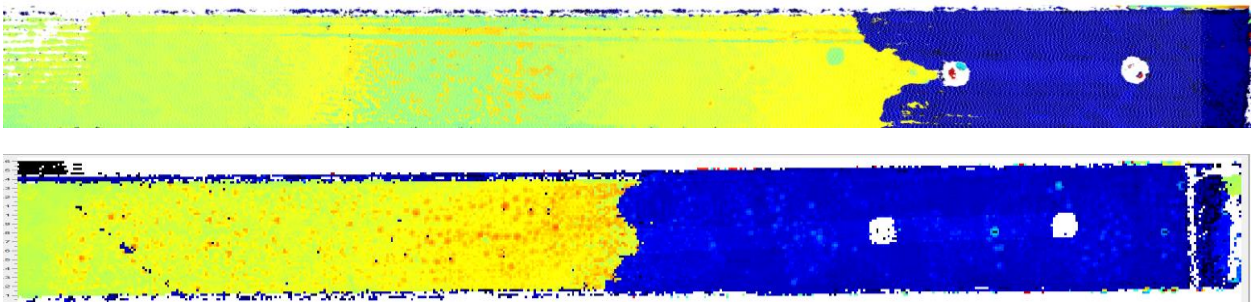

Figure 31: C-Scans during crack progression

6.4 Specimens of Double Width

One of the key assumptions that this work is built upon is the assumption that strip modeling applies to this system. Strip modeling, shown in Figure 32 is such that taking a representative strip of the fastener array and simulating this will provide an accurate representation. The strip is taken to be equal to the fastener pitch, centered about a fastener, and this assumption has been well vetted for regular repeating fastener arrays in metallic structures. However, as discussed immediately prior, in the delaminating case there is crack curvature which is irregular around the fasteners which could possibly invalidate this strip modeling assumption.

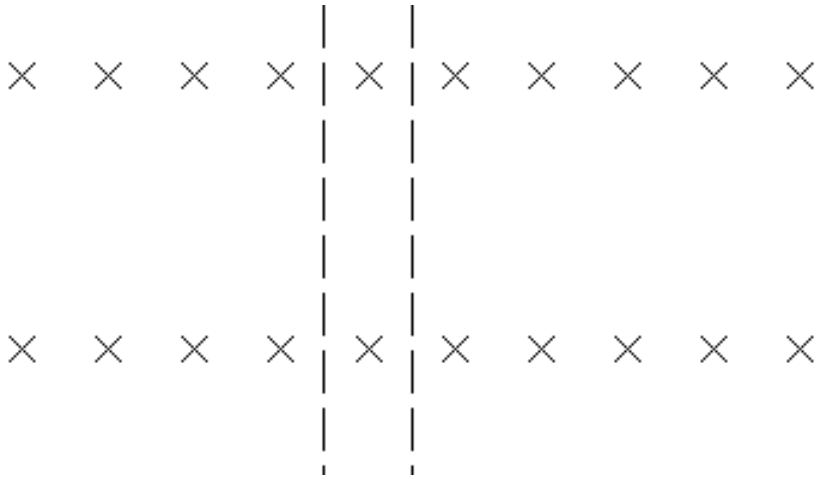

Figure 32: Strip Modeling, one strip highlighted

As a result, specimens were tested which were double the width, and had a 2x2 fastener array installed. This was the maximum size which could be tested utilizing the machines available, and conditions along the centerline of the sample were assumed to accurately simulate the conditions experienced within a large repeating array of delamination arrest fasteners. Shown below in Figure 33 are the normalized load vs. crack growth curves in comparison with standard, single width specimens. The load is normalized to the standard 1.25 inch width, which consists of dividing the measured load by 2.

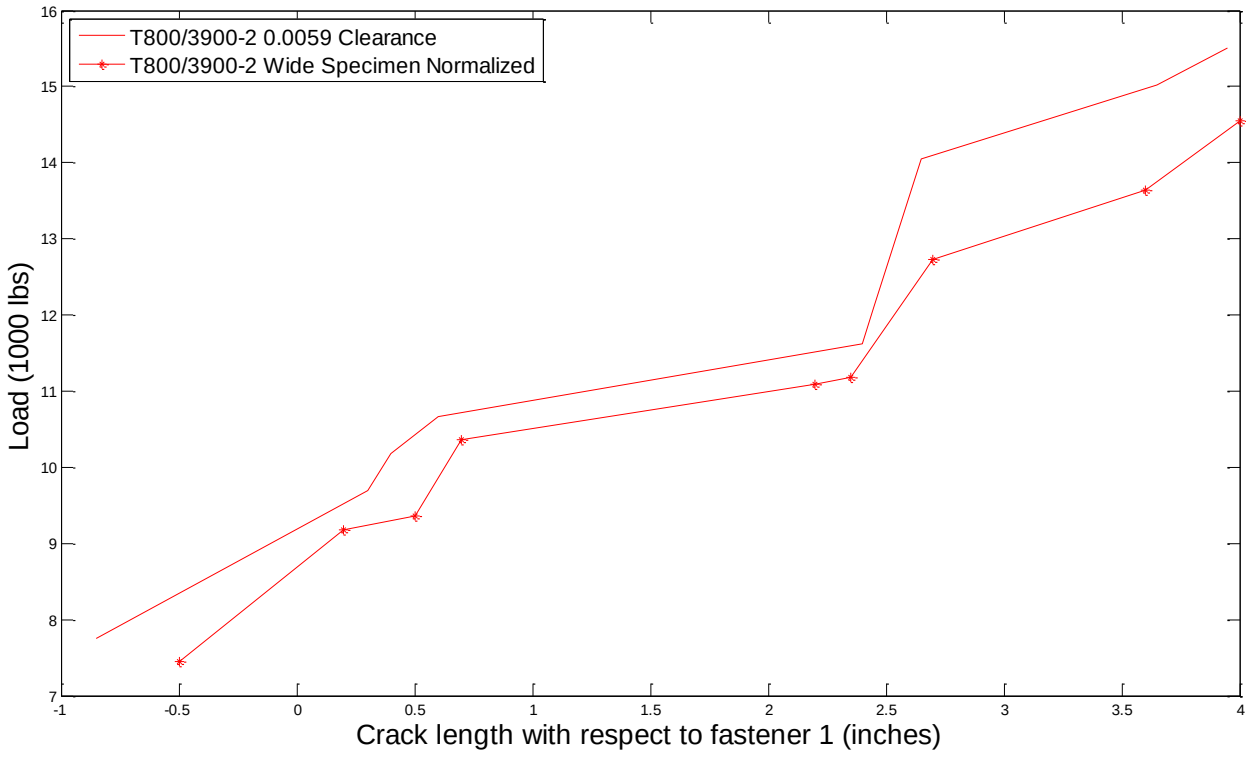

Figure 33: Normalized large specimen load vs. propagation curves

Additionally, C-scans were conducted to evaluate the shape of the crack front within the sample. As shown below in Figure 34, the shape of the crack front around each fastener is highly similar to that of the single fastener wide sample. Down the centerline of the sample, the twin curved

crack fronts do not appear to be interacting to any significant degree, giving confidence to the application of the strip model assumption.

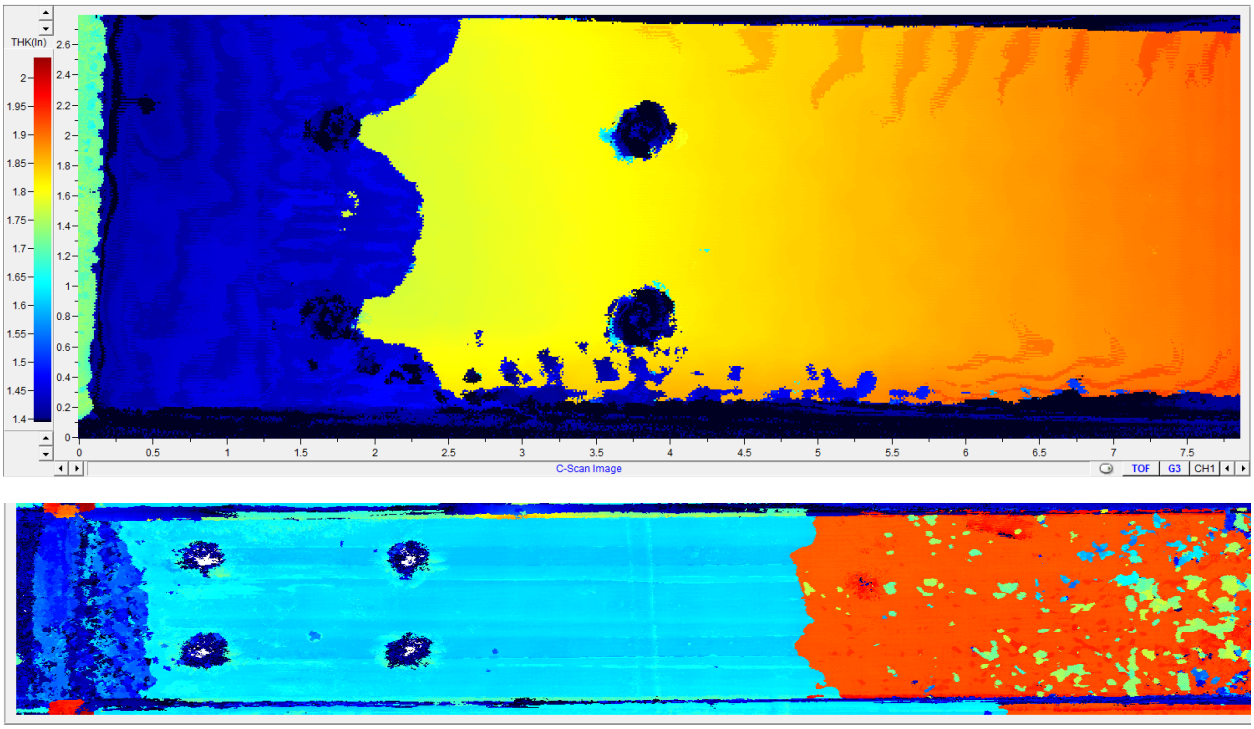

Figure 34: C-Scan of 2x2 fastener array (blue is disbanded)

6.5 Increasing the Fastener Spacing

As mentioned, fasteners only become effective once the crack has reached or passed the fastener itself, prior to this point, the fasteners confer no benefit. As discussed in Chapter 4, simulations showed that increasing the fastener pitch yielded greater crack growth but did not change the general behavior of the multi fastener arrest system. Regardless of the position along the length of the sample, the first fastener always eliminated mode I while the second fastener provided additional arrest capability through load transfer in shear and friction once the delamination had propagated to this fastener. Testing of this was then conducted using a fastener spacing of 3 inches, with the results shown in Figure 35.

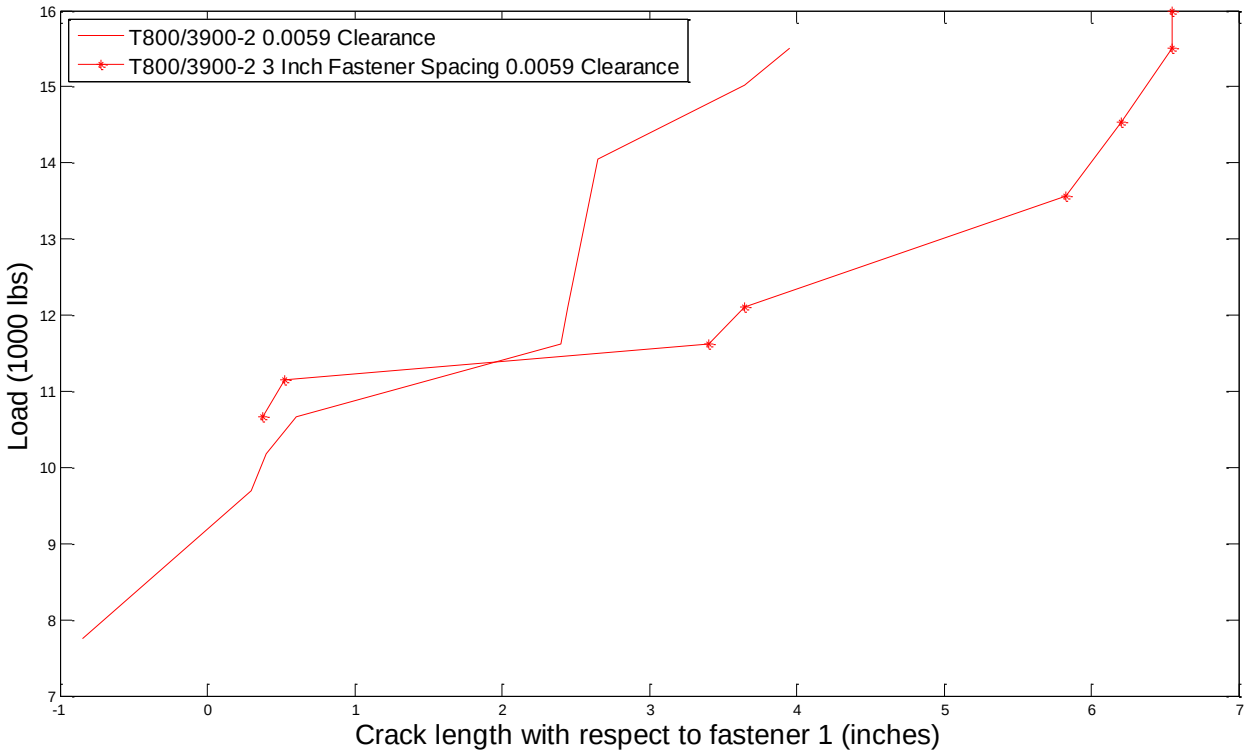

Figure 35: Three vs. two inch fastener spacing

As seen above, the behavior of the two and three inch fastener spacing samples is largely the same, but the crack growth is greater for the sample with the larger fastener spacing. As the fastener cannot provide load alleviation until the delamination has reached it, for the three inch fastener case, the crack can propagate 50% further before the second fastener contributes. However, using a larger fastener spacing saves weight by reducing the number of fasteners utilized.

Similarly, adding a third fastener in series will improve the arrest effectiveness. Each fastener after the first one provides load alleviation through shear engagement and frictional load transfer, so as more fasteners become engaged, there is more resistance to further crack growth. However, when examining the results shown in this chapter, it is important to note that more than two

fasteners may be weight inefficient as the crack will not grow to sufficient length to engage all of the installed arrest features.

6.6 50% zero laminate

In conjunction with the quasi-isotropic laminate being tested, a stiffer laminate, consisting of a 50% zero $((0/45/0/-45/90/0)_{2S}/Crack)_S$ layup was tested using the same procedure described earlier in the chapter. This configuration allowed for the evaluation of the simulation techniques applied to a different laminate configuration, which results in a different laminate stiffness and fastener flexibility. The test data is shown below in Figure 36 with the inclusion of representative quasi-isotropic samples using the same two values of clearance.

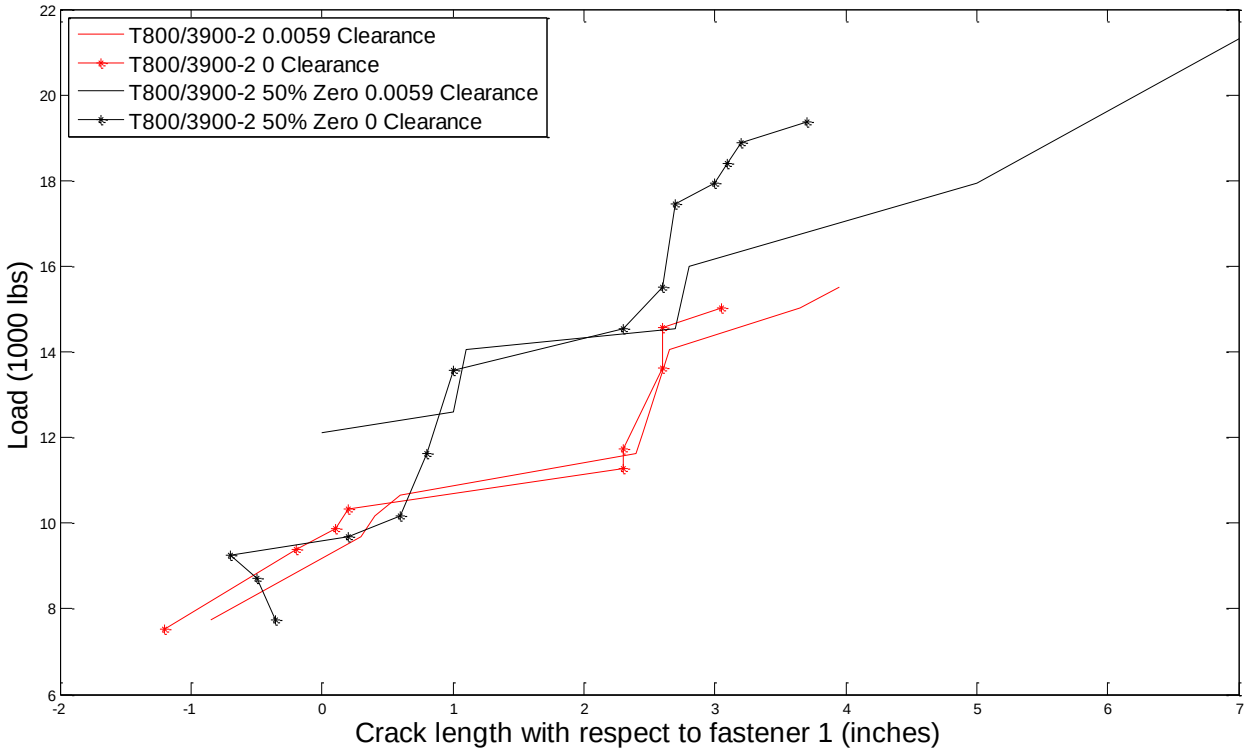

Figure 36: 50% Zero vs. Quasi Isotropic Laminates

As shown in Figure 36, to initiate crack growth, the load is higher due to the greater stiffness of the 50% zero laminate which leads to the fastener conferring less relative benefit, especially when clearance is involved. The takeup of clearance depends on relative displacement of the two laminates, while the crack propagation in this case depends on the relative force and displacement between the two laminates. As the 50% zero laminate is stiffer, there is less displacement for a given force and as a result the same value of clearance requires more loading to close and for the fastener to engage into shear. Consequently, the crack is able to propagate further beyond the fasteners.

Additionally, the load transfer through friction of each fastener remains the same, regardless of the laminate type, provided the interface remains the same, and as the 50% zero sample supports about 40% more tensile loading, the load transfer through friction contributes a smaller percentage towards the arrest.

However, this is not to say that delamination arrest features are not effective for stiffer laminates; the fasteners still provide mode I elimination as well as load alleviation, but are more sensitive to the installation parameters.

6.7 Compression Loading

The results of compression loading showed good agreement with those in tension, as expected. However, the compression results typically showed slightly higher loads for similar crack tip growth, as shown below in Figure 37. This result is theorized to be due to the clamping force of the anti-buckling fixture tending to increase the load transfer through friction artificially. However, as the behavior showed largely the same trends, it is assumed that prior to buckling, compressive and tensile loading does not affect the crack arrest features differently.

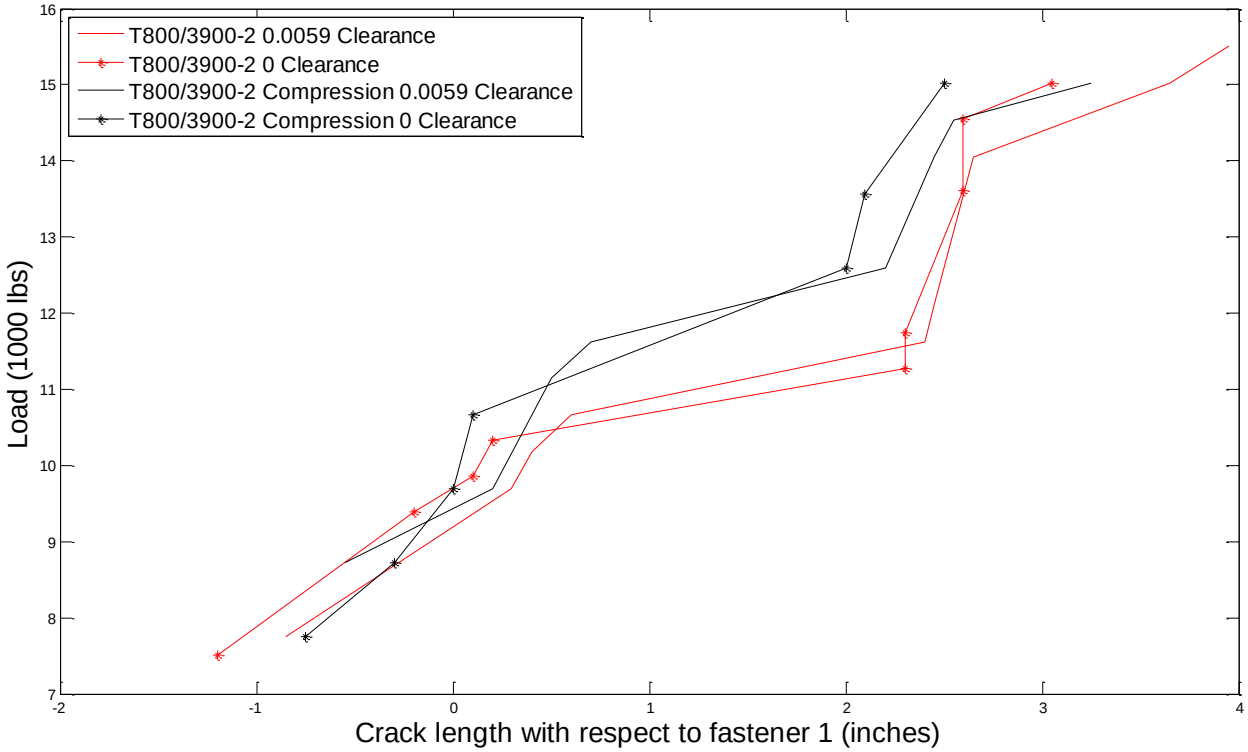

Figure 37: Compression vs. tension testing, Quasi-Isotropic laminates

Additionally, it can be noted that the compression tests were not taken to the same level of loading as the tensile specimens, but were stopped at approximately 15.5 kips. The tests were terminated when the specimen was observed to buckle within the fixture. The decision to use rollers and less than 100% support of the specimen was a tradeoff in stability vs. minimizing the influence of the fixture on the results. Increased clamping of the sample to further reduce buckling would have skewed the results to a greater degree by further increasing the load transfer through friction.

6.8 Failure Modes

The most common failure was filled hole tension at the first fastener, both for 50% zero and quasi-isotropic laminates, as pictured in Figure 38. The stress concentration provided by the hole

resulted in a consistent failure load of the laminates in tension during testing. In spite of the laminate damage, there is minimal visible damage to the cylindrical shape of the hole noted after testing. Although the fastener has shown engagement in the hole, and the laminate can be seen to have been marked by the washers, the holes do not show elongation or damage with the largest change in hole diameter measured as less than 0.0005 inches at the first fastener hole.

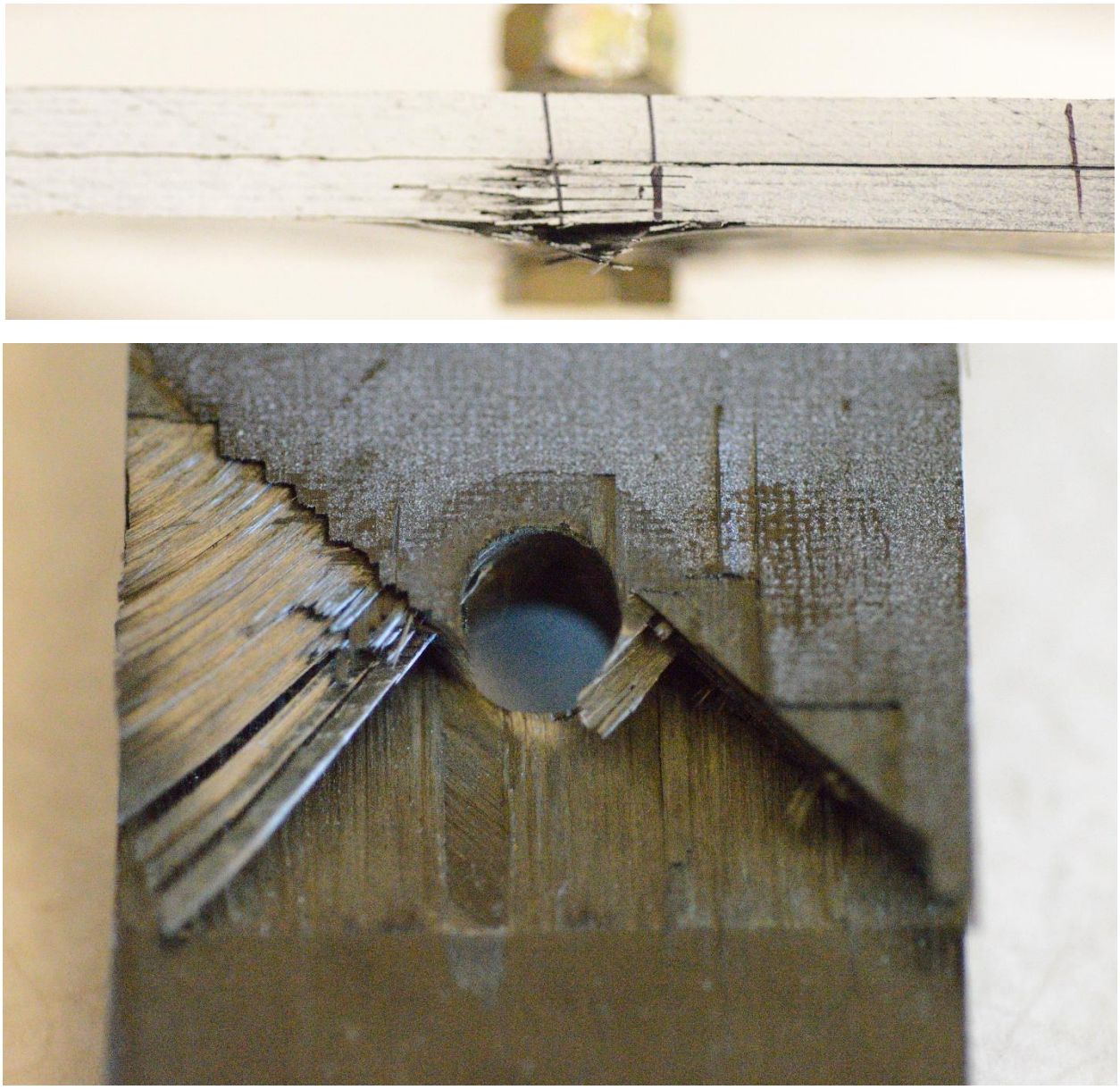

Figure 38: Failure of the laminate, side and top view

Certain samples failed closer to the grips during tensile testing, and this indicated manufacturing defects. One of the primary reasons was that initial samples which attempted to use an insert to control the ply waviness near the crack implantation point used too thick of an insert, damaging the plies at this point. The most effective insert was a segment of a previous delaminated sample as this matched the exact manufactured thickness of the sample.

The final two failure modes were complete delamination of the sample and buckling or crushing in compression. Samples which had very large values of clearance (not shown) or a low value of G_{IIC} such as the material labeled M46J suffered delaminations which propagated across the entire sample. These tests were then terminated once the delamination had approached the lower grip as no further crack growth could occur. Meanwhile in compression, the samples were terminated once buckling or crushing of the sample was observed. Crushing typically initiated at the unsupported notch which allowed for the relative compressive displacement of the two sublaminates, while buckling would occur between the support rollers at high loading.

Chapter 7 Fatigue Delamination Arrest Testing

7.1 Motivation for Fatigue Testing

After the success of quasi-static testing, and the indication that clearance drilled fasteners experience a significant loss in arrest capability, fatigue testing was initiated to measure how effective these fasteners would be under cyclic loading. Under static loading, the fastener shank does not immediately engage in shear and provide arrest. During fatigue loading, if the load level is sufficiently low, it is distinctly possible that the fastener shank would not engage in shear and thus only provide arrest capability through the frictional load transfer.

7.2 Specimen and Test Description

The specimen configurations were identical to those described previously in Chapter 6, with the standard two fastener configuration retained. Testing only consisted of quasi-isotropic and 50% zero laminates with a 2 inch fastener spacing due to constraints. Further configurations were studied analytically and discussed in Chapter 9.

The nuts utilized were elliptically offset stop nuts as these allowed for removal and re-use after each test as compared to Hi-Loks. A second jam nut was installed on the fastener shank as well to minimize the chances of a loss in fastener torque. While found to be largely unnecessary, the second nut was retained during testing. While the nuts and washers were removed, inspected and reused from test to test unless found to be damaged, the fasteners themselves were not reused during the fatigue testing.

These fasteners were not used for multiple tests due to failures of the fastener heads and shanks in fatigue occurring during initial tests when the fasteners were recycled. The eccentric load path

through the laminate causes a minor amount of bending which tends to load the fastener head and shank in bending. As shown below in Figure 39, the direction of bending and fatigue failure can be deduced from the shape of the failed portion, the direction of laminate loading is up/down in the picture.

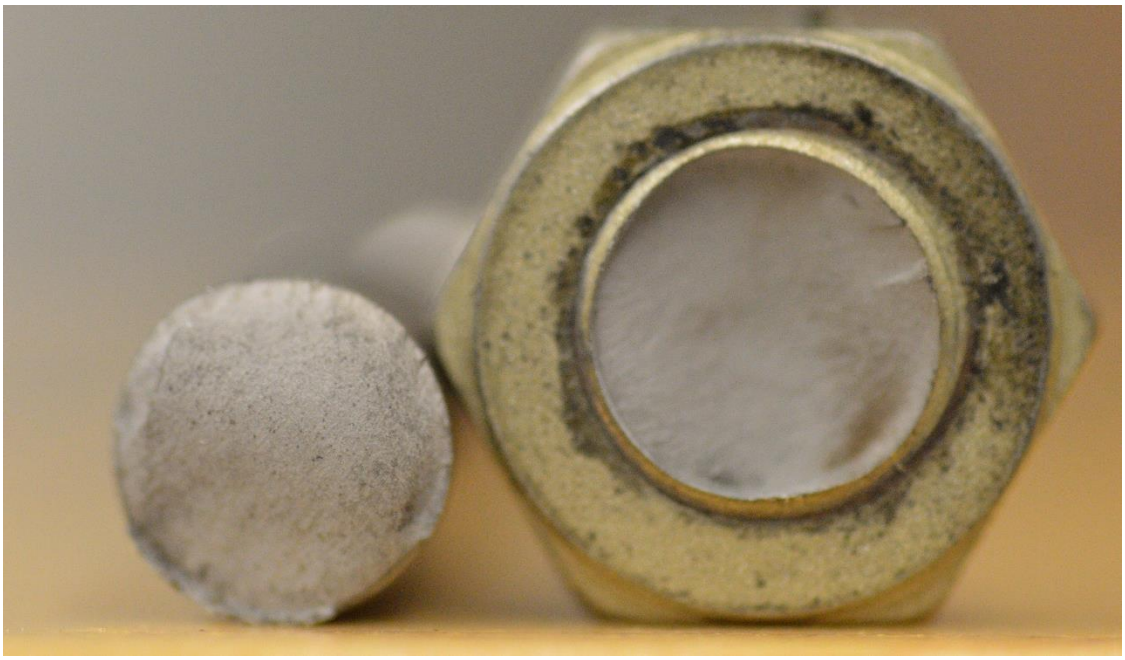

Figure 39: Fatigue failed fastener

The testing frequency averaged 5-10 hz. For samples with greater crack propagation or higher values of loading, the frequency was decreased. This is because the frictional heating was incrased as the area of the sliding contact surface increased. Higher frequencies, while achievable by the testing machine, generated significant heating of the sample and possible changes to the physical response. The highest recorded temperature on a sample whose data was retained was 105°F, the highest recorded temperature on a sample whose data was not retained was 155°F.

All samples were tested using an Instron 8801 servo hydraulic machine with custom fabricated grips to ensure minimal slippage of the samples. The grips were fabricated from heat treated 1018 steel. A pattern was designed to embed within the sample and was cut into the jaws of the grips as shown in Figure 40. The grip pattern is extremely aggressive in order to eliminate slippage of the sample during testing, which was initially a problem using stock grips. This aggressive pattern left a very distinct imprint in the sample however failure was not initiated due to the clamping. Initial quasi-static test samples using these grips continued to fail in filled hole tension failure at the first fastener hole and no visible delaminations were found to be propagating from the gripped area.

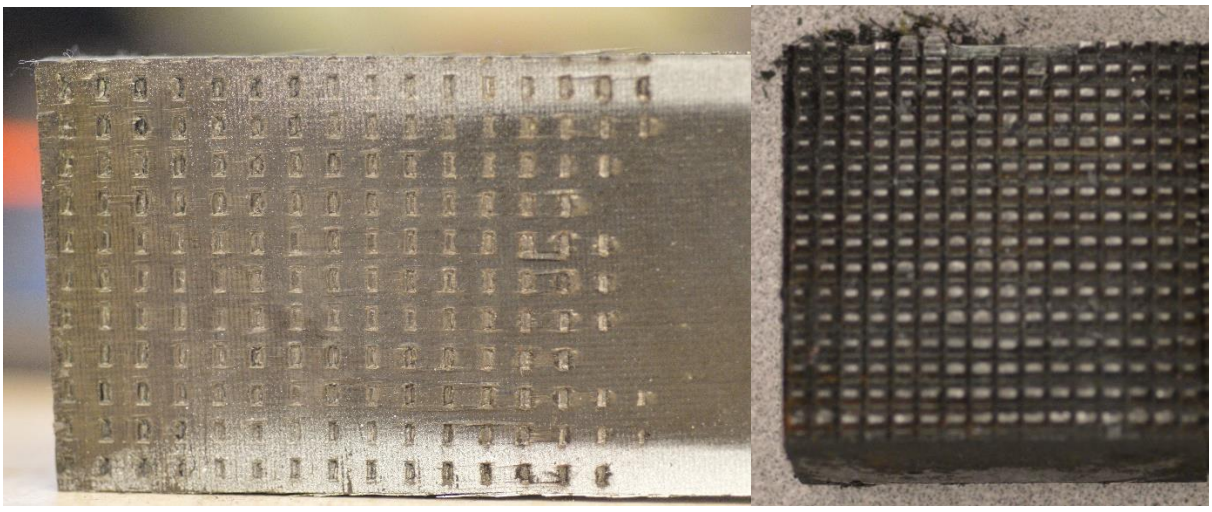

Figure 40: Grips utilized and imprint left on sample

Crack tip tracking was again performed manually, however instead of marking a scale on the sample itself, at predefined cycle intervals. The cyclic loading was briefly paused and the crack tip location was marked on the sample using a felt tipped pen. Because the crack tip remained static during these marking intervals, this solution was feasible for the fatigue loading while not for displacement controlled quasi-static loading.

Fatigue cycling was determined to be load controlled and at constant amplitude. Further work can be conducted for displacement controlled as well as variable amplitude loading but this is outside the scope of the research being presented here.

The initial two loading levels that were chosen were 8,000 lbs. and 12,000 lbs. with an R Ratio of 0. These values were chosen as approximately 50% and 75% of the failure load, with 8,000 lbs. also representing the approximate load at which the crack began to propagate in typical samples. R-Ratio testing was conducted using samples with loadings of 2,000:10,000, 4,000:12,000 and 4,000:8,000 lbs. The first two kept a consistent amplitude of 8,000 lbs. while varying the ratio of the loading, the final test condition used the same maximum load as the R=0 case, but instead with R=0.5. As discussed in Chapter 5, the actual R ratio around the crack tip varied due to the influence of the arrest features, but for classifying the different tests, the R ratio of the loading is used.

Tension-Compression and Compression only testing was also conducted only with an R-Ratio of 0 and -1, because the results were similar to those achieved using tension testing, further testing in compression was decided against due to the relative difficulty of performing compression tests.

Tests were conducted to 250,000 cycles after the final growth of the crack, or failure of the sample in delamination or tension. No sample failed in a mode outside of these three, with the most common result being arrest due to a lack of further crack growth. The sample was cycled and the crack growth recorded. If the sample survived an additional 250,000 cycles after the final crack extension, the delamination was assumed to be arrested for that loading condition. If instead the crack propagated through the length of the sample, the sample was assumed to have

failed in delamination. Finally, certain samples, when tested at high maximum loads, fatigued and failed in filled hole tension failure.

7.3 Results R=0

7.3.i Baseline

Testing the two different baseline loading conditions indicated the importance of clearance, especially as the cyclic load is increased. At relatively low loads, the fastener load transfer through friction provides ample load transfer to bring the value of G_{IIC} below that of the threshold and arrest the crack. Meanwhile, at higher loads, the crack is able to propagate further as a combination of shear engagement of the fastener as well as load transfer through friction succeed in providing crack arrest.

Shown below in Figure 41, the comparison between clearance and zero clearance is very noticeable as the zero clearance system arrests the delamination prior to the second fastener becoming effective at all. The second fastener is in fact contributing nothing to the arrest mechanism of this configuration. This statement was experimentally verified by removing the second fastener during a test, and finding an identical result for the zero clearance test. Additionally, it can be noted that the relative spread of the results is less for the zero clearance fastener. Clearance in the system introduces another variable. All of the sample hole diameters were measured and none of the articles fell outside of the tolerance for the holes. However it is suspected that the increased play in the fastener hole with the inclusion of clearance allowed for the natural variability of fatigue testing to become more evident.

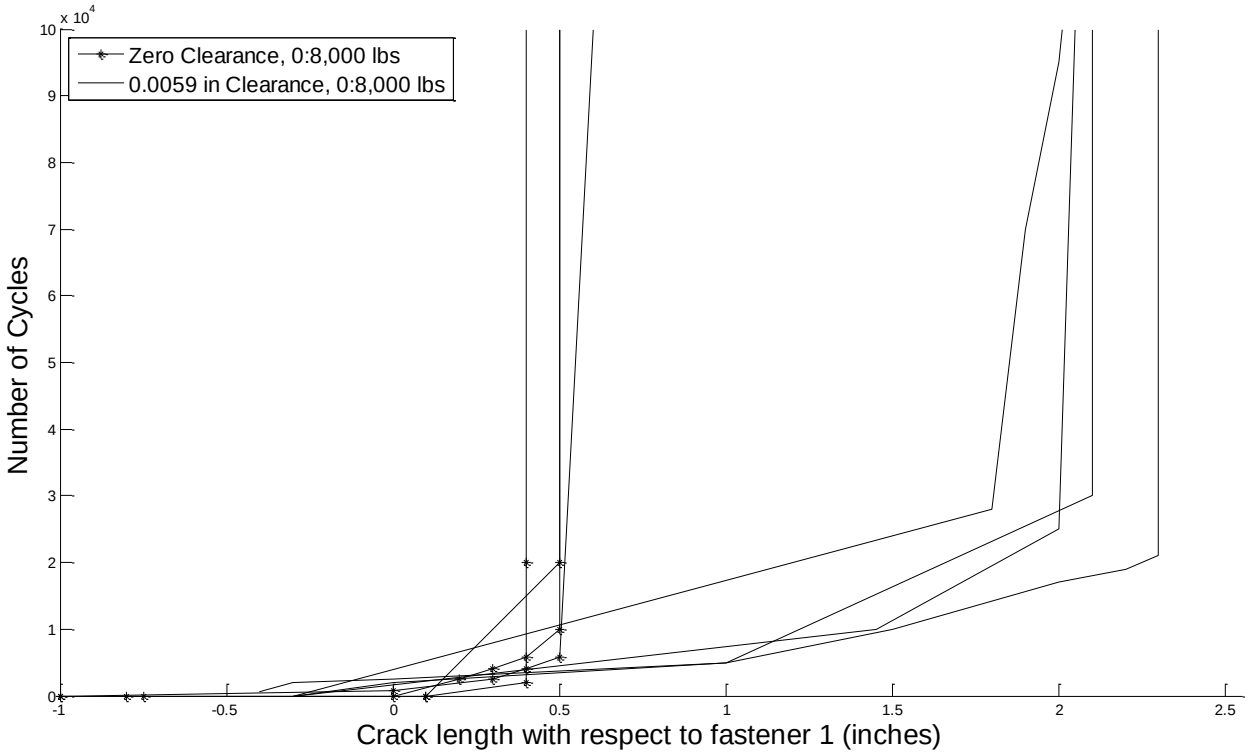

Figure 41: Tensile loading 8,000:0 lbs.

In contrast, shown below in Figure 42, the results for zero clearance and clearance drilled fasteners under high loading are more dramatic. Under a relatively low loading, the first fastener engages both in shear as well as providing load transfer, and can arrest the crack singlehandedly. However, under higher load levels, the amount of load transfer through friction contributes significantly less to the arrest mechanism, resulting in more of the load being required to be taken up by shear engagement of the fastener. The further the crack propagates, the further the fastener "spring" is stretched and thus the greater load it transfers from the loaded section into the unloaded section.

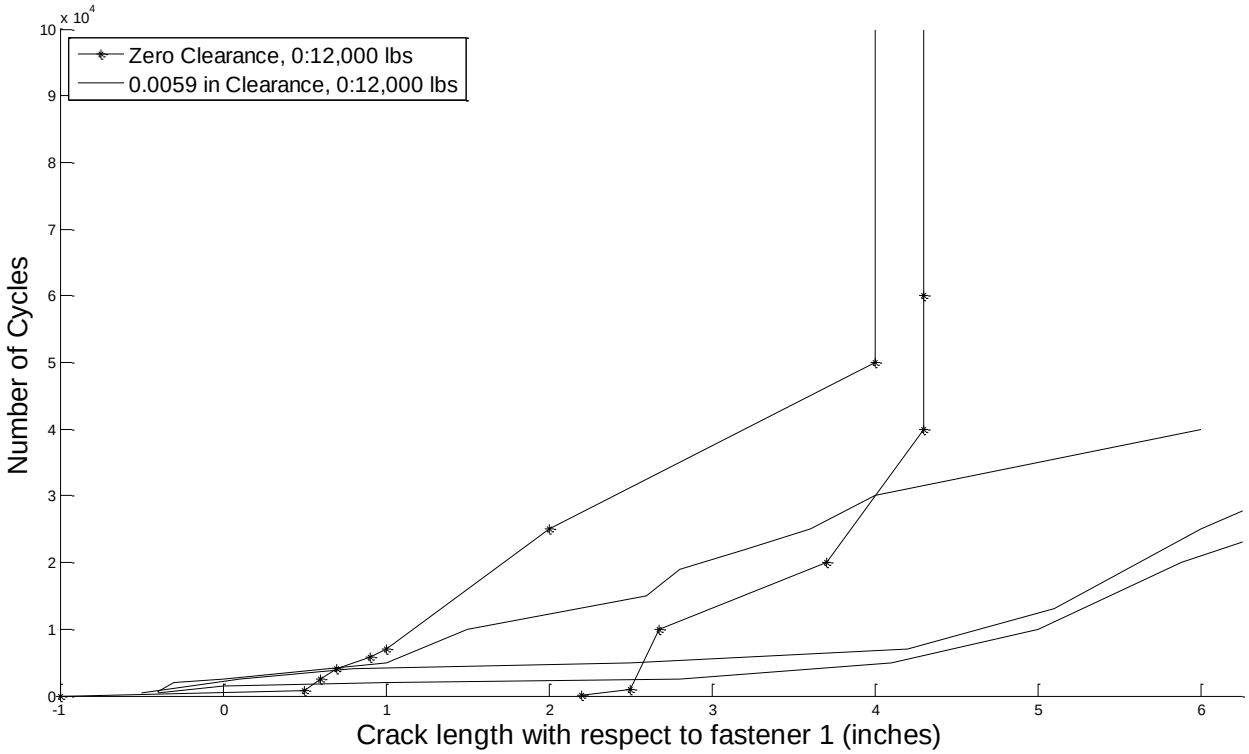

Figure 42: Tensile loading 12,000:0 lbs.

With clearance drilling, the second fastener tends to only contribute primarily through frictional load transfer. When removing the bolts, it can be seen that the first fastener, shown in Figure 43 is heavily marked with carbon from engagement in the fastener hole while the second fastener has only minor marking. These markings subsequently indicate that while the first fastener is heavily engaged in shear during this test, the second fastener is not. However, as shown in Figure 44, the washers can be seen to have marred the surface of the sample, indicating significant clamping of the fasteners occurred.

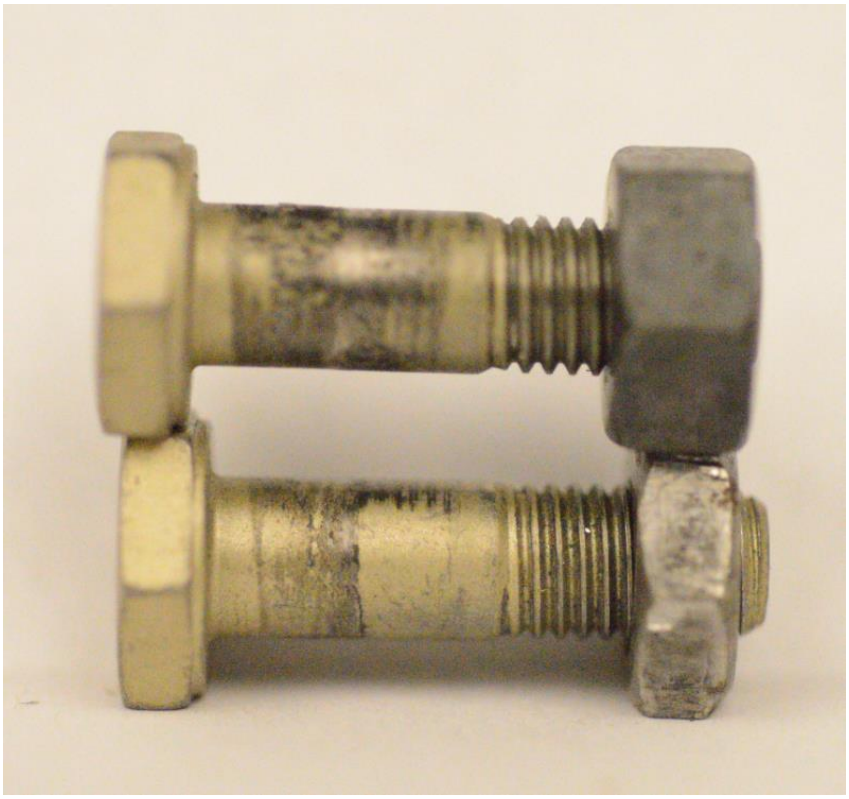

Figure 43: Comparison of fasteners upon removal fastener 1 (upper) and fastener 2 (lower)

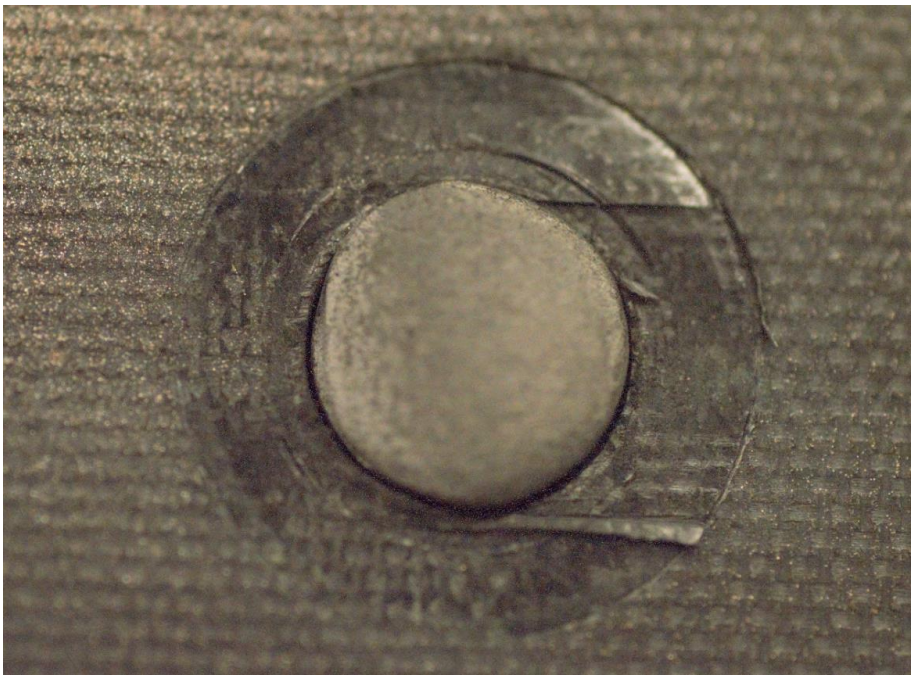

Figure 44: Visibility of washer marks on sample

7.3.ii Tension-Compression testing and Compression testing

Tension-Compression, and Compression only testing was conducted under fatigue loading, with an R-Ratio of -1 and 0, and load levels of -8,000:8,000 lbs. and 0:-8,000 lbs. for comparison to the tensile testing. Due to difficulties encountered during compressive static testing as well as initial attempts, and relatively unremarkable compressive results in Figure 45, a compressive loading of 12,000 lbs. was not tested in sufficient quantity to generate a statistically significant sample set. The primary difficulty was ensuring sufficient clamping of the fixture to prevent buckling as well as avoiding delaminations, sublaminate buckling and crushing of the unsupported ligament, which was necessary to allow for the relative sliding of the two primary sublaminates.

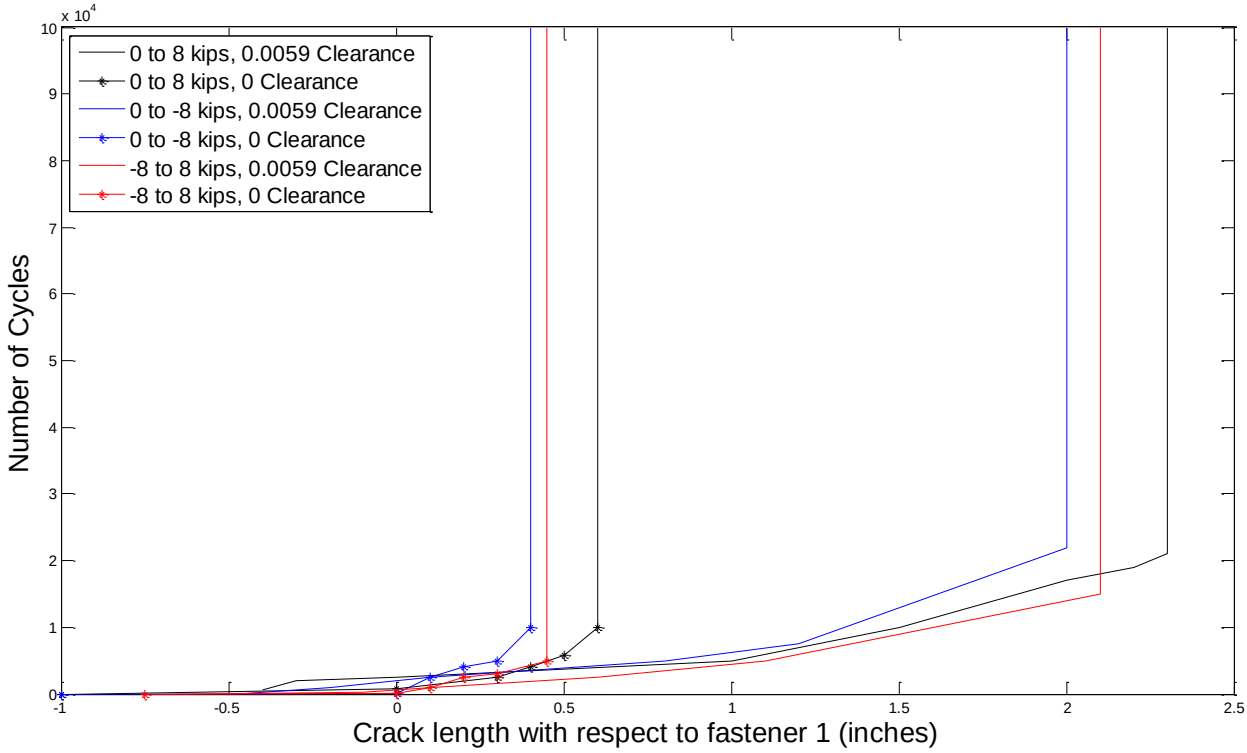

Figure 45: Comparison of Compressive and Tensile Results

As seen in Figure 45, there is good agreement between the compressive and tensile loading configurations, accounting for the additional clamping provided by the anti-buckling fixture. In order to avoid buckling of the laminate during testing, the fixture was required to compress the sample together. This unfortunately creates additional clamping and thus additional load transfer through friction in the same manner as described in quasi-static testing. As a result, the performance of the samples is artificially improved. As well, when testing at R=-1 and accounting for the improvement due to additional sample compression, it is approximately the equivalent of doubling the number of cycles at R=0.

Relatively identical results obtained in compression and tension is ideal. As stated previously, non identical would indicate further directionality of the material beyond that already assumed. If the results were not identical, this would suggest that for a standard 3 ENF, there would be an upside down and a right side up configuration to the sample, however this has not been found to be the case.

7.3.iii Visible polishing of the surface and debris during testing

One result visible under fatigue loading that was not detected under static loading is a visible polishing of the surfaces during the cyclic loading, with carbon dust visible along the edges of the crack as well as on the lower grip, pictured in Figure 46. This dust suggests that the relative sliding of the surfaces with respect to one another while in intimate contact is polishing the interface during the fatigue test. This is further supported by Figure 47 which compares the surfaces of a quasi-static and fatigue test, and the fatigue test surface is noticeably smoother. While for a 0/0 interface, this behavior does not generally produce a significant change in the

coefficient of friction, nor significant wear beyond the removal of broken fibers; for off angle interfaces this behavior may create significant damage.

Figure 46: Carbon dust buildup due to cyclic loading, buildup from 3 tests

Additionally, what may be noted in Figure 47 is that between the fasteners and after the second fastener, the 0 degree interface ply is missing. For quasi-static laminate testing, it was relatively common for this portion of the ply to split and adhere to one of the two sublaminates, with no readily observed preference. However, for the fatigue specimens, this split portion was occasionally missing, more typically for the clearance drilled specimens. While the loading was constant between the clearance and zero clearance specimens, the displacement of the clearance drilled specimens was higher, leading to more extensive rubbing of the two samples together. Some of the carbon buildup during testing was subsequently assumed to be a result of this portion of the interface being ground up.

7.3.iv Hole Damage

After testing, samples were occasionally fully delaminated in order to examine the hole damage at the interface. For the quasi-isotropic laminate, ovalization of the hole and a relatively circular visible damage zone, such as seen in Figure 47 (lower), occurred commonly for the laminates loaded at 12,000:0 lbs. This damage was more readily apparent for the high cyclic stress cases. For the additional test conditions, hole damage was minimally visible and impossible to capture using the photography equipment available.

Measuring the ovalization of the hole, the greatest change in diameter measured was 0.0025 inches, from a value of 0.256 to 0.2585, with the average increase in diameter being 0.0015 to 0.002 inches for highly loaded fasteners in clearance drilled holes. The increase in clearance for transition fit holes averaged 0.0005 inches or less, despite the visible hole damage pictured in Figure 50. For lower loading, as also true with static loading, the increase in diameter was within the margin of error of the measurement equipment.

Figure 47: Comparison of Quasi-Static and Fatigue Specimen interfaces

While the damage zone for the quasi-isotropic laminates was relatively circular, the damage zone for the 50% zero laminates was not as uniform, as pictured in Figure 48, the damage zone shape is highly irregular, and less constrained to the area around the fastener. This phenomenon, while visually interesting, did not appear to affect the results of the tests and thus was not explored further in the course of this research.

Figure 48: 50% Zero fatigue interface and hole damage, direction of propagation is left to right

7.3.v Fastener Loosening during testing and Fastener head Fatigue

The fasteners utilized during testing incorporated elliptically offset locking nuts, which are designed to not become loose due to fatigue cycling. Elliptically offset locking nuts are plastically deformed into an oval as seen in Figure 49. When they are threaded onto the bolt, they elastically deform into a circle and this compressive stress provides a locking action. While the nuts were commonly reused because they never failed in fatigue during testing, they eventually lost their locking capability if not reformed periodically.

Periodic redeformation of the fasteners, standardized to between every 3 tests, was found to ensure consistent locking action and prevented loss in fastener clamping due to the nuts backing off of the fastener shank. Furthermore, a second jam nut was installed above the initial fastener for additional insurance against a loss in clamping. Any test cases where a loss of clamping occurred were discarded from the results shown above.

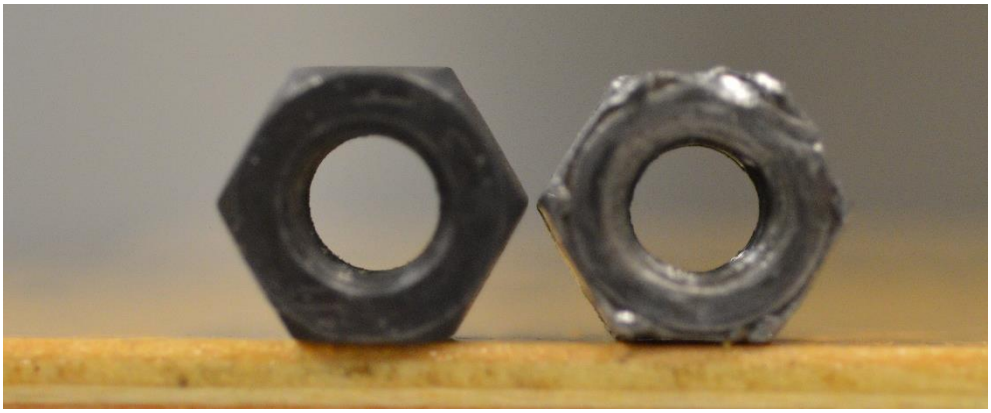

Figure 49: Regular circular nut (left) vs. elliptically offset locking nut (right)

In addition to the loss in fastener clamping due to backing off of the nut, occasionally the fastener heads would be fatigued to failure, causing a catastrophic loss in clamping. The eccentricity of the load, combined with fatigue testing served to produce a bending moment under the fastener head which resulted in failure under fatigue loading. This problem was exacerbated under higher loading and R-ratios closer to 0 as the bending fatigue on the fastener head was greater.

Finally, in order to understand the criticality of fastener clamping in the delamination arrest process, clearance drilled samples cycled from 8,000:0 lbs. were subject to additional cycles with loosened fasteners. These fasteners were tightened so that they would provide zero preload by only having the nuts torqued such that there was no free play between the fastener head and the laminate. Loosening just one of the two fasteners provided significant crack extension, with both fasteners loosened catastrophic crack propagation occurred during cylclic loading with the delamination extending the entire length of the sample.

7.3.vi Hole Damage/Elongation

One damage behavior that was not observed in the static testing which occurred during fatigue testing was the damage and elongation of the holes. Pictured in Figure 50, after testing, the hole has been ovalized to a degree. Before and after testing under a fatigue load of 0:12,000 lbs., the average change in hole diameter was around 0.002 inches, which represents approximately a 33% increase in clearance of the hole when a 0.0059 inch initial clearance was utilized by employing a 6.5mm drill bit.

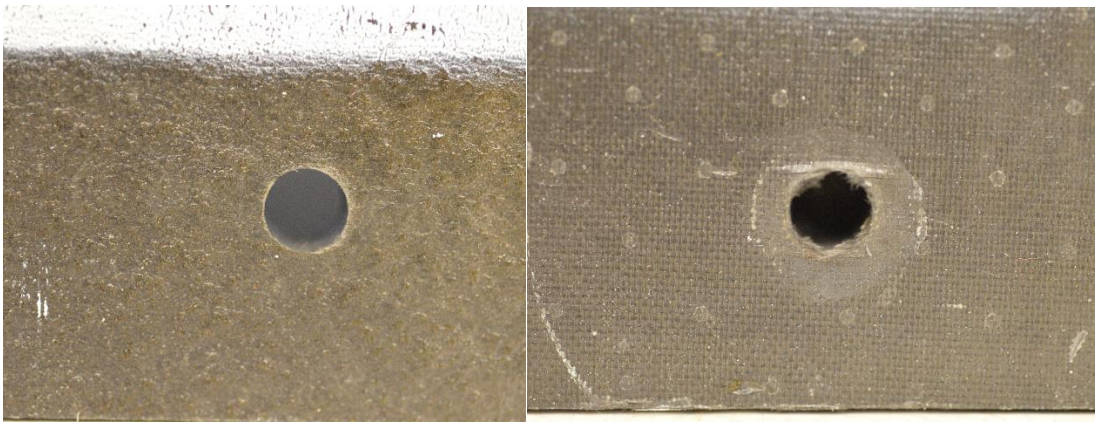

Figure 50: Typical hole as drilled (left) and after testing (right)

As demonstrated previously during testing of samples with and without clearance, any inclusion of clearance, or increase in clearance, will result in further crack growth; the degree of growth is relative to the increase in fastener hole clearance. Additionally, but not investigated in the research here is the size of the damage zone around the hole and whether at fatigue loading levels this damaged hole provided an effective loss in fastener spring stiffness because of this.

One of the most immediately noticeable differences between the two arrest cases is the crack length at the completion of the test, particularly with clearance drilled fasteners. While for zero clearance fasteners the crack was arrested under both loading conditions, the crack was not

consistently arrested under clearance drilled conditions. The cracks extended along most, if not along the entire length, of the sample under this loading condition, indicating that the arrest effectiveness is highly sensitive to the value of clearance.

7.3.vii Sample Discrepancies

Initial samples which contained the dramatic wave in the plies near the crack implantation point as shown in Figure 24 resulted in dramatically superior fatigue results, especially under loading of 12,000:0 lbs., with arrest prior to the second fastener. However, further testing using samples which were manufactured utilizing an insert found this solution to not be consistent. Further testing found that the combination of the bow wave with small resin ligaments resulted in additional load alleviation and an artificially superior sample. As a result, this experimental data was not shown here. The lesson learned from this endeavor is that careful sample design is critical to accurately capturing the true arrest effectiveness.

7.3.viii Lower Maximum load levels

In addition to the experiments described above in this subsection, additional tests were conducted utilizing lower load levels, including 6,000:0 and 4,000:0 lbs. However, there was no crack growth in these samples either to, or past, the first fastener for cyclic loads up to 100,000 cycles. This supports the postulation that there is a ΔG threshold for the matrix material, and for loads below this value, crack growth does not occur. From analysis, this threshold was found to be approximately $G_{II_{Th}} = 5\,\frac{lb}{in}$ for the specific material utilized here.

7.4 Results Varying R-Ratio

Three different additional R ratios of the applied load were tested under tension-tension fatigue loading, 12,000:4,000, 10,000:2,000 and 8,000:4,000 lbs., which represented R-ratios of 0.33, 0.2, and 0.5 respectively. These ratios were chosen as they allowed for the direct comparison between the R=0 loading cases discussed earlier within this chapter, and the three different R ratios maximized the breadth of the study with the resources available. Two of the R-Ratios were also chosen because these utilized the same load amplitude (4,000 lbs.) as the R=0 test case with a maximum load of 8,000 lbs. Tests were conducted on otherwise identical samples, cut from the sample plates and drilled utilizing the same techniques.

It is important to note that the R ratio of the crack tip will vary as the delamination propagation continues down the length of the sample. The crack arrest features are designed to provide load alleviation at the crack tip by transferring load from the loaded plate to the unloaded plate. For an ideal, perfectly stiff fastener, ½ the load would be transferred into the unloaded segment and thus there would be no stress at the crack tip and no driving force. However, the fastener is not infinitely stiff so there is some load differential at the crack tip. As the delamination propagates and the fastener is further engaged, the amount of load transferred increases, changing the R-ratio of the maximum to minimum load seen by the crack tip. For simplicity in this section however, the results are grouped by R-ratio of the applied load.

Seen in Figure 51, with an R-ratio of 0.33 and loading of 12,000:4,000 lbs., there is a non-negligible difference between the clearance and zero clearance results, but in both cases the two fasteners provide good arrest capability, stopping crack growth near the second fastener and with less crack growth compared to the tests with the same maximum load applied but R=0. The

reasons for this are two-fold, both the value of ΔG is lower for this R ratio, as well as the modification of the R ratio itself. The trend of this data further supports the ability to treat the interlaminar region as a homogenous material for fatigue delamination studies.

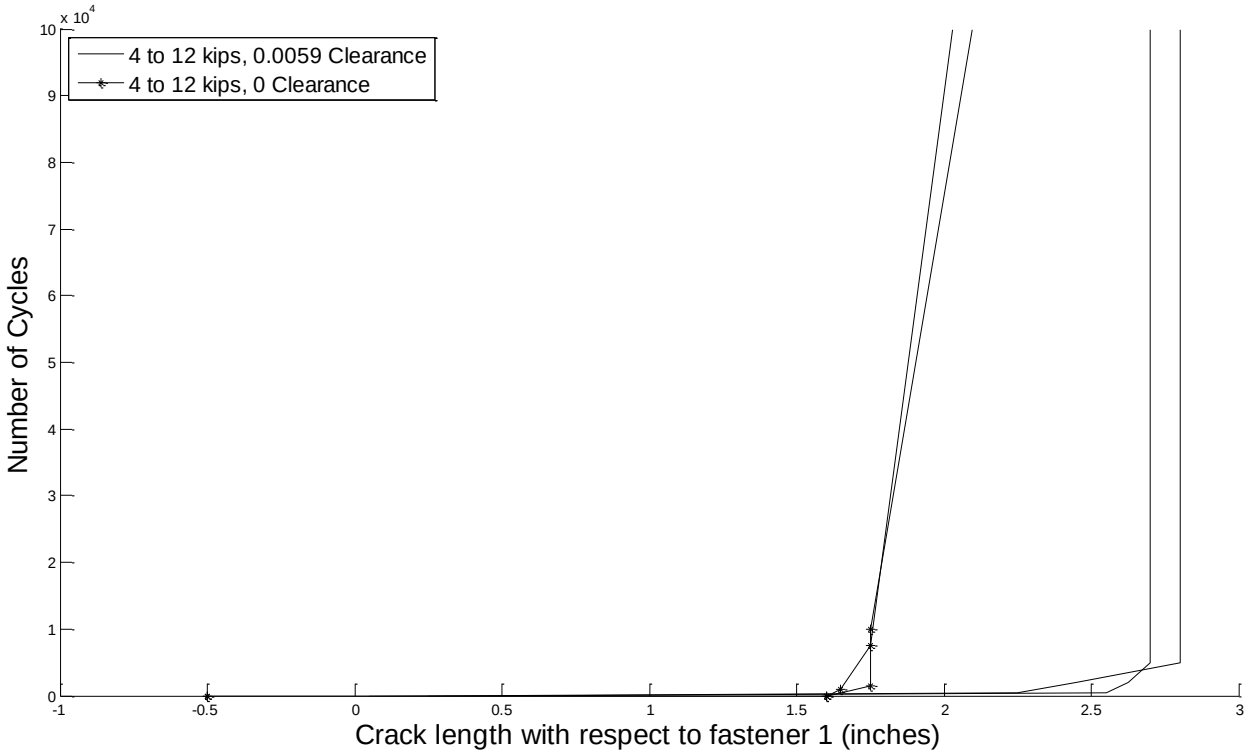

Figure 51: R=0.33 Results

With a lower maximum load, of 10,000 lbs., but same load amplitude of 4,000 lbs., the R-ratio of the tests plotted in Figure 52 was R=0.2. For this test condition, only samples with a clearance drilled fastener were tested due to relatively high data scatter in this segment leading to a comparatively large number of tests being required to adequately understand the delamination propagation behavior.

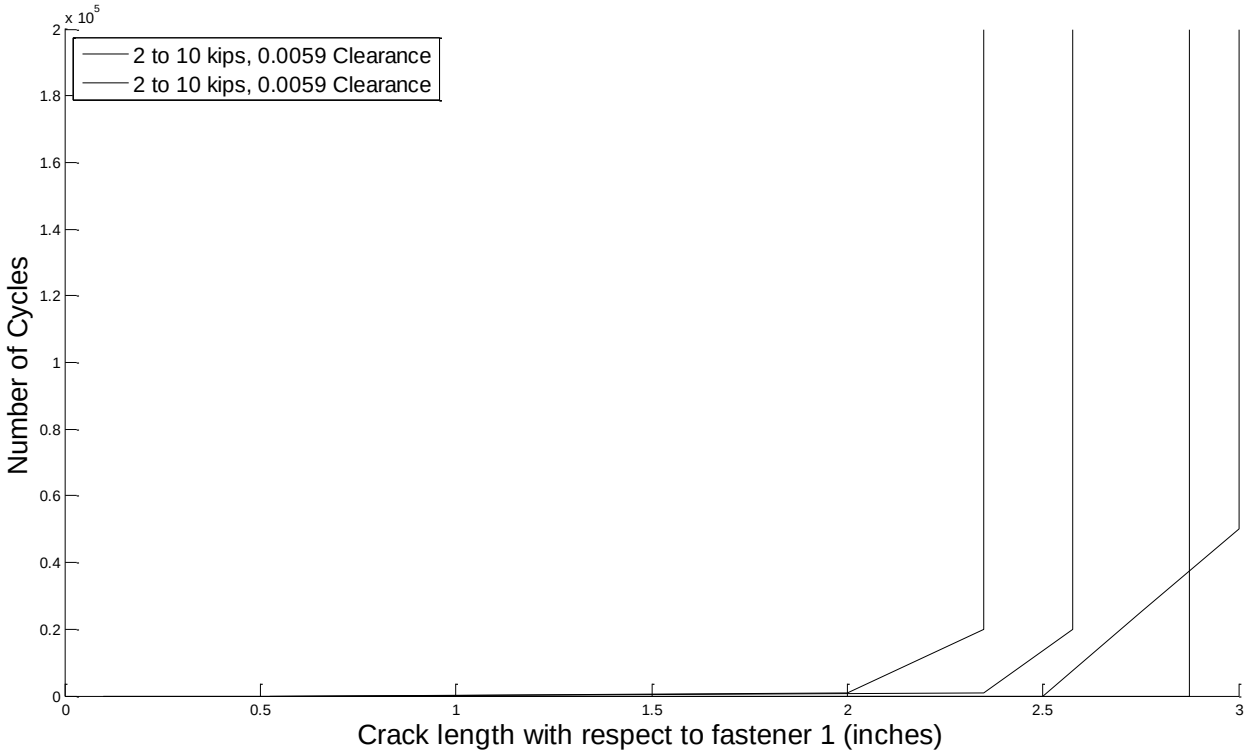

Figure 52: R=0.2 Results

Shown above, the results show a relatively intermediate arrest behavior for this intermediate case, with arrest occurring at slightly lower crack lengths compared to that for the higher loading plotted in Figure 51 and at greater crack lengths compared to previous tests with lower maximum loads.

During testing with a value of R=0.5, at a load level of 8,000:4,000 lbs., the results, shown in Figure 57, demonstrate the clearance and zero clearance fastened results are nearly identical, with the crack arrested near the first fastener. In both cases, it appears that the influence of the first fastener was sufficient to stop the crack from propagating, prior to reaching the first fastener. These results, combined with the R=0 results at this load level suggest crack arrest fasteners provide a very strong benefit to the structure under typical fatigue loading, which will rarely if ever exceed 50% of the ultimate strength.

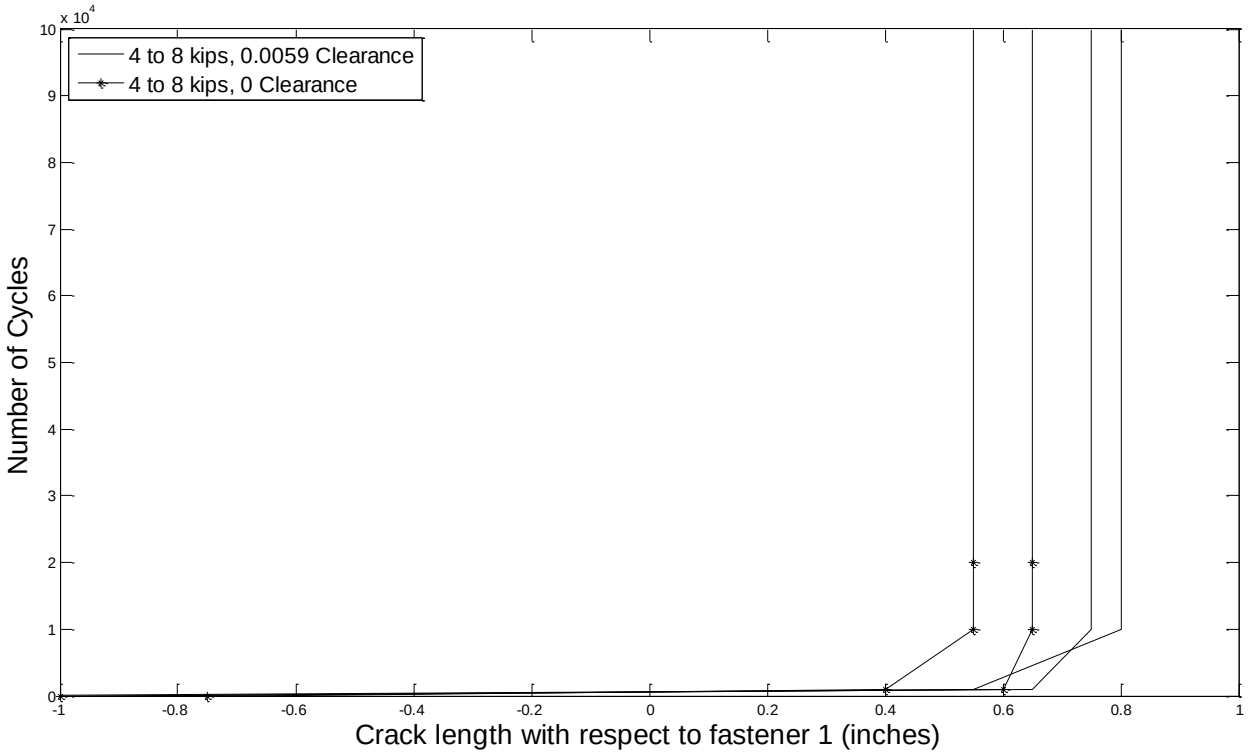

Figure 53: R=0.5 Results

Furthermore, removal of the second fastener provides no loss in the delamination resistance of the laminate, even with clearance drilled holes. The second fastener was removed from a sample and the laminate cycled another 100,000 cycles with no additional crack growth. However, the clamping force of the first fastener remained a critical component of the arrest mechanism. On a different, but otherwise identically tested sample, the first fastener was loosened to provide zero preload, the nut was only tightened enough that the bolt could not slide laterally in the hole. The second fastener was installed to 40 in-lbs. of torque and the sample cycled. The crack rapidly grew to the second fastener where it was arrested and remained so for an additional 100,000 cycles.

7.5 50% Zero

Testing of 50% zero laminates was originally to be conducted at higher alternating stresses because the laminates tested under quasi static loading were shown to support greater loads prior to delamination propagation through the fasteners. Initially, tests were conducted only using 0.2559 diameter holes drilled in the laminate due to resource constraints, and at 12,000:0 and 18,000:0 lbs., which represented similar load ratios as for the quasi isotropic laminate, approximately simulating the initial crack growth load and 75% of the failure load of the laminate. However, as seen below in Figure 54, significant crack propagation was achieved at this load level, and thus a second, lower loading of 9,000:0 was considered as opposed to a higher load level.

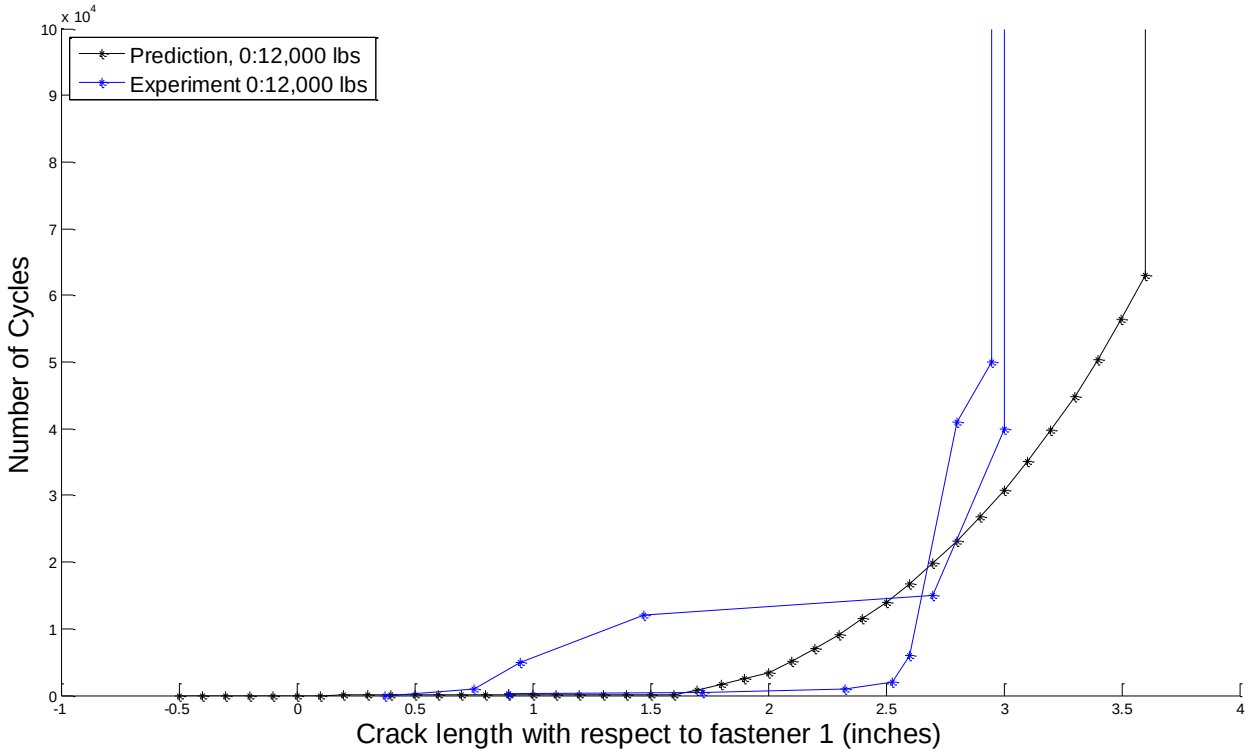

Figure 54: 50% Zero fatigue results

Visible in Figure 54, non-negligible crack growth occurred during the testing, which was unexpected at this load level. This is comparable to the load level at which the crack initially propagates in quasi static loading. It is suspected that because the fasteners are being clearance drilled, they do not transfer any load in shear for a larger distance compared to the quasi-static case of equal load. In both cases, the load transfer through friction is not substantial enough to provide arrest. However, at sufficiently long crack lengths, arrest can be achieved as the fasteners become engaged in shear and provide sufficient load alleviation.

As a result of the above testing at 12,000 lbs., combined with the clearance drilled results in quasi static loading plotted in Figure 36 showing significant crack growth at loads of 18,000 lbs., it was decided to perform tests at a maximum load of 9,000 lbs. using clearance drilled fasteners. Figure 54 shows the experimental results in comparison with the results from the 12,000:0 loading. For the lower loading, the crack is readily arrested by the two fastener system near the second fastener, as the load transfer through friction by the two fasteners provides sufficient load transfer for arrest. This assumption was further supported by loosening the clamping on the second fastener such that minimal load was transferred through friction and performing additional cyclic loading which caused the crack to grow. Subsequent retightening of the fastener arrested the crack again at its new position.

Additional interesting items of note were the experimental results at 9,000:0 lbs., which showed a different curve shape compared to the other experimental specimens. While the delamination stopped growing at a comparable point to other tests, the curve shape did not follow the more common exponential type shape that was commonly observed.

7.6 Key Control Properties

The most important properties which can be controlled during testing are the fastener clearance and fastener clamping. These two parameters have been shown to play a major role in the delamination response under fatigue loading. Either a loss in fastener clamping or an increase in clearance, or both, will result in further crack growth, and improperly controlling these variables will subsequently result in additional scatter within the data.

On the other hand, it is difficult if not impossible to control for the fastener hole damage and fastener fatigue failures which were observed during testing. While acceptable for static testing, re-use of the fasteners cannot occur during the fatigue tests due to potential failure of the fastener heads. Although these can be accounted for when performing life cycle simulations, they typically cannot be prevented during testing, only observed.

Chapter 8 Additional Testing

In the course of the research presented here, additional testing was required in order to accurately model the results of the experiments. These tests served to investigate input parameters that were not publicly available, verify other input parameters and/or investigate any discrepancies in the modeled results compared to the experimental results, especially when these discrepancies could be moderated by tweaking common input parameters such as the load transfer through friction or value of G_{IIC}.

8.1 Material Property Verification

One of the tests performed to verify the accuracy of the modeling is testing the stiffness values of the material and G_{IIC}. The stiffness of the laminate when modeling the system in 1D utilizes classical lamination theory, and the stiffness in the 2D and 3D models utilizes the ply by ply stiffnesses which results in the assembly having a final stiffness which should equal that of the experimental specimen. However, as published values were utilized for the ply by ply stiffnesses, it was not known if the test material utilized would accurately match this, and starting with an improperly matched specimen stiffness would result in a model which would fail to accurately predict the results.

In order to verify the stiffness, a sample which had been completely delaminated was instrumented with opposing strain gages with the fastener removed. The strain gages were installed sufficiently far away from the fastener hole to avoid this influence and the completely delaminated sample was utilized as this load path was symmetric, eliminating the effects of bending. The stress was assumed to thus be uniaxial stress through the laminate. Using the stress

strain curve acquired from strain gages located far away from the fastener holes, a stiffness of $7.9*10^6$ psi was found, which matches the classical lamination theory predicted stiffness of $7.713*10^6$ psi relatively well. Similarly, for a 50% zero layup, the calculated stiffness was $12.5*10^6$ psi, which compares favorably with the predicted stiffness of $11.7*10^6$ psi. For the simulations, both the measured values as well as the predicted values were utilized with minimal difference observed. For the plots produced in the comparison section, the measured stiffness was utilized.

Additionally, the published value of G_{IIC} of the laminate was 14 lb/in, which resulted in predictions that overstated the capability of the laminate in static testing compared to the experimental values. However, simply reducing this value of G_{IIC} shifts the curve of the predictions as discussed in Chapter 4. To avoid simply curve fitting the data, three point end notched flexure (3ENF) samples, as shown in Figure 55, were fabricated in order to test the value of G_{IIC}. Using the procedure outlined in ASTM D7905 [38], the value of G_{IIC} for the samples was found to be 12 lb/in, which resulted in significantly better agreement between the experimental and analytical work.

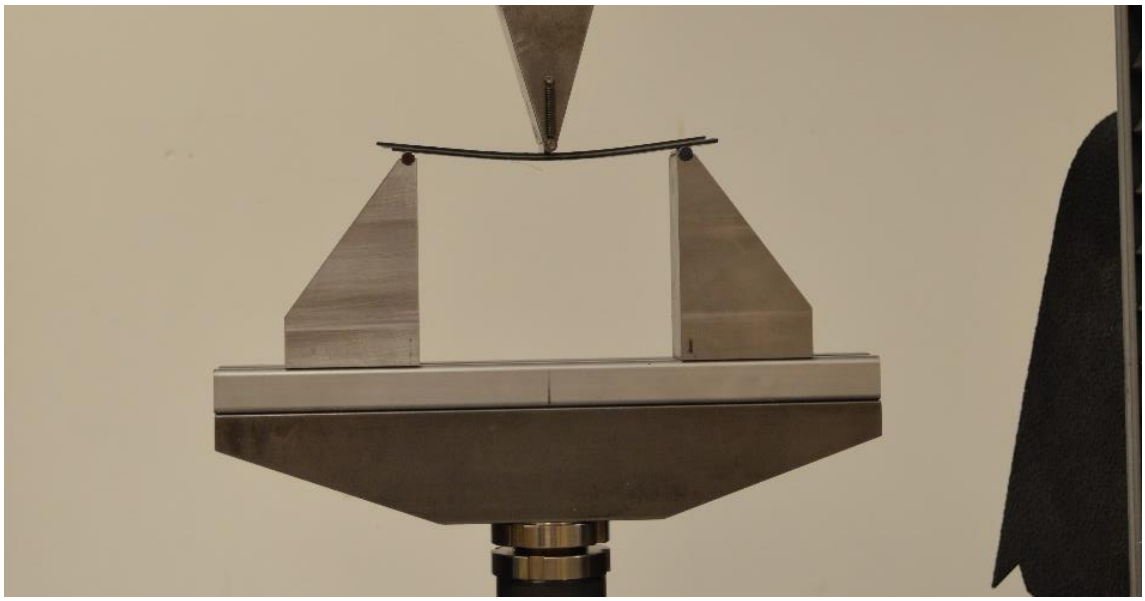

Figure 55: 3ENF Specimens

8.2 Fastener Flexibility Verification

Previous work in the area by Cheung [2] indicated that the fastener flexibility predicted too stiff of a fastener for the work presented here. As a result, test data was generated during this research to understand experimentally the fastener flexibility for the configuration presented here. Tests were performed as shown in Figure 56 using a completely delaminated sample with one and two fasteners installed to varying levels of installation torque. Additional tests were conducted using a single lap shear specimen to allow for a direct comparison between the measured fastener flexibility of the system utilized here and the values predicted by Huth. The same specimen for the previous fastener flexibility testing was utilized for the single lap shear testing as well, using one and two fasteners. Load displacement of the system as well as the strain within the samples was recorded to then allow for the back calculation of the fastener flexibility.

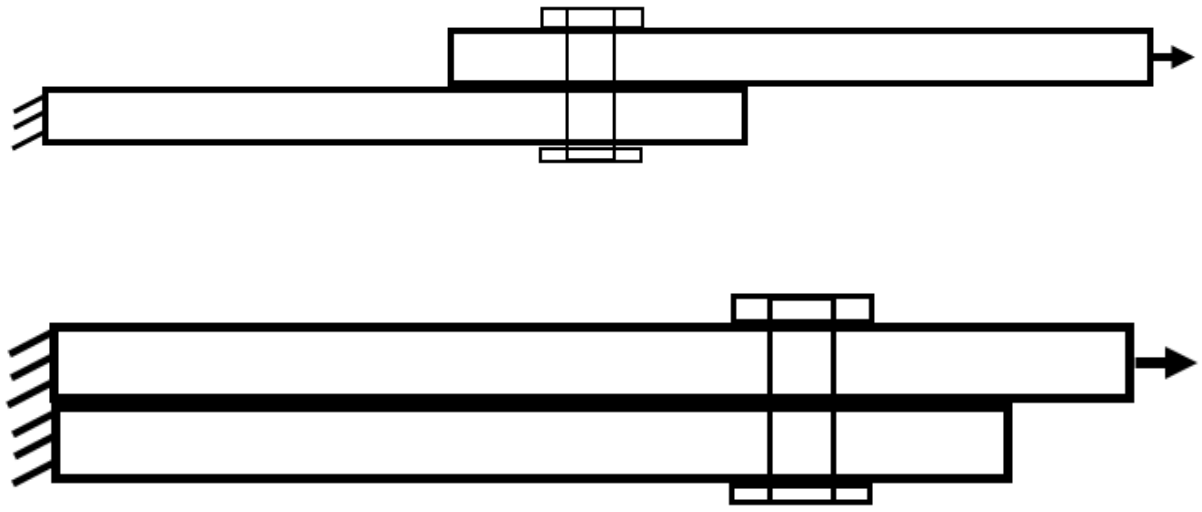

Figure 56: Fastener flexibility testing configurations, single lap (top) and research (below)

Fastener flexibility formulas, as presented, typically include the effects of frictional load transfer within the total predicted value of the fastener flexibility, however the research presented here, particularly for modeling of fatigue delaminations, has found that separating the effects of the shear stiffness of the fastener and the load transfer through friction provides significantly improved results. Thus, the installation torque was varied from "finger tight" which ideally should provide no load transfer through friction, to 80 in-lb, which is the design installation torque.

Data was gathered utilizing opposing strain gages installed on the laminates, both a quasi-isotropic and a 50% zero laminate, in order to compare to finite element based predictions of the system. Furthermore, the relative strain in the loaded and unloaded laminates can be correlated to the amount of load transfer through the fasteners from the loaded to the unloaded section. Comparison of the predicted and measured responses are shown below in Figure 57.

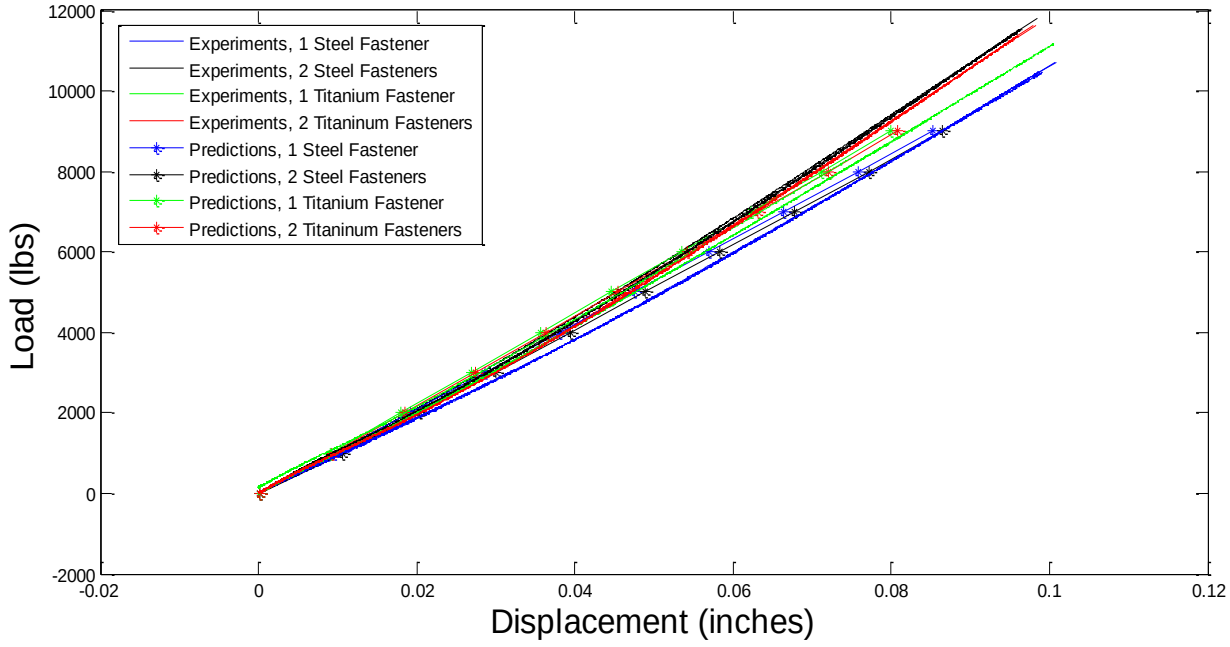

Figure 57: Fastener flexibility testing vs. predictions

As seen above, the predicted and experimental results show good agreement with one another, however it is interesting to note that while the experimental predictions of the delamination response are highly sensitive to the stiffness of the fastener in shear, the load-displacement curves are not. Plotted below in Figure 58, there is minimal difference despite varying the fastener flexibility by a factor of 10 in the below examples. Even at loads approaching the quasi-static failure load of the laminate, there is minimal divergence between the two theoretical configurations. This indicates the need to determine the fastener flexibility through other means, such as measuring the load transfer in shear via strain gages, as the variance between tests is on the same order as the difference between the calculated displacement of the sample when the stiffness is varied.

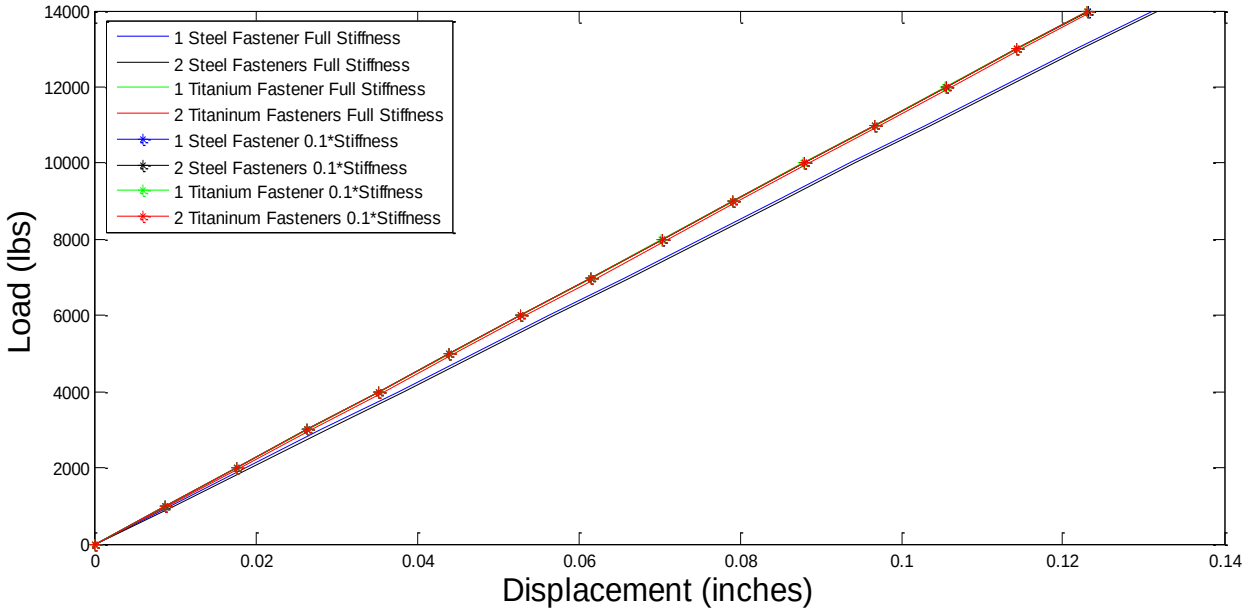

Figure 58: Comparison of Displacement with varying stiffness

Additionally, steel bolts were utilized to understand the general applicability of the fastener flexibility formula. These fasteners were otherwise identical to the 0.25 inch titanium fasteners but had a Young's modulus of approximately 29 Msi compared to 16.5 Msi for titanium [37]. Shown below in Table 3 are comparisons of the values between the experimental and predicted results for the different fastener materials and configurations. Of note, the predictions utilized the correction factor of 0.4*K first postulated by Cheung [2] as the experimental results supported this correction factor.

Table 3. Fastener flexibility values as tested and calculated

	Prediction (with 0.4 correction factor)	Measured, Delamination Configuration	Measured, single lap shear
Titanium 1 Fastener	65,393 lb/in	62,668 lb/in	66,524 lb/in
Titanium 2 Fasteners	65,393 lb/in	55,332 lb/in	63,165 lb/in
Steel 1 Fastener	71,331 lb/in	37,092 lb/in	75,650 lb/in
Steel 2 Fasteners	71,331 lb/in	57,413 lb/in	72,650 lb/in

As visible above, there is good agreement with the tested specimens and the predictive data, with the exception of the single fastener steel specimen in the delamination configuration. It is unknown why this occurred. The experiment was repeated multiple times with good repeatability, however the predictions remained significantly off. This discrepancy was assumed to be a failure of the test article in this specific condition, and was not investigated further due to the agreement of the titanium data.

8.3 Frictional Testing

In conjunction with the fastener flexibility testing, testing of the coefficient of friction of the laminate interface was also performed in order to best understand the two input parameters for the simulation. Work published by Schön [24] indicated that the minimum coefficient of friction between laminates occurred at a 0/0 interface and had a value of approximately 0.25. However, this work used relatively low loads, on the order of 25 lbs. at the maximum, while the assumed preload for the fasteners was on the order of 1000 lbs. Additionally, it was of interest to understand if the three possible sliding surfaces for a fastener, i.e. the interface, as well as between each washer and the laminate, would result in a different “effective” coefficient compared to the tested value using standard methods. When utilizing a fastener with two

washers, each laminate is clamped on two sides; one side is the interface of the crack, the other is the exterior of the laminate against the washer surface. In this case, it was expected that the coefficient would be higher, as for the laminate to move, it must slide against both the interface and the washer surfaces.

Initial testing utilized a standard method of loading, where normal loads are applied using rollers and the value at which the two plates slip was recorded, with the results shown in Figure 59. Load was varied from 900 to 1,550 lbs., with the applied load measured using a load cell inline with the applied normal load and the values chosen to represent an approximation of the applied preload which would be generated by a fastener.

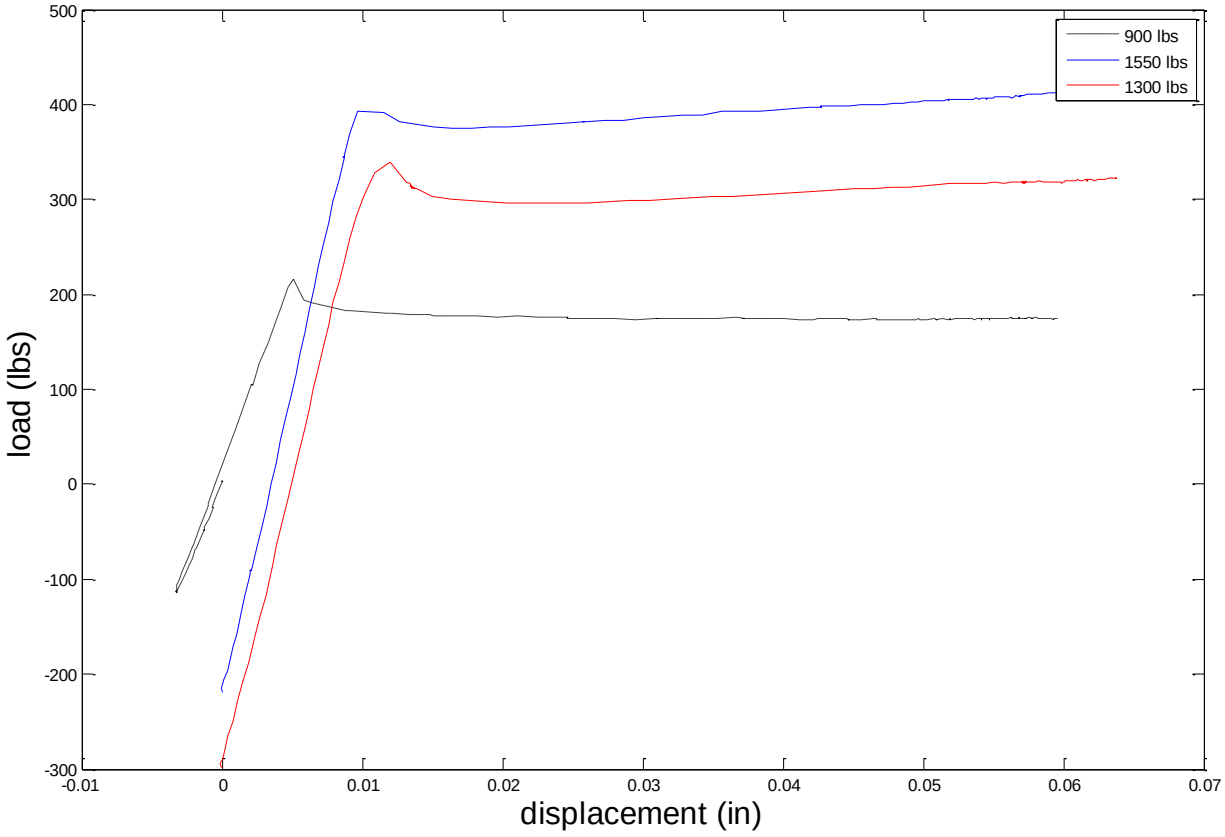

Figure 59: Load vs. Displacement for various values of normal loading

As the test was displacement controlled, there is a small load peak visible which represents the static coefficient of friction and the subsequent approximately flat line represents the kinetic coefficient of friction. As the variation between these two values was not significant, only the static coefficient was employed in the simulations. The tests were repeated three times at each load level to check for consistency, with excellent repeatability found. The static coefficient of friction varied from 0.24 to 0.26 for this testing, which agrees well with previous work by Schön [24], which measured an average coefficient of friction of the same 0/0 interface as approximately 0.25.

Meanwhile, single lap shear samples were tested using a fastener installed to varying levels of torque which could be correlated to preload both by measuring the torque related fastener change in length as well as through previous experimental results which quantified the load vs. torque curve, depicted in Figure 6. Figure 60 plots the load vs. displacement curves of the samples which utilized a fastener in single lap shear.

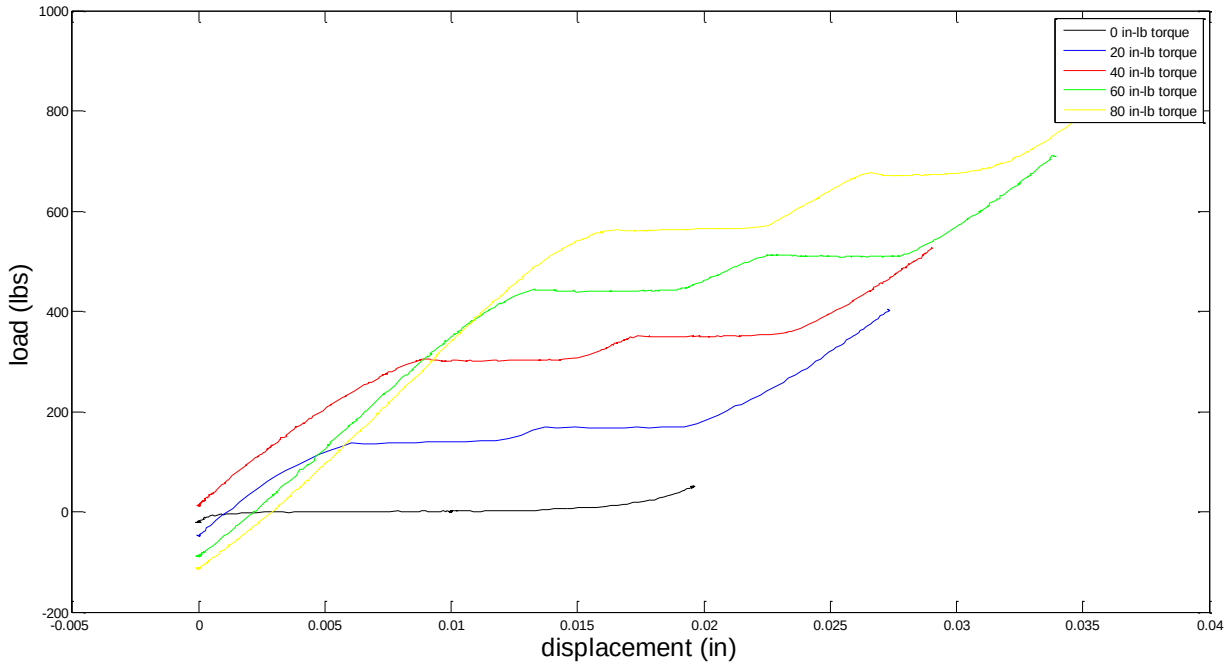

Figure 60: Load vs. Displacement for various fastener installation torques

The samples were initially installed such that the fastener was not loaded in shear, and then pulled in tension until the fastener was engaged in shear, visible by the positive slope at the far right. This positive slope can be utilized to measure the spring stiffness of the fastener, based on the known stiffnesses of the laminates and load/displacement data. Meanwhile, the central portion of the plot can be used to establish the effective coefficient of friction, as this is the load at which the maximum static friction force is exceeded and the samples are allowed to slip. Of note, there is a small increase in load in the center portion of each line, it is unknown exactly why this occurs but the assumption is that this corresponds to when the fastener contacts the hole wall of one of the two fastened components.

In addition to the load transfer being calculated from the strain gages, the load vs. displacement of the delaminations configuration was recorded at varying levels of fastener torque as well as

without a fastener installed. As shown below in Figure 61, with no fasteners installed, the load vs. displacement is significantly lower, as was expected since half of the laminate is not engaged. However, at varying levels of torque, the slopes and values of the curves are not dramatically different, as most of the load transfer is through shear engagement of the fasteners in this test. Load transfer through friction is expected to have varied from between about 0 lbs. (at 0 in-lb of torque) to 700 lbs. (at 80 in-lbs. of torque), which accounts for the discrepancy between the curves.

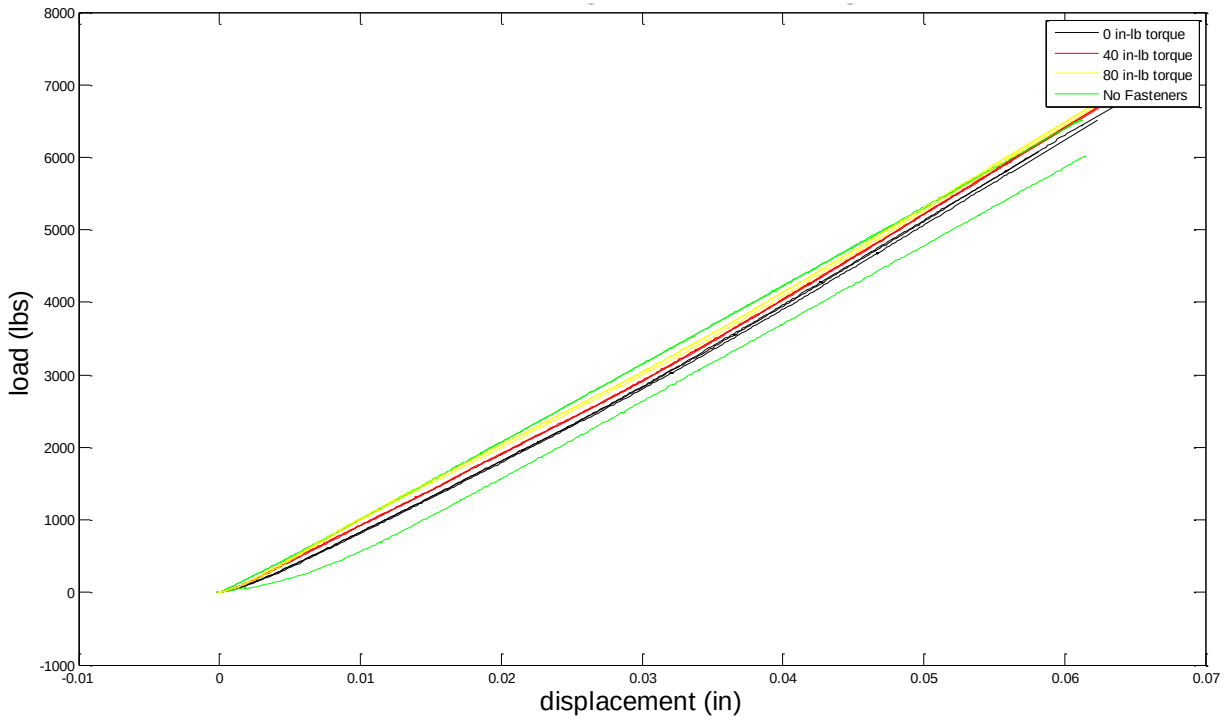

Figure 61: One fastener load vs. displacement curve

Additionally, it can be seen that the curves tend to diverge and then converge as the loading is increased. This can be explained by sliding at the interface once the load is sufficiently high to overcome friction. At lower loading levels, the load transfer through friction plays a significant role and provides a non-negligible portion of the load transfer into the unloaded plate. However,

as the load increases, the frictional force is overcome and the interface is allowed to slide, causing the total displacement to become approximately equivalent regardless of installation torque. This is relevant as, under fatigue loading, this stick-slip condition becomes important in retarding crack growth since at low loads, the R-ratio at the crack tip is reduced.

8.3.i Discussion on Variability in Friction due to Method of Loading

There is a very noticeable difference in the coefficient of friction when comparing the load transfer utilizing the ASTM standard method of measuring this value as compared to the utilization of the fastener to apply the compressive normal force. This can be ascribed to the three sliding surfaces generating additional load transfer through the fastener as shown in Figure 62, comparing and idealized image of the two methods, ignoring the friction between the fastener and washer and rollers and sample.

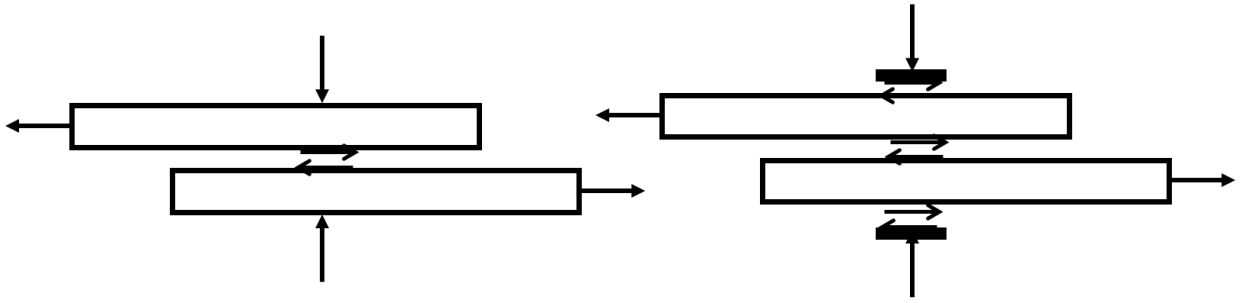

Figure 62: ASTM standard method vs. Fastener load transfer through friction

As can be seen, there are three sliding surfaces when a fastener is utilized to provide the clamping force as compared to the single sliding surface using rollers to clamp the laminates together. The variability is thus assumed to arise from the total load transfer of three surfaces, divided by the preload generated of the fastener to be equal to a coefficient of 0.35, as compared to the measured value of 0.25 when only the single sliding surface is measured. However, it is

also important to note that any changes in the configuration, including interface as well as exterior ply angle or finish has the possibility of influencing the measured coefficient of friction.

8.4 Unfastened Fatigue Properties

In order to accurately predict the fatigue response of the delamination arrest features in the course of this research, the fatigue properties of the laminate under mode II loading were required. The samples tested consisted of three plate symmetric specimens with a quasi-isotropic layup, chosen to mimic the most common laminate configuration of the fastened arrest specimens. An image is shown in Figure 63; visible are the twin symmetric crack fronts whose growth was measured to establish the fatigue properties. A pre-cured insert was utilized to control the initial crack front and initial cycling was performed in order to grow the crack away from the implanted delamination point, with the data from this disregarded.

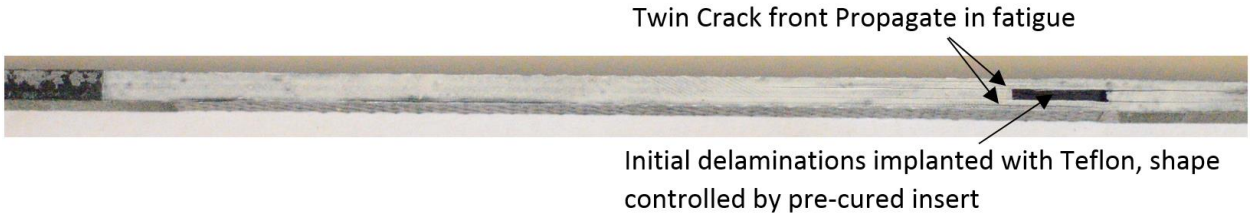

Figure 63: Unfastened fatigue delamination specimen

Testing was conducted using an R-ratio of 0 and various maximum loads in order to establish the $\frac{da}{DN}$ vs. ΔG parameters of the Paris Law. Two of the primary benefits of this sample design over a typical 3ENF sample is that for a constant amplitude load, the value of ΔG remains constant regardless of crack length along the sample. Additionally, the influence of friction is all but eliminated as the plates are not compressed against one another in any manner. For a 3ENF sample, the load application method serves to compress the interface, which provides an

unquantified amount of load transfer through friction in addition to the influence of bending. As much of the research presented here has found that separating the effects of friction presents an improvement in the predictive capability, this characteristic of the 3ENF method was highly undesirable.

While previous work by Gray [16] had noted that the crack length was often asymmetric during quasi-static testing, this was not the observed case during fatigue testing. Regardless of the load application, the crack driving force will be greater for the shorter crack, but for quasi-static testing, the unstable crack growth made asymmetric growth more evident. Under fatigue loading, the microscopic crack growth lead to much more symmetric crack fronts.

8.5 Why mode I was largely neglected in testing

An important item of note is that mode I properties are largely ignored in the research presented here; this is because mode I has been found to be of negligible importance and thus the resources required to test the various parameters were deemed unnecessary. Furthermore, one assumption in the work is that the fatigue is propagated in purely mode II, and there currently doesn't exist a verified method of predicting mixed mode fatigue.

Shown below in Figure 64, when varying the value of G_{IC} by an order of magnitude in both directions, the delamination propagation response is not affected significantly in the region after the fastener, which is the region of interest, by changing this parameter. This agrees well with the simulation results presented in Chapter 4 which showed that mode I is all but eliminated and thus would not affect the results. Prior to the fastener, when the value of $G_{IC} = 16$ lb/in, 10 times the typical value and greater than the value of G_{IIC} in this simulation, the initial propagation force is significantly higher, and similarly, when $G_{IC} = 0.16$ lb/in the initial propagation force is lower.

However as soon as the crack encounters the fastener and mode I is eliminated, the length vs. force curves become nearly identical. There is again divergence at very high loads, above the failure load of the sample, which is attributable to the eccentric load path causing a high degree of bending and subsequent mode I opening of the laminate.

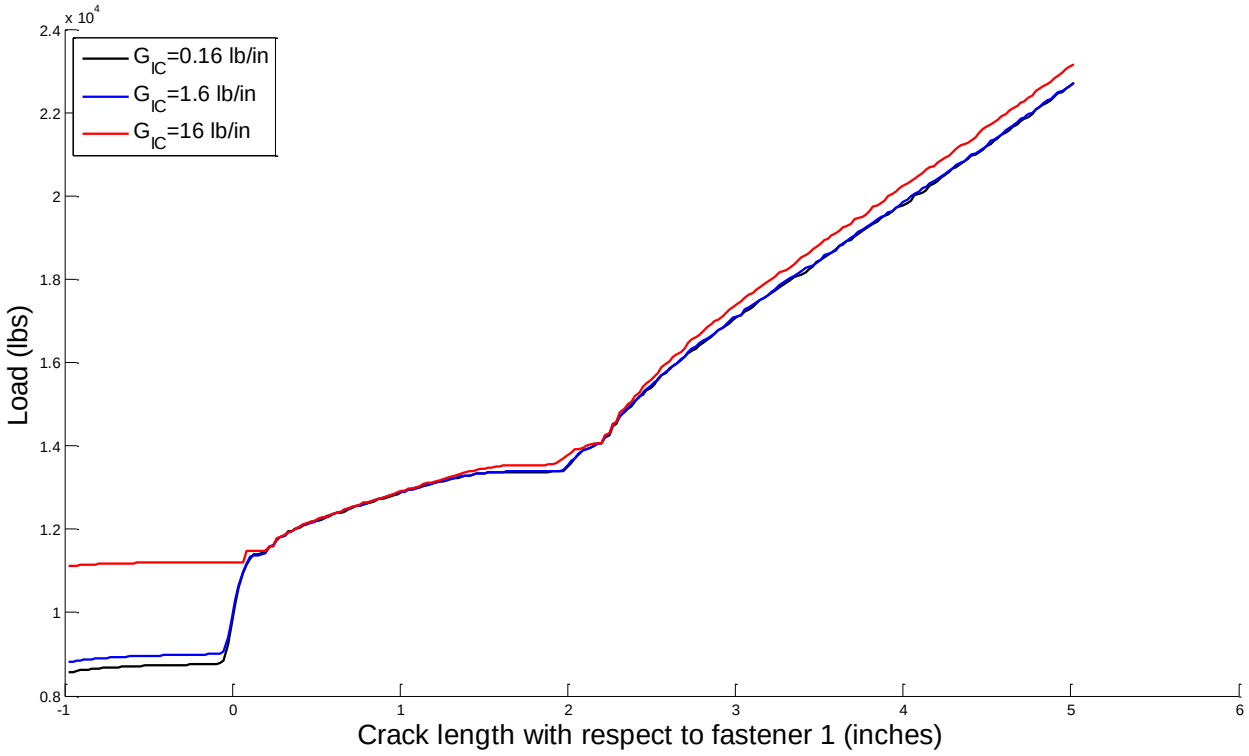

Figure 64: Quasi Static predictions varying the value of G_{IC}

While the above is presented for quasi-static testing, the results will hold true for fatigue testing as well, since the loads at which the specimen are cycled are encountered and exceeded during the quasi static testing with no reoccurrence of mode I. As a result, the assumption of mode I being possible to neglect in fatigue as well as static testing appears valid, and thus mode I fatigue properties were not tested in the course of this research.

Although this assumes that mode I is completely eliminated, this is not exactly true, due to the eccentricity of the loading, where a small value of mode I can always occur, even as the fasteners are providing clamping. However, both experimental and analytical results have shown that the magnitude of the opening mode is negligible and thus can be safely ignored near the presence of fasteners. Notwithstanding the foregoing, in the instances of delaminations of sufficient length, beyond those which have been tested here, it is distinctly possible that arrest feature's zone of influence will be exceeded and thus mode I can reappear.

Chapter 9 Comparison of Experiments and Analysis

One of the primary goals of the research was to accurately predict the delamination response of the arrest features under various conditions. The development of the MATLAB tool allowed for a more direct investigation of various input parameters so that a better understanding could be obtained and the importance of these input parameters could be ascertained. The model was first developed for the static cases and then extended into the fatigue testing. No model calibration was performed in order to generate the predictions, however various key input parameters were experimentally tested and/or verified in order to be utilized in the solution.

The discussions in this section are focused on the experimental results and predictions utilizing the standard material T800/3900-2 as this system was characterized to a sufficient degree in the course of this research to provide all of the input properties necessary to calculate the solution with a reasonable degree of accuracy. The other materials mentioned briefly in Chapter 6 are not compared here as there was insufficient material to experimentally determine the relevant input properties such as G_{IIC}.

9.1 Quasi Static

Selected results of the experiments and the analysis using the MATLAB based prediction tool are shown in Figure 65, which compares the results obtained from experiments with and without clearance to the finite element predictions using the experimentally derived $G_{IIC} = 12\frac{lb}{in}$, and the fastener flexibility correction factor of $K = 0.4K_{Huth}$ established in previous work [2]. In the simulations, no failure load was applied, which is why the predictions show a loading exceeding the tests.

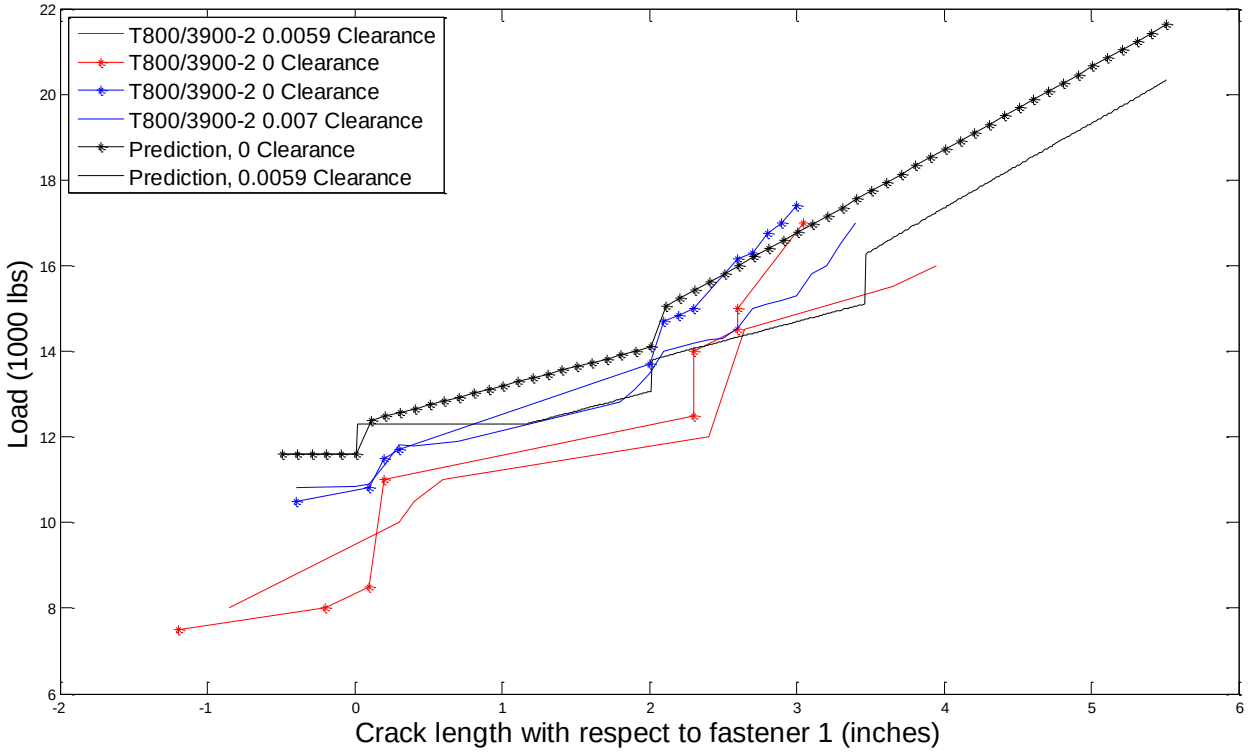

Figure 65: Quasi Static, Quasi-Isotropic predictions vs. experiments

As visible in Figure 65, there is good agreement with the experimental data across different values of clearance. As expected, there is a visible performance decrement predicted by the model which is also visible in the experimental work. However, the loading close to the fastener locations tends to be less accurate, which is to be expected since at this location the crack conditions are much more complex than assumed in this model. Crack curvature has been shown to be extensive and the influence of the load transfer through friction does not occur at a distinct point, however the analysis assumes a flat crack front and that the load transfer through friction occurs immediately at the location of the fastener.

A second comparison, shown below in Figure 66, superposes the predictions and experimental results of the 50% zero quasi-static tests. Reasonable agreement is visible between the test results and the predictions of the arrest performance. Again, no laminate failure theory was included in

the simulations. However, the results show less agreement when comparing the predictions vs. the quasi-isotropic laminates. As the bulk of the work was done using quasi-istropic laminates, the understanding of the dynamics translates relatively well to a harder laminate configuration in capturing the relative behavior of the system, however there is room for improvement in the accuracy.

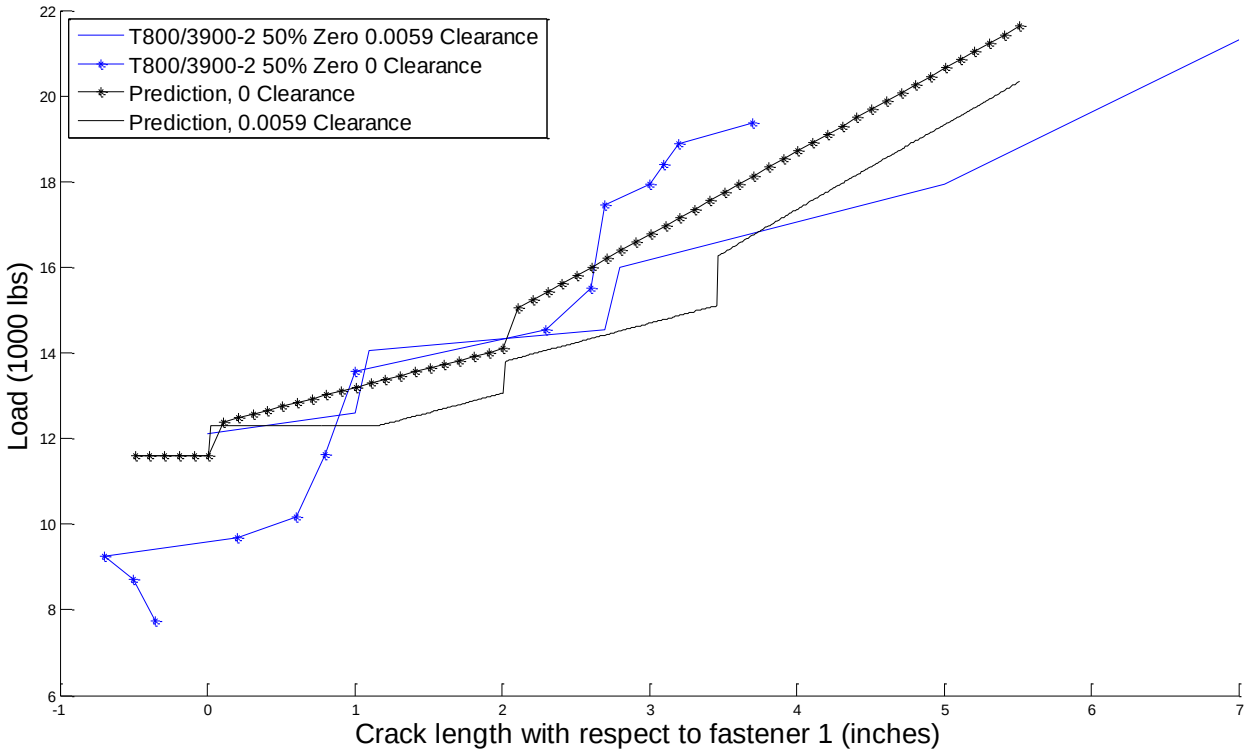

Figure 66: Quasi Static, 50% zero predictions vs. experiments

One of the key parameters that these simulations capture when comparing with the test data is the shape of the curve in both a zero clearance and clearance condition. Figure 66 illustrates the positive slopes of both the experiments and simulations which indicate the delamination arrest features are working as intended.

Overall, the predictive capability of the simulation tool has been shown, demonstrating with various laminate configurations the ability to provide a reasonable estimate of the arrest effectiveness. The above predictions were conducted without any calibration of the model beyond experimental derivation of the properties as described in Chapter 8. Additional calibration can further improve this solution, by tuning the input parameters the solutions can be more finely matched, however, this type of curve fitting exercise does not indicate the ability of the model to make blind predictions.

9.2 Fatigue

The results of the fatigue loading for selected cases are shown in this section, high and low loading of a quasi-isotropic laminate, a varied R ratio of the quasi isotropic laminate and cyclic loading of a 50% zero laminate. This survey of test cases compares the predictive capability of the simulation with the experimental results and reveals areas where the predictive capability is good as well as potentially lacking. Interestingly, there was no consistent trend of under or overprediction which could more easily reveal any specific parameter which is causing the inaccuracy. It is assumed that the imperfect predictions are a result of the relative scatter in fatigue and small variability in parameters which is magnified by the high number of cycles each sample endures. Furthermore, the fastener flexibility reduction factor proposed by Cheung was found to be inapplicable for the fatigue predictions, instead the original fastener flexibility by Huth provided the best agreement. Huth originally developed his formula for fatigue work in joints, so it is theorized that the quasi-static testing performed conformed with the quasi-static loading cases, and his original formula developed from fatigue test data provided better agreement with the fatigue test data presented here [18].

9.2.i Quasi Isotropic Results

Shown in Figure 67 are the experimental vs. predictive comparisons for a loading of 8,000:0 lbs. of load, with both a clearance and a zero clearance drilled fastener. The agreement between the final arrest length is relatively good for these predictions. With no matching of the data, using purely the experimentally derived values of C and m for the research here the agreement is reasonable, but as described in 11.1 altering these values would serve to drop the curves down to more accurately match the experimental results. The final crack lengths show good agreement with the experiments, the two test results shown below were chosen to show the extremes of the disagreement with the prediction.

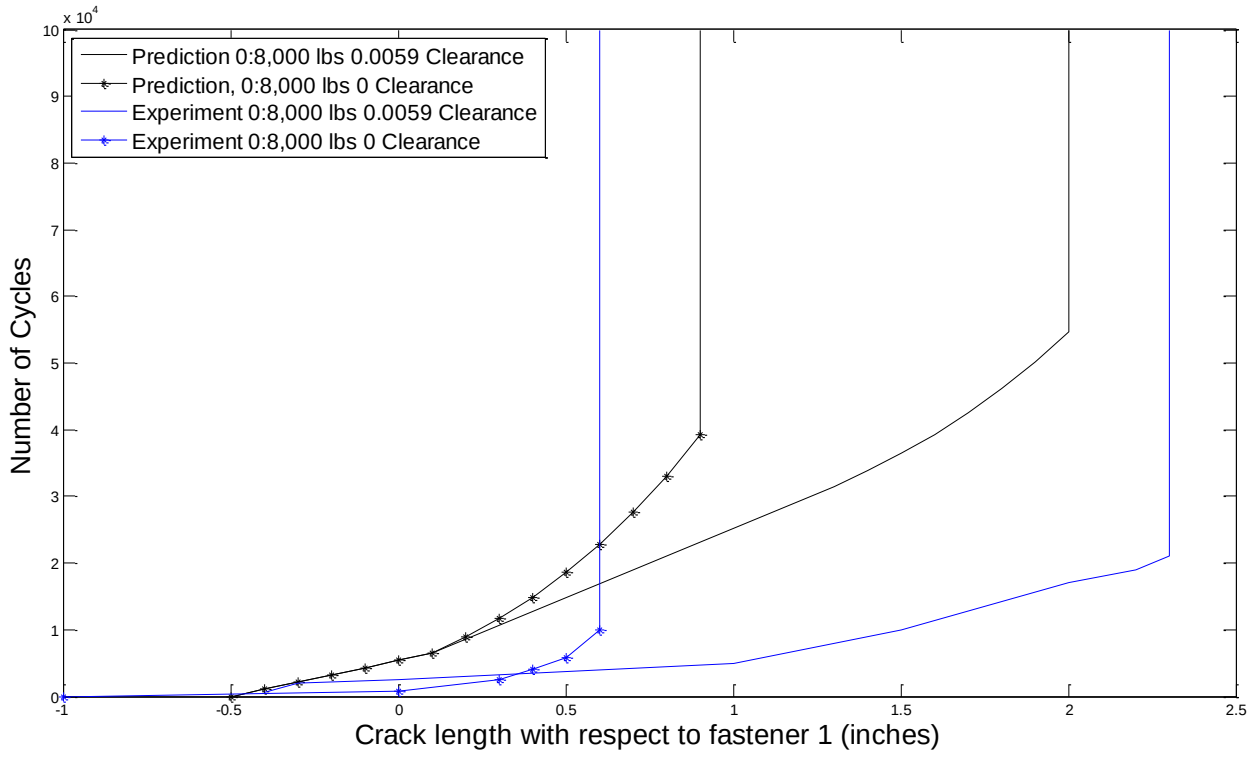

Figure 67: Experiments and Analysis Comparison, Quasi Isotropic, Loading of 8,000:0 lbs.

Additional testing was conducted at higher loading, 12,000:0 lbs., on a quasi-isotropic laminate and is plotted against the predictions in Figure 68. Agreement between the experimental and analysis results are poor, with the theorized reason being hole damage, as shown in Figure 69. The agreement between the clearance simulation and the "zero clearance" experiment shows better agreement. However, measuring the hole diameters after testing, the elongation was 0.001-0.002, not 0.0059. On examination of the sample, the large visible damage zone around the fastener may have provided an equivalent degradation of the stiffness to match an effective clearance of 0.0059.

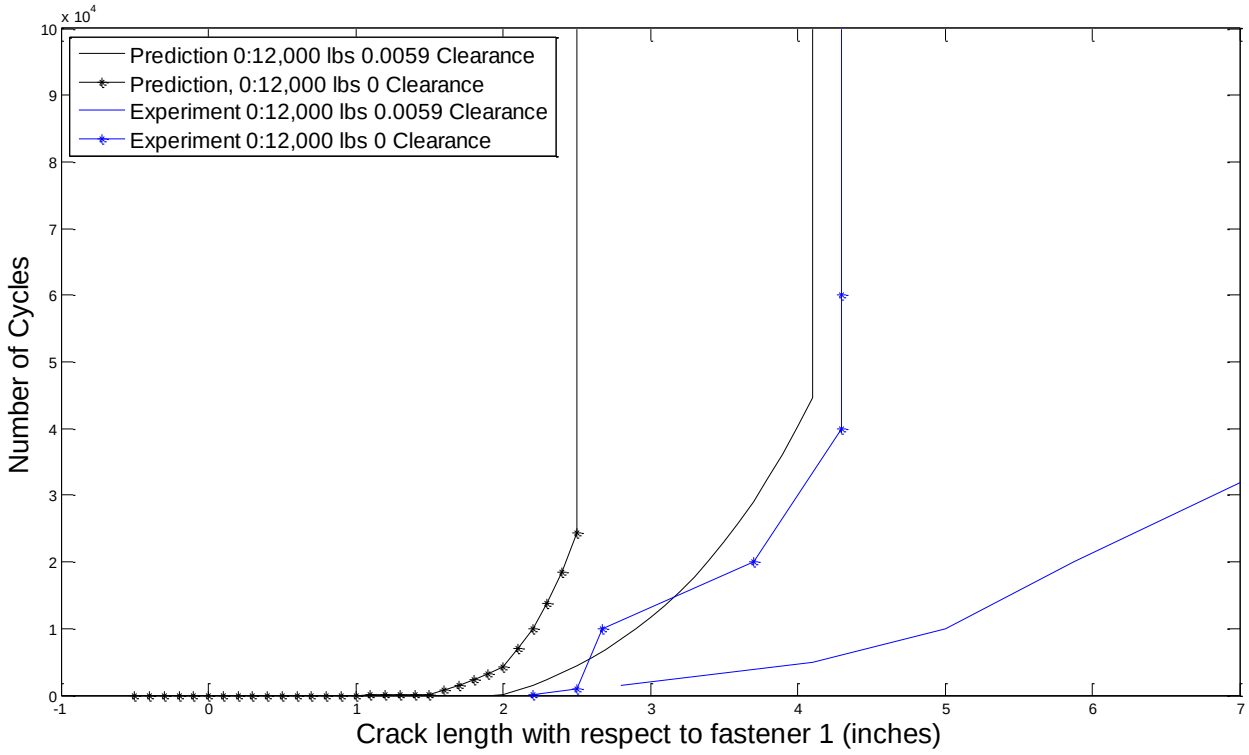

Figure 68: Experiments and Analysis Comparison, Quasi Isotropic, Loading of 12,000:0 lbs.

One possible explanation of the lack of agreement in these results is the effects of hole damage, which is most visible under this loading condition with high maximum and high cyclic stresses. A typical sample is pictured in Figure 69. This damage was not observed in other fatigue tests,

and when comparing the experimental results with the analysis, much better agreement is observed in the other solutions. Hole damage is equivalent to increasing the value of clearance in the system, and, as readily apparent in each of the simulations, increasing clearance results in a loss in arrest capability. This discrepancy could be rectified by making a further non-linear fastener spring with either a spring stiffness that degrades proportionate to the cycles, or a clearance which increases with respect to cycle count.

Figure 69: Hole damage interface (left) and underneath washer (right) after fatigue testing

9.2.ii R=0.33 Results

A comparison of the predictions and experimental results for R=0.33, with a loading of 12,000:4,000 lbs. is plotted in Figure 70. Noticeably better agreement is achieved between the zero clearance results and prediction compared to the clearance drilled prediction which projected much greater crack growth than was observed. This solution is dependent on the crack length at which the value of ΔG passes below the threshold value, which is driven by the assumed value of clearance and the load transfer through friction, both of which provide load alleviation at the crack tip and consequently greater crack arrest than predicted.

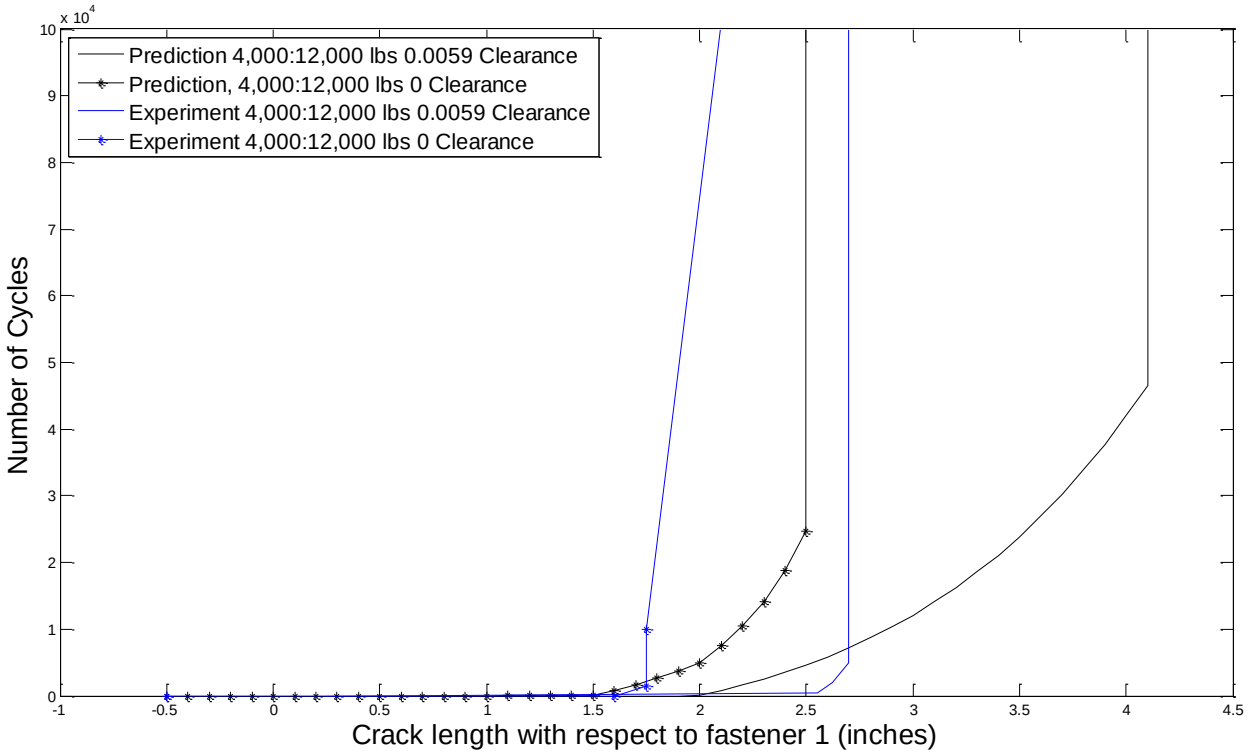

Figure 70: Fatigue Experiments and Analysis Comparison, Quasi Isotropic, Loading of 12,000:4,000 lbs.

9.2.iii 50% zero Results

Figure 71 compares the fatigue experiments and analysis for a 50% zero laminate. Experiments were only conducted using clearance drilled samples at two different maximum loads, 12,000 lbs. and 9,000 lbs., both with an R ratio of 0. Of particular note, with raw predictions, the same input parameters are utilized for these predictions. The solutions capture the general trend of the data, but don't match the number during the crack growth phase. The final crack lengths however show reasonably good agreement.

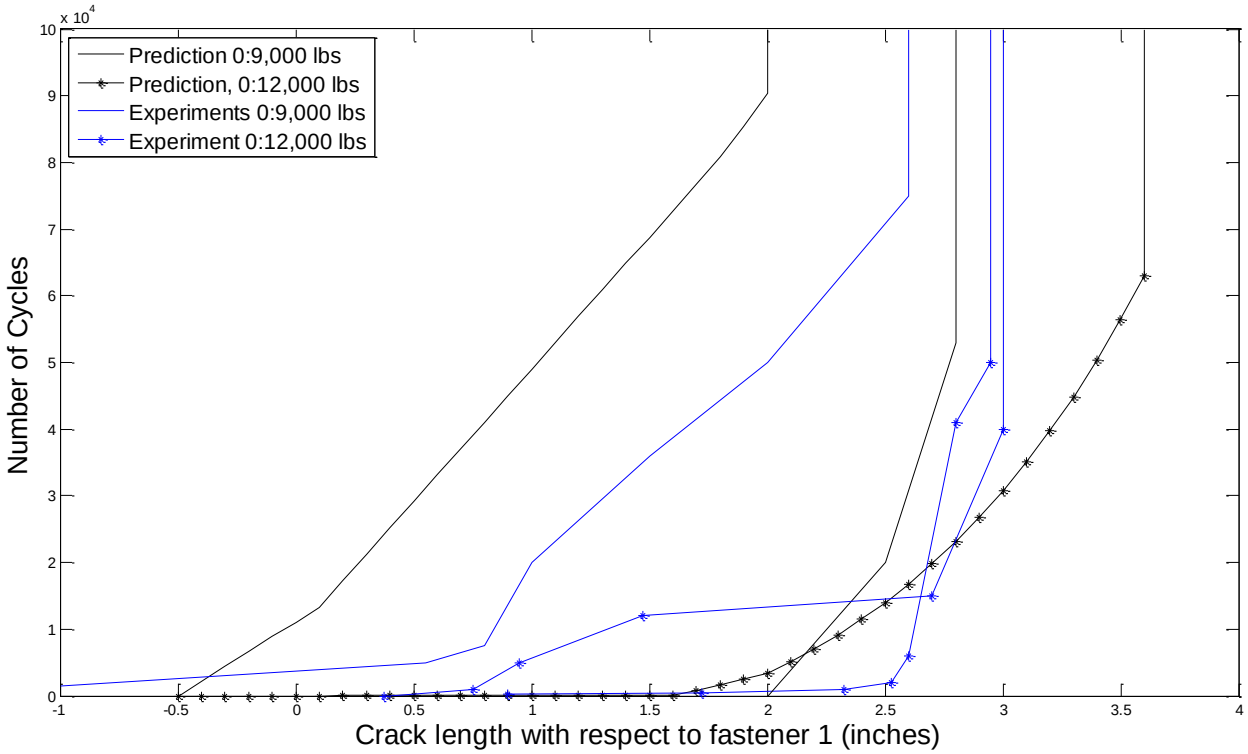

Figure 71: Fatigue Experiments and Analysis Comparison, 50% Zero

9.3 Discussion

For prediction of both quasi-static and fatigue delaminations, the predictive tools have been shown to have good agreement with the experimental results, provided that the input parameters be accurately determined. Under static loading, it was found that G_{IIC} changes resulted in significant changes in the predictions, and accurately measuring the value for the given material system at hand instead of employing published values is necessary for agreement. Similarly, with fatigue loading, accurate measurements of the load transfer through friction and fatigue properties resulted in good agreement across multiple cases.

Of particular note in the fatigue data, there is no consistent over or underprediction of the analysis, and therefore no indication of a specific inaccurate input parameter. Instead, data which

is over and underpredicted is attributable to the loading conditions, clearance and R-ratio. A reason for this variation is the interplay of the hole damage which reduces the fastener effectiveness under high fatigue loading but does not occur under lower loading.

The results of the experiments show a clear benefit provided by delamination arrest fasteners under both static and fatigue loading with a number of different load and laminate configurations. Furthermore, comparisons between the analysis and experimental results shows the ability for relatively accurate predictions of the delamination arrest capability of the fasteners under a myriad of conditions while utilizing a simple one dimensional model.

There remains room for improvement and generalization of the work provided here. The scope of this research is limited to constant amplitude loading of monolithic composite laminates, any deviation from this may result in a breakdown in the predictive capability. Further avenues of study are discussed in 13.7 .

Chapter 10 Various Avenues not further pursued

All of the previous work presented highlights the successful avenues of investigation which yielded beneficial results that enhanced the understanding of the crack growth and arrest in the presence of delamination arrest fasteners. This chapter will instead highlight some of the less successful and thus less pursued areas of study.

10.1 Smaller sized samples

The unfastened fatigue delamination samples were created using a thinner laminate in comparison to the fastened fatigue samples in order to maximize efficiency of time and materials. One concept that was explored during the initial research was testing sub-scale fastened fatigue specimens, of 1/3rd the thickness, as pictured in Figure 72. The choice of 1/3rd the thickness was made because the original quasi-isotropic sample sublaminates had a three times repeated and then symmetric layup. Having the same quasi-isotropic, symmetric layup but not repeated then yielded a 1/3rd scale sample. The sample width was also cut to 1/3rd of 1.25 inches, and the fastener installed in the sample was approximately 1/3 the diameter, the closest size was D=0.0860 inches, which is $\frac{1}{2.9}$ times the diameter of the stock ¼ inch fasteners.

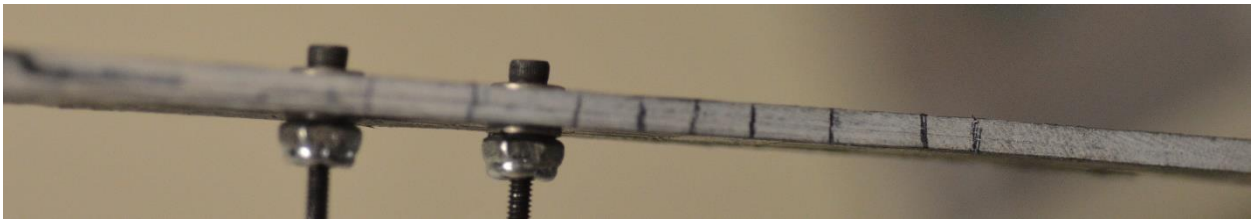

Figure 72: Subscale samples

The markings above, where the crack was measured at regular cyclic intervals, show that on these smaller samples, the fasteners provide delamination arrest capability in the same manner as the greater sized samples. However when attempting to measure the crack growth, the variability in measurements, in part due to the resolution of the tools and method of crack length measure was too great to compare with predictions beyond a qualitative impression.

10.2 Countersunk Fasteners

Another one of the original ideas was to compare the performance of countersunk vs. protruding head fasteners, as it was theorized that the countersinking would improve the performance due to greater engagement. Two different types were employed, those with a relatively large head Figure 73, left, and a small head which required less cutting of the laminate, Figure 73 right.

Figure 73: Typical Countersunk titanium fasteners

However, under quasi-static loading, the delamination response was largely the same when tested using a quasi-isotropic laminate only, although the smaller headed fasteners could not support as great installation torque due to their relatively small contact area with the laminate. For fatigue loading however, the countersunk fastener heads tended to very consistently fail. After numerous recurrences of fatigue failure, countersunk heads were abandoned.

10.3 High values of Clearance

Testing of samples in quasi-static loading originally consisted of tests performed utilizing E, F and H drills, which represented 0, 0.007 and 0.016 inches of clearance respectively between the fastener shank and hole. However, initial experiments resulted in highly unstable crack growth for the largest value of clearance, and this was subsequently abandoned. While the H drilled fasteners can be assumed to eventually engage in shear, their arrest benefit was so poor that the current sample length of 17 inches was not long enough for the arrest response to be adequately captured.

Continuing into fatigue, it was noted that the F drilled fasteners tended to not engage in shear under low loads, with friction accounting for the load alleviation required to arrest the crack. When subjected to higher loading, the samples had extensive crack propagation. The next smallest available drill bit was 6.5mm, or 0.2559 inches in diameter, which reduced the clearance, by 0.001 inches, and this drill size was subsequently utilized for the fatigue testing.

10.4 Smaller Fasteners

During the course of this project, it has been noted multiple times that the tensile properties of the fasteners greatly exceeds what is necessary in order to effectively eliminate the mode I component of delamination. As a result, smaller diameter, 6-32 fasteners (D=0.1380) were utilized to compare the delamination response. However, as the quasi-static arrest performance of these was poor, further variations were not pursued.

This is not to say that smaller fasteners, arranged appropriately, will not provide an arrest benefit since smaller diameter fasteners did provide mode I elimination, and some shear load transfer.

However the challenges of appropriately designing the arrest pattern and installing this was considered superfluous to the core of this research.

10.5 Post Damage Installation of Fasteners

Under static loading, samples were generated with only a single fastener in order to compare their response to the single fastener experiments conducted previously [2]. Typically the samples were loaded such that the crack grew past the planned installation point of the second fastener. They were then unloaded and the second fastener installed. Reloading of the sample showed a change in the load vs. crack length curve to a curve which matched the tests conducted on entirely two fastener samples.

During the course of the fatigue testing, fastener heads would occasionally fail due to bending. As the machine was programmed to stop if the displacement grew too rapidly, indicating extensive crack growth, it was possible to remove the sample and reinstall a fastener after additional or minimally arrested crack growth occurred. Restarting the samples showed a subsequent restoration to the original delamination arrest capability, despite the additional crack growth.

This suggests that installation of the fasteners is insensitive to the pre-existing crack growth and post-damage installation provides equivalent arrest capability to installation immediately after manufacturing.

10.6 Off-center holes

Occasionally, samples were generated where the holes, either one or both, were not located along the centerline of the laminate, as seen in Figure 74. As these samples were already constructed,

it was decided to also test their response under quasi-static loading as they represented an extreme case of a failure in the manufacturing process.

Figure 74: Offcenter hole

Testing of these samples, recorded in Figure 75, showed a surprisingly close delamination response, and thus a relative insensitivity of the delamination arrest feature to the location of the hole across the width. Although C-scans were not taken of the sample, it is assumed that the crack shape around the fastener varied such that the tip of the inverted V was centered on the fastener hole, leading to a highly asymmetric crack tip. In the interests of time and resource efficiency, the limits of this capability was not investigated, only samples which could not be utilized in the primary research due to poor quality were employed to investigate this. As a result, a statistically significant sample set was not obtained, but from qualitative observation, there was a relative insensitivity.

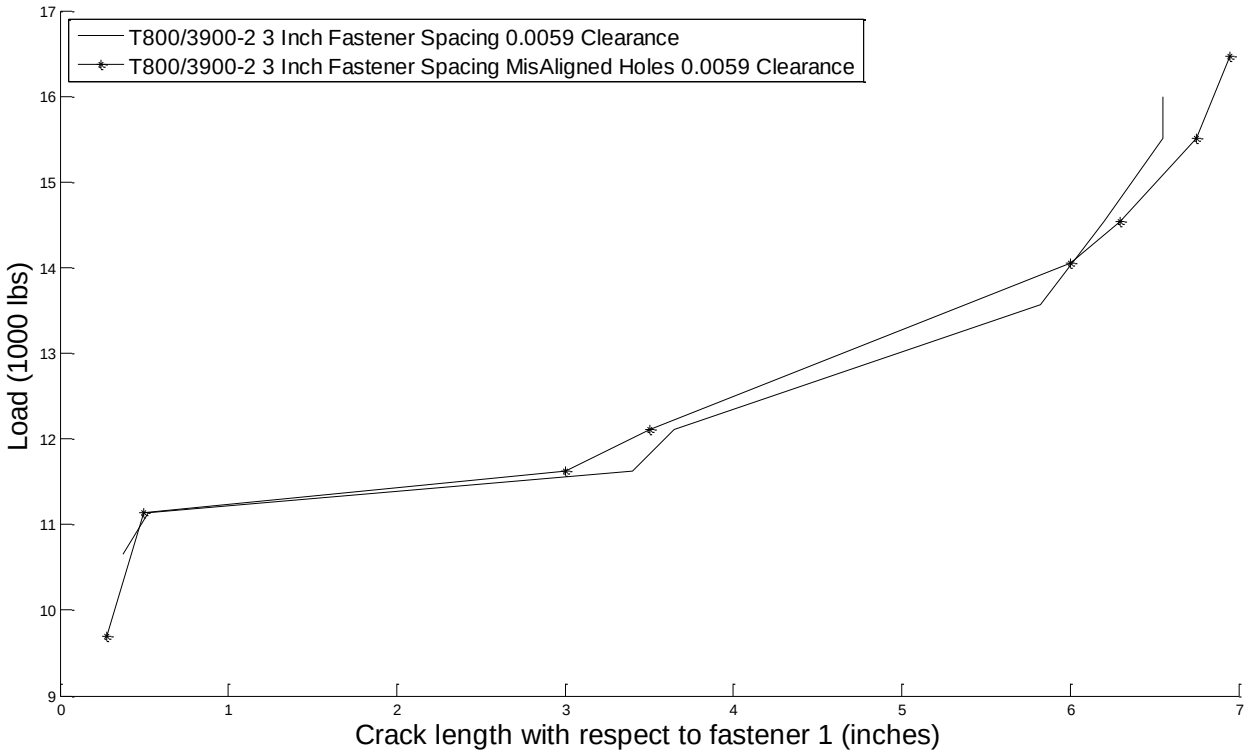

Figure 75: Offcenter hole vs. centered hole response

Chapter 11 Parametric Studies using Prediction Tool

One of the primary benefits of the predictive tool is the ability to customize various parameters in order to perform parametric studies as well as better understand which input parameters played the most critical roles in accurate prediction of the final delamination arrest performance of the laminate. The influence of some of the key input parameters were subsequently discovered using this method.

Six different studies are described in this chapter which represent five of the most important design considerations as well as the importance of friction when creating a part which utilizes delamination arrest fasteners to improve the damage tolerance. Sections 11.1 and 11.2 represent material selection choices, as these are material properties which are not altered by the arrest feature design. The following two sections, 11.3 and 11.4 discuss controllable design parameters, changing both the size and spacing of the fasteners. Section 11.5 compares the predictions with and without the inclusion of frictional load transfer in fatigue. Finally, section 11.6 represents situations where the crack is not propagating along the centerline, or if the part design calls for an asymmetric laminate.

11.1 Changing C and m in the Paris Law

In particular, for fatigue loading, the Paris law ($\frac{da}{dN} = C\Delta G^m$) relies on coefficient C and exponent m in order to describe the crack growth vs number of cycles. For a given material system, these values are fixed material properties. Additives to the matrix, which serve to improve the static delamination resistance, may aid in improving the fatigue life as well.

Changing the values of C and m in the Paris law serve to alter the slope of the line which represents the crack growth per cycle for a given value of ΔG. For fastened fatigue specimens, this changes the number of cycles required to reach a certain crack length at a fixed load, as shown in Figure 76. When including a threshold value of ΔG_{th} in the analysis, which in effect assumes the crack growth halts below this value, changing C or M does not change the final crack length. If no threshold is found, then the final crack length for a given number of cycles is increased.

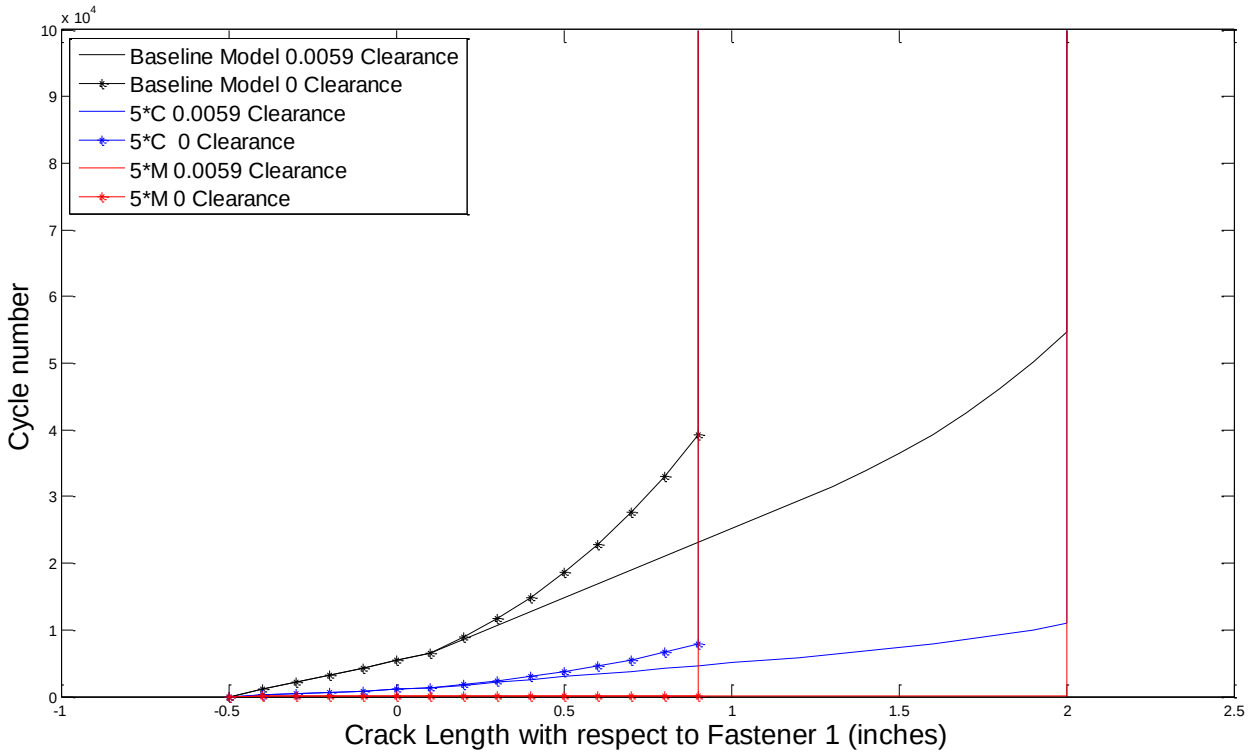

Figure 76: Results of Changing C and m in the Paris Law

Seen above in Figure 76, changing the value of C and m, which correspond to the rate of crack growth per cycle, alters the number of cycles, but for a constant ΔG_{th}, does not alter the ultimate crack length at arrest. Increasing the value of either C or m will lower the curve, which when comparing previous experimental and analytical results, can improve the agreement between the

curves. Similarly, accurate prediction of the values of c and M is critical to the accurate prediction of the crack growth curve of a laminate, particularly with delamination arrest features which alter the value of ΔG as the crack extends down the length of the laminate.

11.2 Using a $G_{II_{crit}}$ and ΔG_{th}

Typically, materials have a fatigue threshold. In metallic structures it is more commonly referred to as ΔK_{th}, but for composites, where the strain energy release rate G is utilized instead, $\Delta G_{II\,th}$ is utilized. This value is experimentally derived by testing samples at various ΔG levels and finding the point at which the crack does not grow. Similarly, at high values of G_{II}, mode II delaminations will occur, typically the quasi-static value of G_{II} is then denoted as G_{IIC}. However, in the course of this research, it was found that a second value of G_{II}, which was lower than G_{IIC} caused crack growth at rates significantly greater than predicted by application of the Paris Law. This values is then denoted as $G_{II_{crit}}$ in order to delineate it from the quasi-static G_{IIC}.

Figure 77 plots a number of different combinations of $G_{II_{crit}}$ and $\Delta G_{II\,th}$. Examining the results, changes in $\Delta G_{II\,th}$ are much more readily apparent than those of $G_{II_{crit}}$. Changing the value of $G_{II_{crit}}$ only changes the initial crack growth response, which at high values of ΔG_{II} is still quite rapid, even when applying the unaltered Paris law at all values of G_{II}<G_{IIC}. However, changing the value of $\Delta G_{II\,th}$ changes the results of the simulation dramatically. The assumption is that once $\Delta G_{II} < \Delta G_{II\,th}$, then $\frac{da}{dN} = 0$ and the crack stops growing. For fastened delamination specimens, as the crack grows, the value of ΔG_{II} decreases as the fastener engages more and more in shear and thus for lower values of $\Delta G_{II\,th}$, a greater crack length is required for $\Delta G_{II} < \Delta G_{II\,th}$.

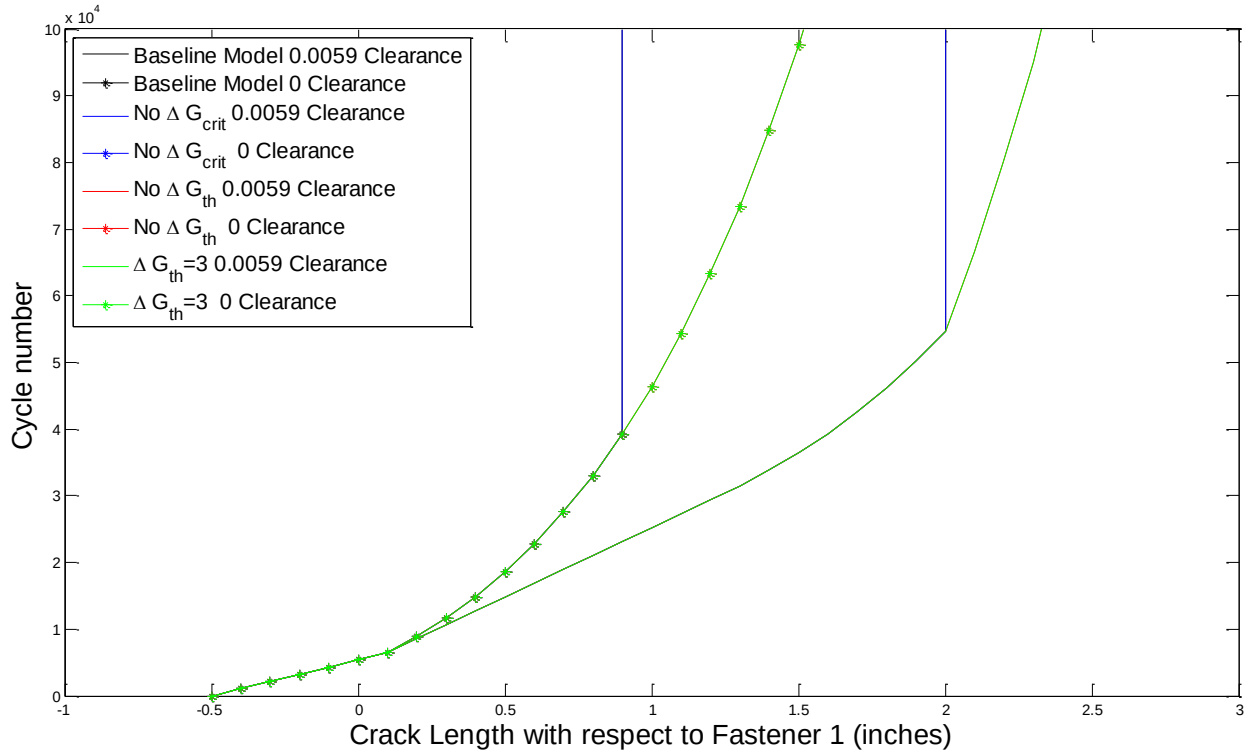

Figure 77: Results of changing $G_{II_{crit}}$ and ΔG_{th}

As visible above, by decreasing the value of ΔG_{th} from 5 lb./in to 3 lb./in, the curves diverge, but decreasing it further to 0 does not result in further divergence in the area shown. Further crack growth is required and divergence of the $\Delta G_{th} = 0$ and 3 lb/in curves occurs only at approximately 300,000 cycles, beyond what was typically observed in the research here. Each material system will have a different ΔG_{th} so experimental investigation is required for each change in material.

11.3 Fastener sizing

The size of the fastener determines both the weight added due to its installation as well as the strength loss in the component due to the drilling of holes and loss in net section area. As discussed in previous work by Cheung [2] and tested briefly in the research presented here, the

0.25 inch fasteners utilized for shear engagement are dramatically oversized for mode I elimination. Samples were tested with 6-32 bolts, which have a diameter of 0.1380 inches. These smaller fasteners served to completely eliminate the mode I component but did not perform well under mode II loading and thus were not pursued further in the course of this work.

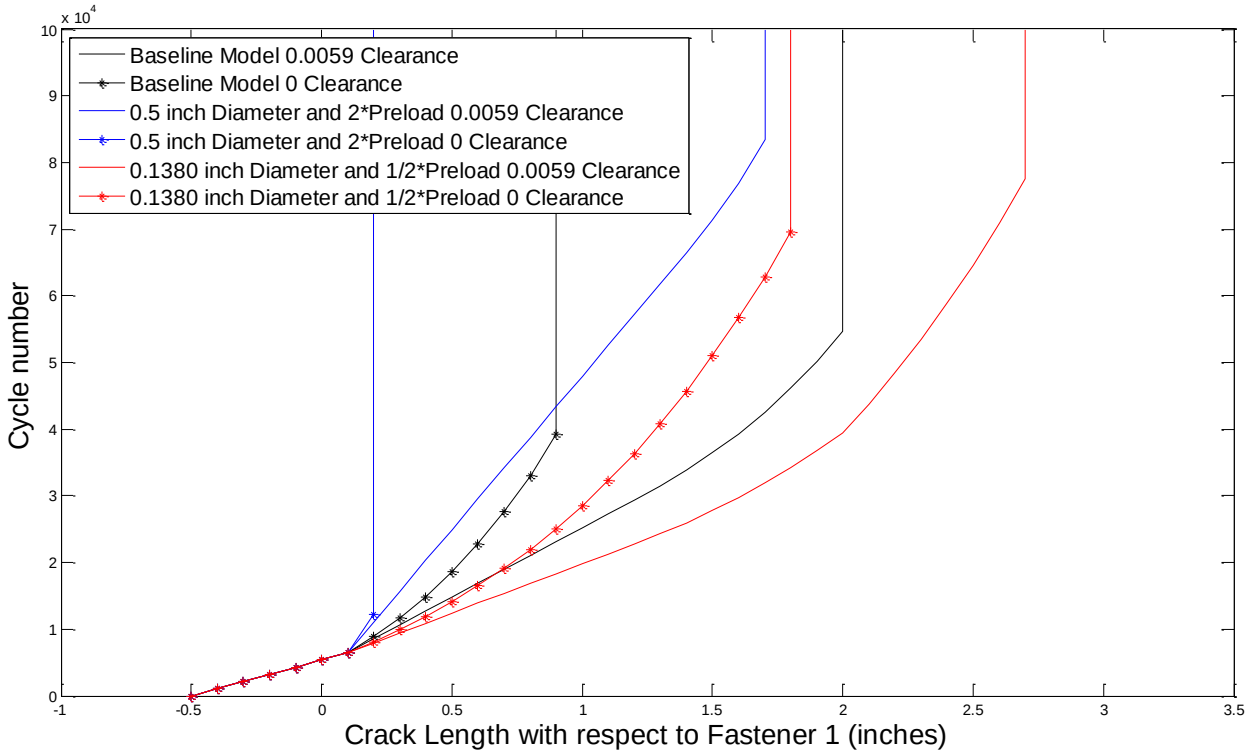

Figure 78: Results of changing the fastener size

As seen above, smaller fastener diameters provide less arrest capability, with the tradeoff of less weight. Each reduction in the diameter by ½ reduces the weight of the fastener by approximately 4 times, leading to an optimal design which balances the performance/weight ratio. The reasons for this reduction in effectiveness is that smaller diameter fasteners have a lower fastener flexibility and thus provide less load transfer through shear. Additionally, they cannot support as high of a preloading, reducing the load transfer through friction. For the above simulations, the preload was assumed to be ½ the baseline preload. Conversely, stiffer fasteners provide greater

load transfer through shear, and in the above, were assumed to withstand 2x the base preload, showing significantly better arrest capability, particularly with zero clearance. When clearance is utilized, the benefit is not as dramatic because although the fastener provides more load transfer in shear, the crack must extend by the same amount before the fastener can engage.

11.4 Fastener Spacing and Number

Changing the fastener spacing can be seen to have a dramatic effect on the maximum crack length achieved, but not a significant effect on the shape of the response. Comparisons of a fastener spacings of 1.25, 2, 3 and 4 inches, which correspond to 5, 8, 12 and 16 times the diameter of the fastener are shown below in Figure 79. Each response has the same typical 2 points where the load required to propagate the crack increases and the slope of the line becomes steeper, however the location at which this occurs varies based on the fastener location. The closer fastener spacing can be seen to arrest the crack by causing the propagation load to exceed the failure load at a shorter overall distance, therefore the spacing ultimately becomes a design decision based on the maximum allowable crack length for a given component.

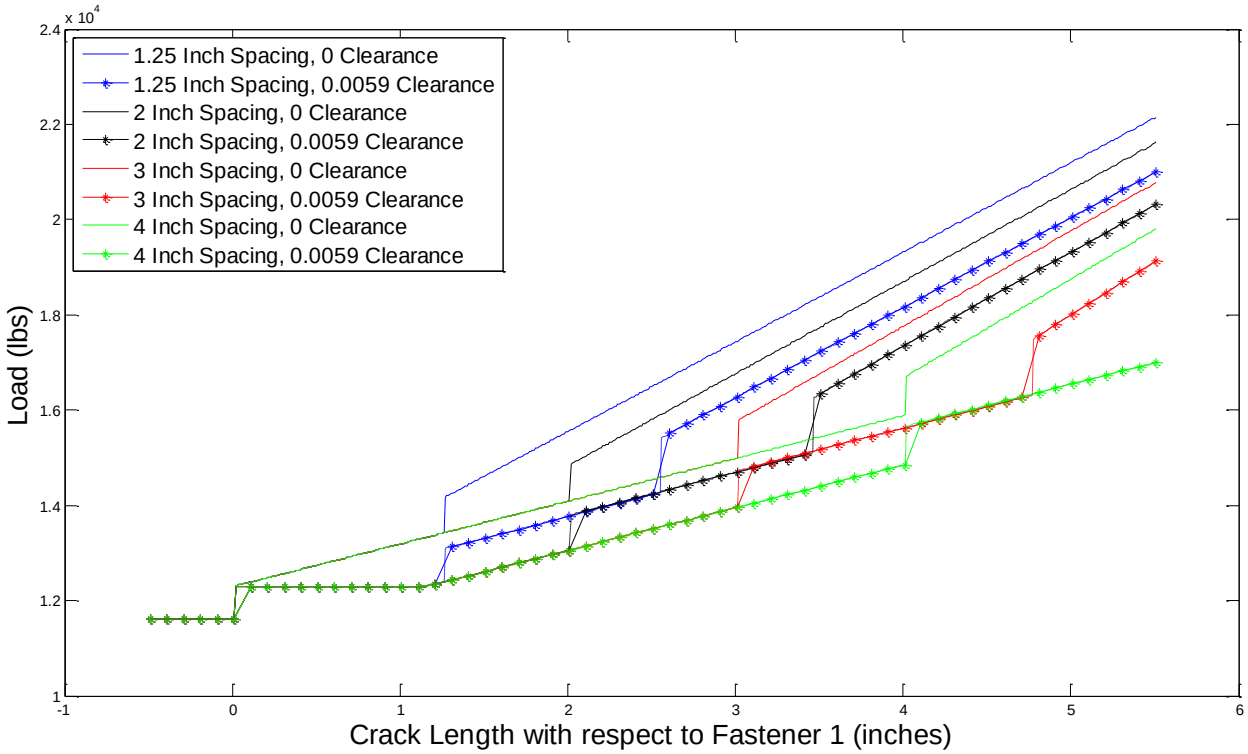

Figure 79: Changing the Fastener Spacing

Similar results can be obtained by increasing the number of fasteners. Each fastener will contribute in exactly the same manner as the second fastener, providing additional load transfer through friction and shear. The slope of the propagation curve will then become steeper as each fastener engages in shear until the point at which the laminate fails due to a competing mode. In conjunction, a fully fastened laminate will be inefficient as noted for various cases discussed in previous chapters; arrestment would occur prior to the delamination reaching a third fastener, thus this third fastener would only be adding weight, not capability under these conditions.

Similar results are obtained under fatigue loading. As seen in Figure 80, increasing the fastener spacing from 2 to 3 inches causes additional crack growth under clearance drilling conditions, but the behavior is unchanged for zero clearance conditions with a loading of 8,000:0 because the crack is arrested prior to the second fastener. When the fastener spacing is increased to 3

inches, the crack extends further but is then arrested due to the greater load transfer in shear by the first fastener and in fact, the second fastener is contributing no arrest capability in this situation.

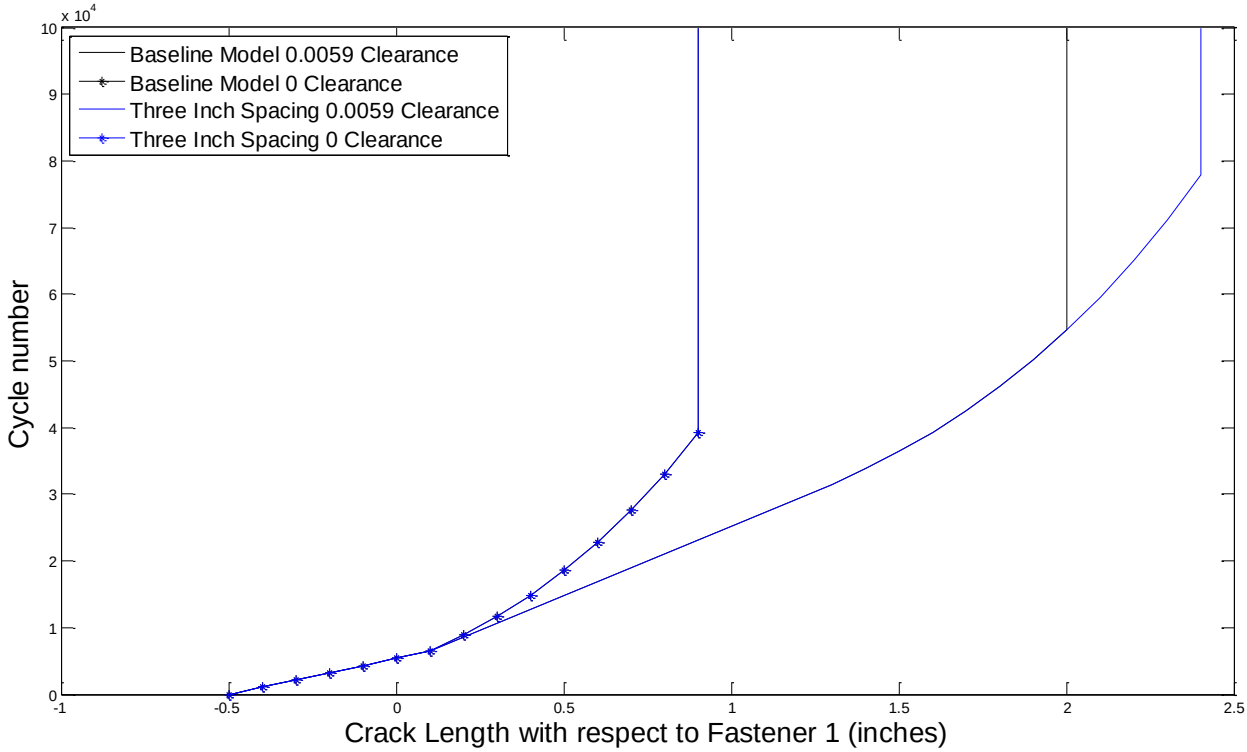

Figure 80: Increasing the fastener spacing under fatigue loading

11.5 Zero Friction

Commonly in analysis, the effect of friction is ignored, however in the research presented here, it should not be, as inclusion provides improved agreement with the test data. Furthermore, the more accurate predictions allow for increased weight savings by eliminating redundant fasteners from the system.

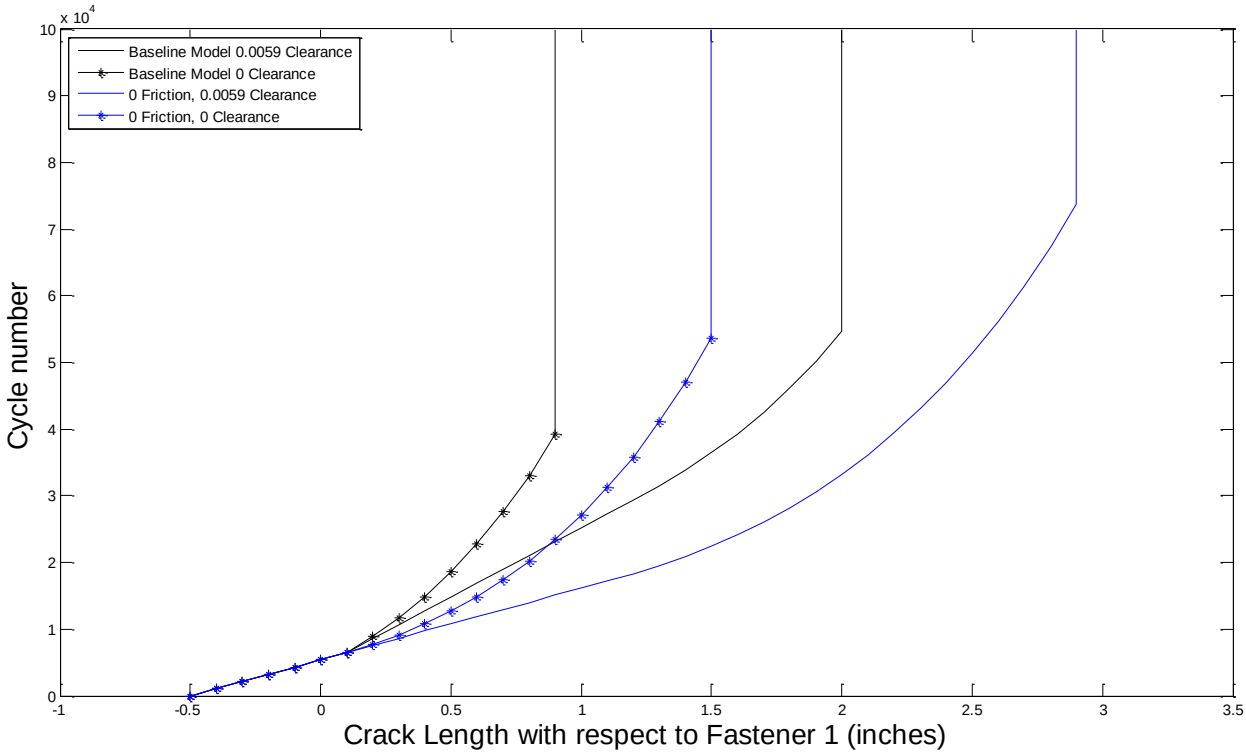

Figure 81: Eliminating the friction loading of 0:8,000 lbs.

Figure 81 compares the predictions with and without the inclusion of friction at a loading level of 0:8,000 lbs. Without the inclusion of friction, the crack length grows at least 50% longer compared to the predictions with friction included.

11.6 Asymmetric Specimen Stiffness

For cracks which occur not along the centerline, or for disbonds which occur between two components of unequal stiffness, the driving force of the crack can be increased or decreased in comparison to a baseline symmetric laminate system. One example is that it is common for the skin and stringer to have different layups. The method of loading, in this case loading either the stiffer or softer component, also plays an important role in the growth of the delamination.

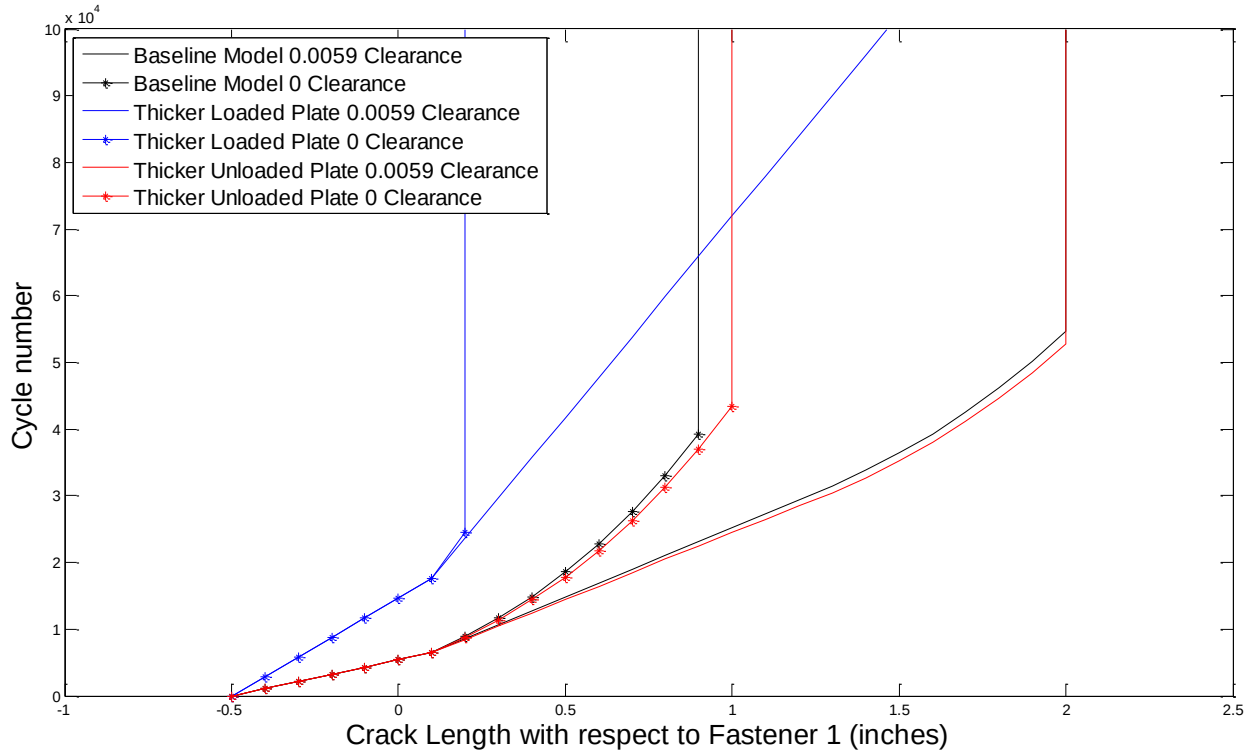

Figure 82: Changing the relative stiffness of the two plates

As visible above in Figure 82, increasing the stiffness of the loaded portion has a much more dramatic effect on the delamination response as compared to increasing the stiffness of the unloaded portion. The portion which is loaded, when stiffer, either because it is thicker or made of a harder laminate, will carry more load without stressing the crack tip, which is highly beneficial to preventing delamination growth. Another important suggestion of this parametric study is that having an asymmetric configuration, either intentionally or unintentionally due to the crack location through-the-thickness does not dramatically reduce the arrest capability of the fastener system.

Chapter 12 Discussions on Application of Delamination Arrest Fasteners

Delamination arrest features represent an added weight and expense in the design of a structure. Also, arrest fasteners, among other solutions, degrade the ultimate strength of the component and require additional steps during the manufacturing processes. However for fail safe structures such as aircraft, or for improved longevity in other structures such as ground vehicles, they provide a benefit in damage tolerance and for certification. Minimizing their number and impact on the structure thus should be the goal of a designer. The research presented here is intended to guide the designer when determining areas of interest for arrest features.

12.1 The need for delamination arrest features

In order to provide fail safety of strength limited structures in delamination, delamination arrest features are necessary, particularly if there is a potential for mode I delaminations occurring. Not shown, but for the same delamination specimen, loads of 6-8,000 lbs. were sufficient to cause the delamination to grow through the entire length of the specimen if no fasteners were installed. The typical failure load of the quasi-isotropic laminate was 16,000 lbs., meaning that if the mode I delamination was not arrested, the laminate fails in delamination at less than ½ its ultimate strength. Similarly, under fatigue loading, the installation of the fasteners improves the life from 1 cycle to 250,000+ cycles.

These dramatic improvements in damage resistance both in static and fatigue loading indicate the need for delamination arrest features. Fasteners are one of many different arrest features, each with their own pros and cons. The research here focused on thick laminates which most

commonly employ fasteners as the other methods such as z-pins or stitching are unable to penetrate laminates of this size.

From a material science standpoint however, improvements in matrix formulations can continue to reduce the need for, and in some cases eliminate, delamination arrest fasteners. The original matrix materials were highly brittle and prone to delamination. The introduction of toughenners has reduced the need for delamination arrest features as the matrix itself is more highly resistant to delaminations. Good analysis techniques, combined with a knowledge of the material system, can then investigate areas of the structure where improvements in matrix toughness obviate the need for arrest features.

Finally, delamination arrest features serve as a damage resistance and damage tolerance device for the aircraft structure. Impact damage [1] can create extensive delaminations. Arrest features serve to limit the growth of these cracks both during their formation as well as during the component's service life. Without these arrest features preventing growth due to structural loads, the tolerance of the part to potential in service damage would be significantly lower.

For various configurations, it is impossible to remove the need for delamination arrest features, but minimizing their impact to the structure is of high importance. One way to accomplish this is to have all the fasteners in the structure serve as dual use fasteners. The primary employment of these fasteners is the attachment of components, such as shear ties, with analysis also showing their capability for delamination arrest.

12.2 Expected level of benefit and limitations

The expected level of benefit a delamination arrest fastener can provide is highly dependent on a number of factors both within and beyond the designer's control. The final decision on the implementation of fasteners as an arrest feature is subsequently an interplay between these various parameters which will serve to arrest the delaminations.

It is key to balance the expectations of the capability of delamination arrest fasteners. The above research has shown arrest fasteners excel with relatively tough laminates with relatively high fatigue delamination resistance. As briefly touched on in the experimental work of Chapter 6, for more brittle laminates, the delamination arrest fasteners provide significantly less benefit, especially when installed with clearance. Crack growth under these conditions was extensive, and different means of reinforcement, or redesign to tolerate extensive cracking may be required.

12.2.i Controllable parameters

The first and foremost conditions of fasteners as an arrest feature is that they do not become effective until the crack has reached them. Prior to the crack reaching the fastener, they provide no arrest benefit in mode II, through shear or frictional load transfer. Depending on the stiffness of the laminate, they may begin to eliminate mode I prior to the crack reaching the fastener, with stiffer laminates experiencing mode I elimination at slightly shorter crack lengths. However in all of the cases tested here, visible mode I elimination was 1-2 fastener diameters away from the fastener hole at the maximum.

The above caveat relates to the maximum crack length which is allowable for the component. The maximum allowable crack length is a design parameter which depends on the application. For a composite beam in pure bending under constant load, this length may be determined as the

point at which the bending stiffness is excessively degraded due to delamination. However, as the fasteners cannot provide significant load alleviation until the crack has reached or passed said fastener, it is necessary for the fasteners to be placed such that they engage significantly prior to the maximum allowable crack length.

Furthermore, fastener pitch is constrained by the diameter of the fasteners, and each fastener does not engage until after the crack has passed the fastener, meaning that the minimum fastener pitch constrains how quickly additional fasteners can become effective in arrest as the crack grows. Spacing, size and number will then be affected by the maximum allowable crack length. For short maximum allowable crack lengths, a single larger fastener may provide more efficient arrest at a tradeoff of greater impact on the pristine laminate strength. The fastener pitch between two smaller fasteners may be too great for the allowed crack length. Tools such as those developed here can help optimize the design, facilitating studies to attempt to find the most appropriate configuration of fastener size and pitch.

The fastener flexibility is controlled by the fastener size and to a lesser extent the material. As seen in Table 3, nearly doubling the modulus of the fastener only changes the fastener flexibility by 10%, and the increase in density, switching from titanium to steel does not justify this change. However, increasing the diameter will increase the stiffness of the fastener in shear and provide increased load transfer, changing from a 0.25 to 0.30 inch fastener increases the shear stiffness by 13% for the quasi isotropic sample specifications, trading off a greater loss in the ultimate strength of the part due to larger holes. Although larger is better for delamination arrest, the maximum fastener size is constrained by best practices in order to avoid compromising the tensile strength of the laminate.

Meanwhile, as the crack propagates along the length of the part, engaging each fastener in shear, the first fastener to be engaged is providing sequentially more and more load transfer. Thus, a long installation of fasteners in shear will not provide as dramatic of an arrest capability as the striking installation of fasteners would suggest. The fastener furthest from the crack front will be carrying the bulk of the load while the fastener closest to the crack tip will be carrying a minimal load and all fasteners which the crack has not reached will provide no benefit at all. This again reinforces the idea of the careful weighing of the benefits of fewer stiffer fasteners vs. a greater number of small fasteners.

The last design specification which is largely controllable is the clearance within the fastener hole. Seen throughout the research presented here, clearance is a key design parameter, the introduction of clearance leads to significant losses in delamination arrest capability, especially under fatigue loading. As the fasteners cannot engage in shear, minimizing the clearance of the system will result in fastener shear engagement of the fasteners, albeit with the tradeoff of potentially increased manufacturing difficulty.

Finally, all of the above does not consider fastener failure, which for various configurations is a valid concern. Under fatigue loading, the fastener head failure has been observed, and for static loading, using too small of a fastener may result in overloading and failure of the shank in the same manner as overloaded non-bonded joints.

12.2.ii Relatively Uncontrollable Parameters which affect benefit

In contrast to the above parameters, such as fastener size and pitch, which are controlled by the design engineer, two properties that affect the benefit of the arrest features which are typically not controllable in the design are the matrix properties and the load transfer through friction.

These are largely material properties, both of the laminate and the fastener system and typically are much more difficult to change.

The delamination properties of the matrix, both in quasi-static and fatigue loading are difficult to change during the design of the part. Typically the matrix is chosen due to desired manufacturing processes, compatibility with the fiber type and availability. For production parts, designing, testing and certifying a new resin system is unlikely to happen, so the designer is left with the properties provided by the matrix at hand. Under these conditions, generally tougher matrices will provide more arrest benefit in conjunction with the fasteners as the resistant material provides the ability for the fastener to engage in shear prior to catastrophic delamination failure. For brittle materials, delamination growth will tend to be more rapid and the fasteners will be unable to provide significant benefit prior to large crack lengths.

A second parameter, which controls the load transfer through friction, is the installation torque. This provides the preload which provides the normal force that causes load transfer through friction during the delamination process. The typical coefficient of friction of the interface is a minimum of 0.25 [24], with an "effective" coefficient found to be about 0.35 in the course of this research. While this is ideal to account for in the analysis, it is imperative to consider the stress relaxation of the laminate during long term service and estimate the final preload that the fastener is providing. This will then establish the minimum approximate value of load transfer through friction. Increasing this value, if possible, will improve the arrest benefit of the fastener system, but typically this value is a result of the configuration and cannot be manipulated to a significant degree.

12.3 The need for high quality control

Delamination arrest fasteners have been seen to be highly sensitive to the hole clearance as well as the installation torque. As a result, process control becomes critical when relying on these fasteners to provide delamination arrest capability in a structure. Discrepancies between the assumed and actual values have the potential to generate a significant departure in performance from that which was predicted.

Various drill sizes were utilized in the course of this research, as discussed in Chapter 10, however the results are largely shown for either a custom E drilled, F drilled, or 6.5mm drilled holes. An E drill is precisely 0.2500 inches in diameter, in order to get a tight transition fit, this drill bit was ground slightly to match the fastener diameter of 0.2495 inches. Installation of these 0 clearance fasteners then required slight pressure to press the fastener into the hole. Under research conditions this a reasonable endeavor, however under industrial conditions, careful installation may not be possible and specifying this tight tolerance could lead to more laminate damage than benefit in delamination arrest.

Interestingly however, despite the preceding commentary on the need for quality hole drilling to ensure consistent clearance, drill punch-out did not affect the response to a detectable degree. Occasional samples suffered punch-out, usually indicating a failure in the backing material or a need to sharpen the drill bit, however these samples were tested anyway and the quasi-static behavior was unchanged compared to samples with the highest quality holes.

As discussed previously, the load transfer through friction also plays an important role in the arrest capability of the fasteners, particularly under fatigue loading at relatively low peak loading, where frictional load transfer represents a proportionally larger amount of the total load.

Also discussed previously is the observation that fasteners occasionally lost clamping during fatigue testing, indicating the need to accurately control both the original installation torque as well as ensure continued clamping of the laminate through its service life.

12.4 Post-damage installation

In contrast with the various other reinforcement mechanisms which are inserted into the laminate during the manufacturing process of the composite, fasteners are installed after the curing cycle is completed. This can be both a drawback, as drilling composites is not ideal, as well as a benefit, as post-damage installation of delamination arrest fasteners is possible. This method of enhancing damage tolerance post damage is not possible with other arrest features.

During the course of this research, cracks were grown under arrest by one fastener, and after a second fastener was installed, the arrest curve shifted from the single fastener to the two fastener behavior. More discussion of this is in Chapter 10. Reloading the sample resulted in the sample load vs. crack length curve changing from the one fastener behavior established by Cheung [2] to the two fastener curve as found in this research.

While not as formally tested, this behavior is expected to also occur in fatigue delaminations as well. Under fatigue loading, the first fastener head occasionally failed in fatigue bending, resulting in additional crack growth due to a loss in clamping and shear load transfer. While these results are not shown in the previous chapters due to the departure from the standard test conditions, after the discovery of the fatigue failure, a new fastener was installed and the testing was resumed. For the various conditions, the re-installation of the fastener re-established the arrest capability of the two fastener system, resulting in re-arrest of the delamination. By extension, after the discovery of delaminations in a part which cannot be readily repaired through

other means, fastener installation can improve the fatigue delamination resistance, provided the structure can support them. This feature is unique among arrest delamination features as it only requires access to one side of the structure.

Chapter 13 Conclusions

13.1 Static Arrest Features

Under static loading, delamination arrest features are highly successful at shifting the failure mode away from delamination, even with the introduction of clearance. Not surprisingly, more fasteners provide more benefit, assuming that the crack extension is sufficient for each fastener to become engaged. Prior to engagement, additional fasteners just add weight.

The first fastener shuts down mode I delamination and subsequently provides load alleviation at the crack tip through shear and frictional load transfer. As mode I delaminations remain effectively eliminated, additional fasteners provide benefit only through load alleviation and shear. For quasi-static testing, as the propagation loads are relatively high, fastener engagement in shear tends to be the dominant arrest mechanism, with frictional load transfer providing a marginal benefit.

As a result of shear engagement dominating the arrest situation, clearance of the fastener becomes the most important manufacturing parameter which will alter the delamination arrest capability. Increasing the clearance between the fastener and hole wall results in a greater delay in shear engagement of the fastener and subsequently greater crack lengths. For a sufficiently large value of clearance or brittle laminate, it is possible for failure to occur prior to engagement.

Comparing the results of the quasi-isotropic and 50% zero laminates, the critical parameters remain the same but the relative benefit provided is less for the stiffer laminate, particularly with the introduction of clearance. The 50% zero laminate carries proportionally more load prior to delamination failure, thus the installed fasteners are incapable of increasing the propagation load

to the same degree as in the quasi-istropic system. Similarly, for an equivalent amount of clearance, a laminate must displace the same amount to take up this value of clearance, but the stiffer laminate requires more load to achieve this, and thus stresses the crack tip more. Finally, the load transfer through friction is a constant value regardless of laminate configuration.

13.2 Fatigue Arrest Features

As the work here combined with previous testing has indicated the very good capability of fasteners in the delamination arrest role for quasi-static loading, the second focus was understanding the arrest solution under fatigue loading. Comparing the predictions made using only experimentally derived parameters and a one dimensional model with the experimental results gives good confidence of the capability of both the arrest features themselves as well as the prediction of the relative benefit a configuration will offer.

13.2.i Important findings

One of the most important assumptions that was verified is that the Paris Law, utilizing ΔG instead of ΔK, appears to be applicable to the arrested delamination propagation. The research presented here suggests that the delamination fatigue behavior is unchanged in the presence of fasteners, with the exception that the fasteners serve to reduce the value of ΔG at the crack tip. Furthermore, the virtual crack closure extraction of ΔG also yields accurate results.

There is a distinct mesh sensitivity inherent in applying these parameters. For a complex loading situation, it is not possible to integrate the Paris law to obtain the number of cycles for a given crack length change, $da,$ because ΔG is a function of crack length which, in the most general case, cannot be readily expressed. However with a sufficiently small mesh at the crack tip,

$\Delta G(a) \approx \Delta G(a + da)$ and thus the integration is much simpler. For the problem to be analyzed, a mesh sensitivity study must be performed.

In addition, testing and analysis comparisons have indicated that the standard correction for R ratio utilized in fatigue of homogenous materials applies to interlaminar fatigue as well. Reasonable agreement was achieved between experiments and analysis under a wide range of fatigue loading. A more detailed examination of the parameters may yield improvements, the scale of the testing program which derived these parameters, while detailed, is by no means comprehensive.

When applying the R ratio correction factor, it is critical to apply the R ratio of the loads at the crack tip, not the applied/global loads. Typical fatigue loading is not concerned with this as there are no arrest features which serve to alter the stresses at the crack tip, but for delaminating samples, as the delamination extends down the length of the sample, the value of the loads at the crack tip, G_{Max}, G_{Min},and ΔG all change.

Another outcome of the experimental work is the understanding of a ΔG_{th} and G_{crit} of the matrix material. Section 11.2 details the effect of these two parameters; in general, the response is less sensitive to alterations in ΔG_{Crit} compared to ΔG_{th}. The threshold value is utilized to find the location at which the delamination is assumed to be arrested as the crack tip stresses pass underneath the fatigue limit. Changing this value will then alter the final predicted crack length.

13.2.ii Experiments and analysis

Under high loading, the arrest benefit of the fastener is less and the effects of clearance are pronounced, with high loading and clearance resulting in delamination failure of the laminate. The speculated reason for the poorer performance at this high load, 75% of the failure load of the

lamina, is that there is hole damage which reduces the effective stiffness of the fastener. This hole damage was visible during post-test inspections of the laminate. In clearance, this problem is exacerbated by the repeated impacting of the fastener shank into the hole wall. Meanwhile, load transfer through friction in this case represents a proportionally smaller amount of the total load transfer necessary to provide load alleviation at the crack tip.

Under low loading, the fasteners provide significant arrest benefit, with arrest readily occurring, even prior to the second fastener under certain conditions. The load transfer through friction has been found experimentally, as well as through analysis, to play a significant role in the arrest capability. Analysis without the inclusion of friction tends to underpredict the performance and testing where the frictional load transfer is intentionally minimized tends to show more extensive crack growth.

Visible to a greater degree in the heavily loaded samples is hole damage, which did not appear in the statically loaded specimens. The continued loading and unloading of the fastener shank against the hole wall is assumed to be the driver behind this. The damage also qualitatively appeared worse for clearance drilled holes, presumably because the fastener shank completely disengages and then impacts the hole more forcefully during each cycle.

When comparing the 50% zero results to those of the quasi-isotropic results, as in the quasi-static testing, the 50% zero laminates obtain less benefit from the installation of fasteners. The delamination resistance is still dramatically improved due to the elimination of mode I delaminations by clamping, but with the inclusion of clearance, delaminations occurred at a lower percentage of the ultimate load of the sample compared to the quasi isotropic design.

13.3 Critical parameters for design and analysis

The most important input parameters for fatigue and static analysis are

- G_{IIC}: shifts the quasi-static curve vertically
- Fastener Flexibility: stiffer fasteners transfer more load and reduce G_{II} at the crack tip
- Load transfer through friction: greater load transfer reduces G_{II} at the crack tip
- Laminate Stiffness: used to calculate the fastener flexibility and determines engagement of clearance drilled fasteners
- C and m for the Paris Law in ΔG: changes the slope of the fatigue curves
- ΔG_{th}: higher ΔG_{th} indicate delaminations will arrest in a shorter distance

13.4 Parameters which have minimal influence

In contrast, certain parameters were found to have minimal influence on the analysis

- G_{IC}: fasteners effectively eliminate mode I delaminations in both static and fatigue testing
- Fastener spacing: there has been no interplay between fasteners found at typical spacing values
- G_{crit}: typically G_{crit} is very close to G_{IIC} and thus only plays a significant role in very low cycle fatigue
- Fastener Young's Modulus: Huth's formula tends to be insensitive to $E_{Fastener}$
- Fastener location through the width: variations in fastener location across the width during testing did not affect the results

13.5 Application of the work presented here

Not surprisingly, except in very special cases such as runouts, it is unusual for a delamination to occur entirely across the width and for only ½ of the total laminate to be loaded. More commonly in aerospace structures, it would be assumed that bending of the structure would generate the necessary mode I and mode II components to propagate delaminations through the structure. While the samples tested here are thus not generally representative of a typical delamination, the arrest mechanisms are applicable.

Under fatigue loading, one of the key drivers of arrest is the frictional load transfer. For common certification, friction is not accounted for in order to improve the conservatism of the predictions. However, failing to utilize this may be leaving weight savings on the table as even utilizing the minimum values of friction measured results in a substantial improvement in both agreement and predicted performance. As well, in bending, additional load transfer through shear can be generated due to the contact of the two parts in bending, independent of the fastener preload. Accounting for this interaction as well will further improve predictions of the performance.

Load transfer through shear is the other key parameter in this work. Delaying the engagement of the fasteners in shear has been shown to consistently negatively impact the delamination arrest benefit provided. Tightly controlling clearance offers a way to improve the delamination arrest capability with minimal impact to the general design.

13.6 Future Usage

The recommended usages of delamination arrest fasteners is as dual use fasteners, particularly in thick laminates as well as potentially for post-damage mitigation. Fasteners are one of the only arrest features which can be utilized in thick laminates as well as after the part has been fabricated. The recommendation for thick laminates arises because the load transfer through shear of a fastener is reduced as the laminate is thinned, and for thinner laminates other arrest features may provide more benefit. The research presented here has shown that for relatively thick laminates, delamination arrest fasteners provide benefit under fatigue and static loading and their performance can be predicted.

13.7 Future Work

There currently exists a number of potential areas of future work in this area which expand the details of the project in different directions. Building on the fatigue delamination arrestment work, additional efforts can be directed into increasing the understanding of this phenomenon under different conditions.

One of the most important extensions of this work would be into variable amplitude loading. Real structures are subject to variable, not constant amplitude loading during their life cycle, but the scope of this work was too great to be tackled in the current research. Extending the current constant amplitude solutions to predict variable amplitude loading however is a suggested area of further work.

Additionally, fasteners tend to eliminate delaminations in mode I, but mode II and possibly mode III are included. Mode III is often ignored, and was neglected in the work presented here, however it is possible that this mode will arise under various loading conditions, and being able to account for this can provide additional confidence in predicted behavior.

While briefly touched on in the scope of this work, continued three dimensional modeling is of potential interest in capturing the curved crack shape. Accurately capturing the crack front is of particular interest for simulating various other potential fastened delamination scenarios of higher complexity.

Three dimensional modeling can work in conjunction with experiments to investigate the results of non rectangular fastener patterns. The research here verified the strip assumption used in the modeling, but was limited to rectangular fastener patterns. The non-flat crack front may be better resisted by a different fastener array.

A final solution which is of particular concern is the effects of post buckling on the re-introduction of mode I delaminations due to sublaminate buckling. While the fasteners tend to eliminate mode I delaminations at and past their location, if the sublaminates buckle, this assumption has the possibility to break down and result in extensive delaminations driven by mode I growth.

References

[1] Kim, H. “Impact Damage Formation on Composite Aircraft Structures” Proceedings of JAMS Review 2014, UW Seattle

[2] Cheung, C.H. “Delamination arrestment in bonded-bolted composite structures by fasteners” PhD Thesis, Dept. Aeronaut. and Astronaut. Univ. Of Wash. Seattle, WA, 2016.

[3] Singhal, T. “Weak bond detection in composites using solitary waves Weak bond detection in composites using solitary waves” MSAA Thesis, Dept. Aeronaut. and Astronaut. Univ. Of Wash. Seattle, WA, 2015.

[4] Hiley, M., Stringer, G. “A Comparison of Through-Thickness Reinforcement Methods: Z-Pinning and Stitching”. Proceedings of ICCM16 (2007)

[5] Davidson, B. “A Predictive Methodology for Delamination Growth in Laminated Composites,” U.S. DOT/FAA, Springfield VA, DOT/FAA/AR-97/87, 1998.

[6] Wang, J. and Pizhong, Q. “Fracture Analysis of Shear Deformable Bi-Material Interface,” Journal of Engineering Mechanics, pp. 306-316, March 2006.

[7] Tracey, D. “Finite Elements for Determination of Crack Tip Elastic Stress Intensity Factors,” Engineering Fracture Mechanics, vol. 3, pp. 255-265. 1971.

[8] Datta, D. (August 2013). Introduction to the eXtended Finite Element (XFEM) Method. Cornell University Library [Online], available: http://arxiv.org/abs/1308.5208v1.

[9] Hattori G. et al. “New anisotropic crack-tip enrichment functions for the extended finite element method,” Comput Mech, vol 50, pp. 591-601, March 2012.

[10] Dong, L. and Atluri, S. “Fracture and Fatigue Analyses: SGBEM-FEM or XFEM? Part 2: 3D Solids,” CMES, vol 90, no.5, pp379-413, 2013.

[11] Mabson, G, “Fracture Interface Elements,” 46th PMC General Session of Mil-17 (Composites Materials Handbook) Organization, Charleston, SC, 2003.

[12] Cheung, C.H., Gray, P. and Lin, K.Y. “Analysis of Fasteners as Disbond Arrest Mechanism for Laminated Composite Structures,” FAA JAMS 2010 Technical Review Meeting, Seattle, WA, 2010.

[13] Deobald, L. et al., “Interlaminar Fatigue Elements for Crack Growth Based on Virtual Crack Closure Technique,” 48th AIAA Structural Dynamics and Materials Conference, Honolulu, HI, 2007

[14] Chandra, N. Topic: “Theoretical and Computational Aspects of Cohesive Zone Modeling,” Department of Mechanical Engineering, Florida State University, Tallahassee, FL

[15] Elices, M. et al. “The cohesive zone model, advantages, limitations and challenges,” Engineering Fracture Mechanics, vol. 69, pp. 137-163, 2002

[16] P. Gray “Experimental and Analytical Study of Mode II Interlaminar Failure of Bolted and Bonded Composite Structures,” MSAA Thesis, Dept. Aeronaut. and Astronaut. Univ. Of Wash. Seattle, WA, 2012.

[17] Tate, M.B., Rosenfeld, S.J., 1946. Preliminary investigation of the loads carried by individual bolts in bolted joints. Technical Report 1051, NACA, Langley Memorial Aeronautical Laboratory, Langley Field, Va, May.

[18] Huth, H., 1986. Influence of fastener flexibility on the prediction of load transfer and fatigue life for multiple-row joints. ASTM Special Technical Publications 927, 221–250.

[19] Dell'Anno, Giuseppe et al. "Exploring mechanical property balance in tufted carbon fabric/epoxy composites". Composites Part A. Vol 38, Issue 11, November 2007

[20] Pingkarawat, K and Mouritz, A.P. “Improving the mode I delamination fatigue resistance of composites using z-pins” Composites Science and Technology, Vol 94 February 2014

[21] Pegorin et. Al. “Mode II interlaminar fatigue properties of z-pinned carbon fibre reinforced epoxy composites” Composites Part A: Applied Science and Manufacturing Vol 67 December 2014

[22] Cheung, C.H., Gray, P.G., and Lin, K.Y., “Fastener as Fail-Safe Disbond/Delamination Arrest for Laminated Composite Structures,” Proceedings of the 18th International Conference on Composite Materials (ICCM18), Jeju Island, Korea, August 21-26, 2011.

[23] Cartie, D. et. Al. “Fatigue delamination behaviour of unidirectional carbon fibre/epoxy laminates reinforced by Z-Fiber® pinning” Engineering Fracture Mechanics, Vol 76 Issue 18

[24] Schön, J. “Coefficient of friction of composite delamination surfaces” Wear, 2000, Vol.237(1), pp.77-89

[25] Pegorin, F. et. al “Delamination Fatigue Properties of Z-Pinned Carbon-Epoxy Laminate Using Metal or Composite Rods” Proceedings of ICCM 20 (2015), Copenhagen, Denmark

[26] Elisa, P. “Virtual Crack Closure Technique and Finite Element Method for Predicting the Delamination Growth Initiation in Composite Structures” Advances in Composite Materials – Analysis of Natural and Man-Made Materials, 2011 pp. 463-480.

[27] Zhang, J. et. al “Fatigue delamination growth rates and thresholds of composite laminates under mixed mode loading” Int. Jnl. Fatigue, Vol. 40 (2012), pp 7-15.

[28] Hojo, M. et. al “Effect of Matrix Resin on Delamination Fatigue Crack Growth in CFRP Laminates” Eng. Fract. Mech. Vol. 49, No.1 pp. 35-47

[29] Richard, L. “Analytical and experimental studies on delamination arrest features in aircraft composite structures” Proceedings of ICCM 20 (2015), Copenhagen, Denmark

[30] Esmaeili, F. Chakerlou, T.N., Zehsaz “Investigation of bolt clamping force on the fatigue life of double lap simple bolted and hybrid (bolted/bonded) joints via experimental and numerical analysis” Engineering Failure Analysis, Vol 45 (2014) pp. 406-420

[31] Schijve, J. *Fatigue of Structures and Materials*, Delft, The Netherlands: Springer, 2009

[32] Krueger, R, "The Virtual Crack Closure Technique: History, Approach and Applications," NASA, Langley VA, ICASE Report No 2002-10, NASA/CR-2002-211628, April 2002.

[33] Zi, G. and Belytschko, T. "New crack-tip elements for XFEM and applications for cohesive cracks," International Journal For Numerical Methods in Engineering, vol 57, pp. 2221-2240, March, 2003.

[34] Mar, J. W. and Lin, K. Y., "Fracture of Boron/Aluminum Composites with Discontinuities," Journal of Composite Materials, Vol. 11, pp. 405-421 (1977).

[35] Liu, W. "Analysis of delamination arrest fasteners in bolted-bonded composite structures" M.S. Thesis, Dept. Aeronaut. and Astronaut. Univ. Of Wash. Seattle, WA, 2014.

[36] Rodriguez, P. "Analytical study of delamination arrest features in Abaqus FEA", Master's Thesis, University of Washington, Seattle, WA, 2015.

[37] "Modulus of Elasticity of Young's Modulus and Tensile Modulus for common Materials" Engineeringtoolbox.com http://www.engineeringtoolbox.com/young-modulus-d_417.html

[38] ASTM D7905/D7905M-14, "Standard Test Method for Determination of the Mode II Interlaminar Fracture Toughness of Unidirectional Fiber-Reinforced Polymer Matrix Composites," ASTM Book of Standards Vol. 15.03.

Appendix A – Obtaining Raw Propagation Data and Source Code

Source code, data reduction code and raw data provided on request. Code is written in Matlab (.m extension). Raw data is provided in .dat (raw crack/load data), .csv (load displacement) or .txt (strain data).